Journal of FOOD PROCESS ENGINEERING

Edited by D. R. Heldman, Michigan State University

FOOD & NUTRITION PRESS, INC.
WESTPORT, CONNECTICUT 06880 USA

VOLUME 2, NUMBER 3 QUARTERLY

JOURNAL OF FOOD PROCESS ENGINEERING

Editor: D. R. HELDMAN, Chairman, Department of Agricultural Engineering, Michigan State University, East Lansing, Michigan

Editorial Board:

A. L. BRODY, Mead Packaging, Atlanta, Georgia

J. M. HARPER, Head, Agricultural Engineering Department, Colorado State University, Fort Collins, Colorado

C. G. HAUGH, Agricultural Engineering Department, Purdue University, Lafayette, Indiana

C. J. KING, Chairman, Department of Chemical Engineering, University of California, Berkeley, California

R. L. MERSON, Department of Food Science and Technology, University of California, Davis, California

N. N. MOHSENIN, Agricultural Engineering Department, Pennsylvania State University, University Park, Pennsylvania

F. W. SCHMIDT, Department of Mechanical Engineering, Pennsylvania State University, University Park, Pennsylvania

All articles for publication and inquiries regarding publication should be sent to Prof. D. R. Heldman, Michigan State University, Department of Agricultural Engineering, East Lansing, Michigan 48824 USA.

All subscriptions and inquiries regarding subscriptions should be sent to Food & Nutrition Press, Inc., 265 Post Road West, Westport, Connecticut USA.

One volume of four issues will be published annually. The price for Volume 2 is $50.00 which includes postage to U.S., Canada, and Mexico. Subscriptions to other countries are $60.00 per year via surface mail, and $67.00 per year via airmail.

Subscriptions for individuals for their own personal use are $30.00 for Volume 2 which includes postage to U.S., Canada, and Mexico. Personal subscriptions to other countries are $40.00 per year via surface mail, and $47.00 per year via airmail. Subscriptions for individuals should be sent direct to the publisher and marked for personal use.

The *Journal of Food Process Engineering* is published quarterly by Food & Nutrition Press, Inc. — Office of Publication is 265 Post Road West, Westport, Connecticut 06880 USA.

Application to mail at second class postage rates is pending at Westport, Ct. 06880.

JOURNAL OF FOOD PROCESS ENGINEERING

JOURNAL OF FOOD PROCESS ENGINEERING

Journal of
FOOD PROCESS ENGINEERING

VOLUME 2
NUMBER 3

Editor: D. R. HELDMAN

FOOD & NUTRITION PRESS, INC.
WESTPORT, CONNECTICUT 06880 USA

ISSN 0145-8876

Printed in the United States of America

CONTENTS

MEETINGS

JUNE 1979

June 10—13: 39TH ANNUAL MEETING & FOOD EXPO FOR INSTITUTE OF FOOD TECHNOLOGY. Alfonzo J. Cerdantes Convention Center, St. Louis, Missouri. Contact C. L. Willey, Institute of Food Technologists, Suite 2120, 221 North LaFalle Street, Chicago, Illinois 60601.

June 24—27: SUMMER MEETING OF THE AMERICAN SOCIETY OF AGRICULTURAL ENGINEERS. In cooperation with the Canadian Society of Agricultural Engineers. University of Manitoba, Winnepeg, Canada. Theme: International Dimensions in Engineering. Contact R. R. Castenson, Manager of Public Relations, American Society of Agricultural Engineers, 2950 Niles Road, St. Joseph, Michigan 49085.

AUGUST 1979

August 27—31: SECOND INTERNATIONAL CONGRESS ON ENGINEERING & FOOD, FOOD PROCESSING AND ENGINEERING 1979. Helsinkie University of Technology, Helsinkie, Finland. Contact Dr. J. Larinkari, P.O. Box 244, SF-101031 Helsinkie, Finland.

MEASUREMENT OF THERMAL CONDUCTIVITY OF DAIRY PRODUCTS AND MARGARINES

VINCENT E. SWEAT

Agricultural Engineering Department
Texas A&M University
College Station, Texas 77843

AND

CARLTON E. PARMELEE

Animal Science Department
Purdue University
West Lafayette, Indiana 47907

Received for Publication August 2, 1978
Accepted for Publication November 21, 1978

ABSTRACT

A line heat source thermal conductivity probe was used to measure the thermal conductivity of 28 dairy products and margarines at 0, 20, and 40°C. Water and fat contents and mass density of each sample were also measured and correlated to thermal conductivity.

There was a strong positive correlation between thermal conductivity and water content, and an inverse correlation between thermal conductivity and fat content. Temperature did not appear to be a significant factor over the limited temperature range studied. Although there was some correlation between mass density and non-fat solids fraction, no correlation was observed between mass density and thermal conductivity.

INTRODUCTION

Virtually all dairy products and margarines are heated or cooled during processing. Recent emphasis on energy utilization and conservation has caused renewed interest in efficiency of heat transfer processes in food processing. Thermal properties of the products being processed must be known to analyze accurately the rate and amount of heat transfer involved.

Some thermal conductivity values are available for milk and cream, but practically none have been determined for cheeses, other non-liquid dairy products and margarines. Thermal conductivity has been shown to be affected by product temperature, density, and composition in regard

Journal of Food Process Engineering 2 (1978) 187—197.

to water, fat, and sugar content. All of these properties vary from product to product within the dairy industry so the thermal conductivity of dairy products varies accordingly. The measurement of thermal conductivity of every type of product under every conceivable condition would be an enormous task, therefore the use of models to predict thermal conductivity using other more easily measured properties appears to be the best way to assure the availability of data. Before such models can be generated, considerable data must be collected.

Literature Review

Thermal conductivity of liquid dairy products has been measured by several investigators, but very few values were found for non-liquid products such as cheeses and butter. Leidenfrost (1959) measured the thermal conductivity of unsweetened condensed milk at various concentrations and temperatures. Konrad and Rambke (1970) worked with whole milk, skim milk and cream at different concentrations. A study by Fernandez-Martin and Montes (1972) included skim milk, half and half, and whole milk at various concentrations and temperatures from 5 to 75 °C. Equations were developed to express thermal conductivity as a function of fat content, solids-not-fat-content, temperature and the ratio of fat to solids-not-fat.

Lepilkin and Borisov (1970) measured the thermal conductivity of milk and cream products over a range of fat content from 3.2 to 96%. Reidel (1949) and Spells (1960) reported conductivity data for butterfat. Butter and margarine were included in a study by Hooper and Chang (1953).

Several factors have been shown to affect thermal conductivity of dairy products including temperature, water content, and fat content. The influence of water content and temperature has been established for other types of foods, but the higher fat contents and the reversal of phases of some dairy products and margarines make them unique with respect to prediction of thermal conductivity.

The objective of the present study was to measure thermal conductivity of several dairy products and margarines and to relate thermal conductivity to water content, fat content, temperature, and density of the samples. Many different samples were tested to broaden the scope of the data.

EXPERIMENTAL

A line source thermal conductivity probe similar to those used previously by the author for meat, and fruits and vegetables was used

(Sweat *et al.* 1973, 1974). The thermal conductivity measurement procedure was automated by using a computer to control the probe heater and to collect temperature data under program control.

Line Source Thermal Conductivity Probe

The probe used in this study was hypodermic tubing 3.2 cm long and 0.58 mm in diameter attached to a plastic handle. Constantan wire 0.05 mm in diameter with enamel insulation was utilized as the heater wire and it was doubled. Thermocouple wires were enamel-coated chromel and constantan with plastic spaghetti tubing insulating the thermocouple junction. The heater wire and thermocouple wires were insulated from each other and the hypodermic tubing (Fig. 1).

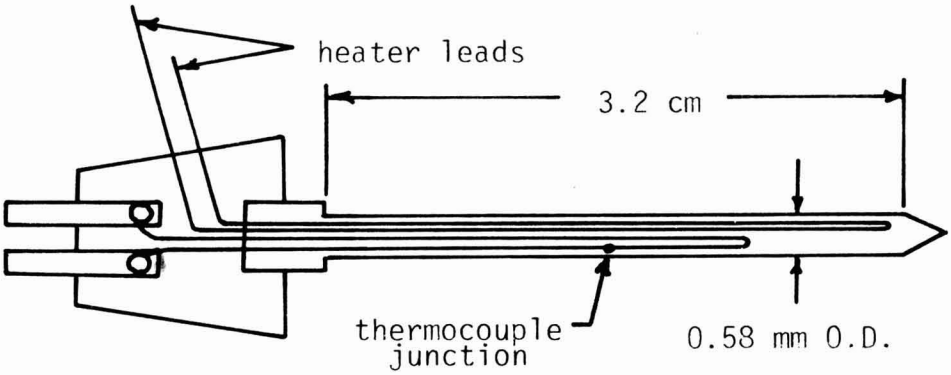

FIG. 1. CROSS-SECTION OF THERMAL CONDUCTIVITY PROBE

Probe Theory

For detailed theory, see the development by Nix *et al.* (1967) or other authors who have reviewed the theory in detail. Briefly stated, the probe heater approximates an infinite line heat source. After the heater is turned on, there is a short transient period in the plot of probe temperature versus logarithm of time (Fig. 2). Then this curve becomes linear with a slope equal to $Q/4\pi k$, where Q is the power generated by the heater and k is the thermal conductivity of the sample.

Equipment

Figure 3 shows the thermocouple circuit and the probe heater circuit.

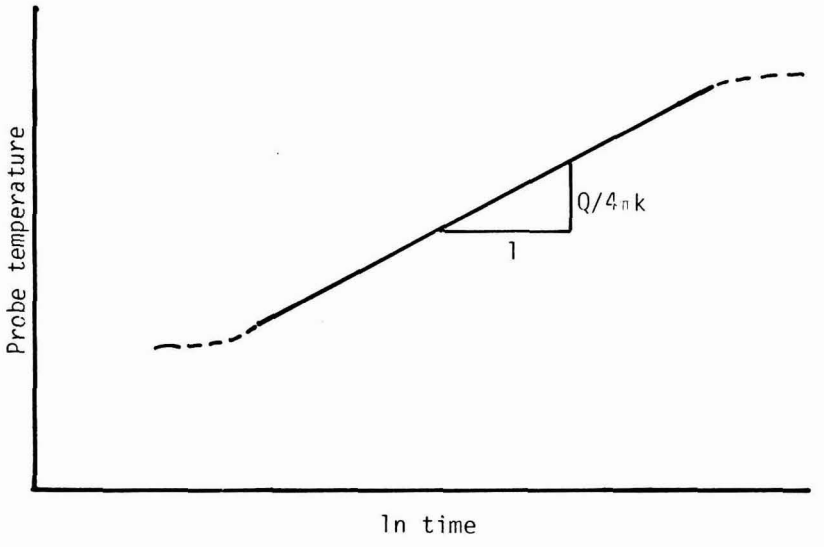

FIG. 2. PROBE TEMPERATURE VERSUS ln TIME

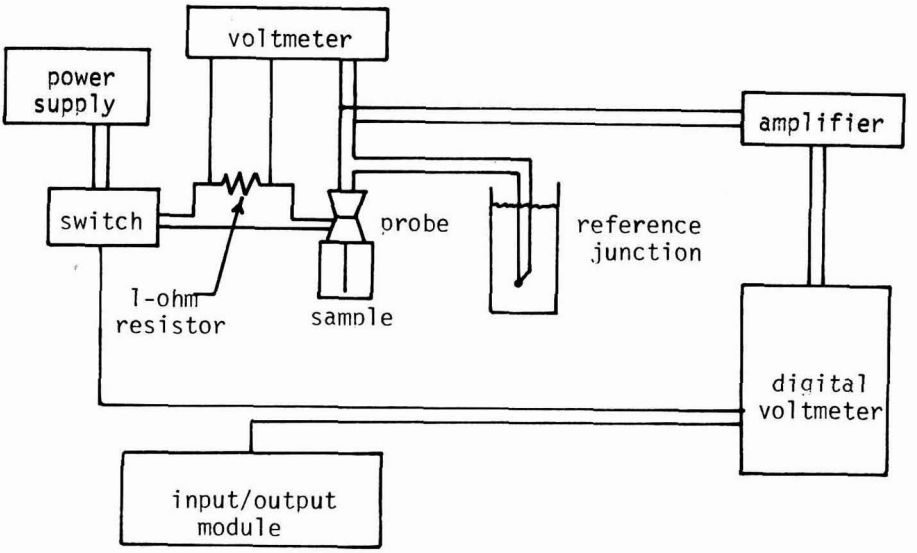

FIG. 3. THERMOCOUPLE, PROBE HEATER AND CONTROL CIRCUITS

The probe heater was turned on and off under program control to simplify the testing procedure and to synchronize the time of the heater activation with the initial temperature measurement. The current to the probe heater was controlled by a two-stage transistor switch capable of being activated by logic level signals from the computer. The current level was measured to the nearest 0.1 milliamp with a digital voltmeter by measuring the voltage drop across a standard 1-ohm resistor, which was in series with the probe heater. The signal from the probe thermocouple was amplified by a factor of 1000 and then at the computer this signal was passed through a 1-Hz low pass filter, a solid state multiplexer and into a high-speed sample-hold amplifier which drove the analog-to-digital (A/D) converter. The multiplexer and A/D converter were operated under program control of the associated digital computer. A digital voltmeter was connected across the thermocouple output for observation of the probe temperature prior to and during a run.

Thermal Conductivity Measurement

When measuring thermal conductivity of a sample with the probe, the sample was first equilibrated at the appropriate temperature. Temperatures of 0, 20, and 40 °C were used. Samples were placed in an expanded plastic insulated bucket containing a mixture of water and crushed ice for the 0 °C tests. A temperature controlled laboratory bath/circulator was used to circulate water in the same container for 20 and 40 °C.

Three samples of each product were tested. Three glycerine samples were always included for probe calibration. The thermal conductivity probe was placed in a sample. The probe temperature was monitored by observing the thermocouple output on the digital voltmeter to ensure that the sample was at a constant temperature before initiating the conductivity measurements.

Tests were conducted under computer control. The initial sample temperature was printed out. Then the probe heater was activated. After the heater was turned on, time and probe temperature were recorded 25 times per second. After six seconds had elapsed, the probe heater was turned off. A linear regression line was fitted to the (ln-time)-temperature data between 2 and 6 s by the least squares method. A straight line was normally obtained with a food sample in less than two seconds. The temperature rise in the sample was estimated as 3—5 °C based on a temperature rise of 10—15 °C in the probe thermocouple and a very rapid temperature drop to within 3—5 °C of the initial sample temperature after the heater was turned off.

A correlation coefficient was calculated to describe the linearity of the (ln-time)-temperature curve. The run was normally rejected if the correla-

tion coefficient was less than 0.999. Thermal conductivity of the sample was calcualted and printed out, using the equation $k = Q/(4\pi M)$ where Q is the heat supplied by the probe in watts/m and M is the slope of the (ln-time)-temperature curve in degrees C.

Six successive measurements were made in each sample at two-minute intervals. This equilibration time provided for reestablishment of a uniform temperature throughout the sample. The mean thermal conductivity and standard deviation were printed out. Reported thermal conductivity values for each product are the averages of the mean thermal conductivity values for the three samples tested. The 40 °C tests always were conducted last because some of the samples were partially melted at that temperature.

Products

All products tested were procured from local retail stores or commercial sources and kept refrigerated until tested, either the same day or the following day. Samples for water content, density, fat content, and thermal conductivity were taken from similar locations within one block of cheese or the same container of butter or other product.

For thermal conductivity testing, samples were placed in 1.9 cm inside diameter brass cylinders which were then sealed at the top with polyethylene and 1.6 mm rubber sheet cut from an inner tube. The rubber sheet was used to maintain a water proof seal during and after placement of the thermal conductivity probe into the sample. For the solid cheese products, a cork borer was used to obtain a cylindrical shaped sample which would fit the brass sample holders.

For each product, four separate measurements were made for density, water content, and fat content. Density of solid cheese products was measured by measuring the volumetric displacement of water at 20 °C for a sample of predetermined mass. For fluid products, the samples were poured into containers of known volume (approximately 50 ml), then weighed. The liquid products tested were sufficiently viscous to retard convection currents around the probe at the power level used.

Water content was determined by drying 2—4 g samples in a 100° atmospheric oven until they reached constant weight. Usually this occurred at about 48 h.

Fat content was determined by the Babcock method, modified for the particular type of product tested, except for butter and margarine (modified Kohman method) and evaporated milk and pudding (Pennsylvania test) (AOAC 1970).

RESULTS AND DISCUSSION

Table 1. Thermal conductivities of dairy products and margarines

Product	Water Content % by wt	Fat Content % by wt	Density Kg/m³	Thermal Conductivity W/m°C 0°C	20°C	40°C
Colby Cheese	37.3	32.0	1050	.32	.31	.29
Colby Cheese (sharp)	37.8	30.0	1090	.31	.28	.27
Cheddar Cheese	37.2	32.0	1090	.32	.31	.30
Meunster Cheese	44.3	31.5	1070	.34	.34	.31
Port Salute Cheese	47.3	24.5	1060	.36	.32	.34
Cream Cheese	55.4	32.0	1010	.34	.38	.36
Cream Cheese (low fat)	64.5	22.9	1000	.42	.37	.40
Swiss Cheese (without eyes)	35.2	32.0	1110	.33	.29	.34
Monterey Jack Cheese	39.5	33.0	1090	.33	.32	.32
Gjetost Cheese	19.1	24.6	1230	.32	.33	.30
Romano Cheese	31.3	27.3	1210	.29	.30	.29
Brick Cheese	43.5	29.9	1090	.32	.30	.30
Mozarella Cheese	45.5	17.0	1140	.34	.37	.38
Cheesespread	47.8	19.5	1130	.36	.37	.38
Neufchatel Cheese	65.2	22.0	1080	.42	.40	.40
Smoked Cheese	45.1	25.9	1130	.32	.32	.33
Butter	16.5	80.6	910	.20	.21	----
Margarine	16.0	81.7	960	.20	.19	----
Whipped Margarine	16.2	81.6	650	.15	.17	----
Diet Margarine	56.7	40.1	1070	.34	.36	----
Pudding (DelMonte, Chocolate)	72.4	23.6	1070	.50	.53	.54
Sour Cream	75.0	17.2	1000	.47	.46	.49
Filled Evaporated Milk	77.0	7.8	1080	.46	.47	.46
Sweetened Condensed Milk	30.1	11.0	1310	.33	.33	.32
Evaporated Milk	77.0	7.7	1070	.46	.46	.45
Half & Half	82.2	9.3	1010	.43	.47	----
Cream	60.4	16.7	990	.33	.36	----
Ice Milk Mix	68.6	5.6	1090	.46	.49	.47

Results of this study are shown in Table 1. Water contents ranged from 82.2% for half and half to 16% for margarine. Fat contents ranged from 5.6% for ice milk to 81.7% for margarine. The "filled evaporated milk" was Milnot which has vegetable fat substituted for the original milk fat. The correlation between fat content and water content is shown in Fig. 4. Although water content generally decreased as fat content increased, several products such as sweetened condensed milk and Gjetost cheese did not fit this general pattern probably due to the higher sugar

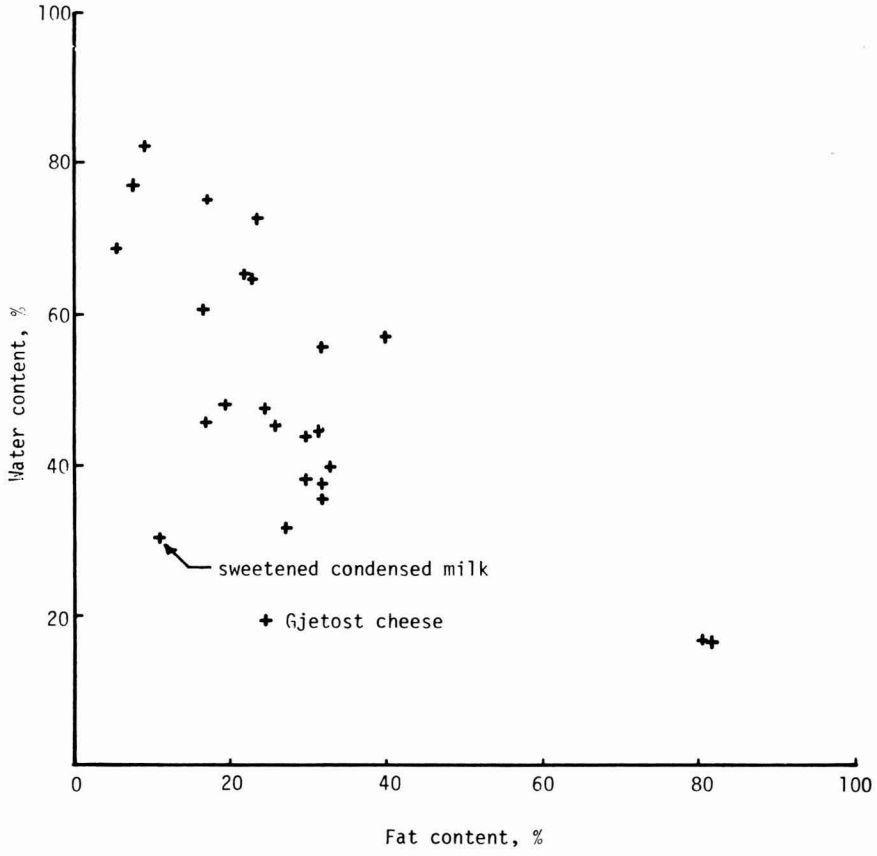

FIG. 4. FAT CONTENT VERSUS WATER CONTENT FOR DAIRY PRODUCTS AND MARGARINES

content of these products. Density did not vary greatly for most products. The most notable exception was whipped margarine which had a density of only 650 kg/m^3 as compared to 960 Kg/m^3 for regular margarine. Some correlation between the fraction of non-fat solids and density is seen in Fig. 5. No correlation was observed between density and thermal conductivity.

Figure 6 illustrates the strong correlation between thermal conductivity and water content at 20 °C (correlation coefficient = 0.93). Notable exceptions are pudding, sweetened condensed milk, and ice milk mix, which contain sugar; and Gjetost cheese, which has a comparatively low total fat and water content, but relatively high lactose content. These products were not included in the calculation of a linear regression line. The equation for this line is $k = 0.141 + (0.00412 \times W)$ where k is thermal con-

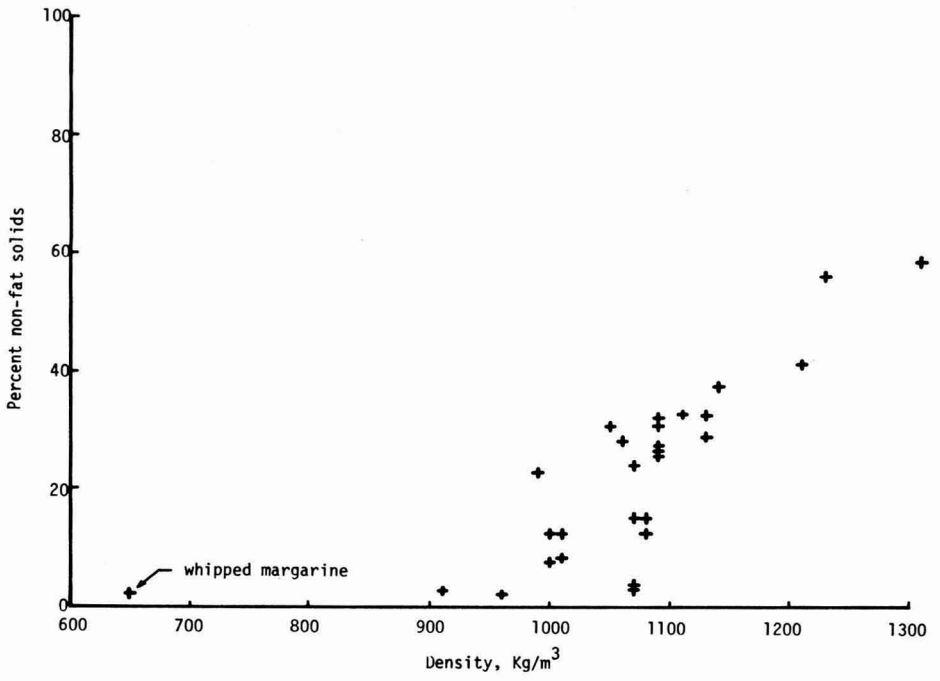

FIG. 5. DENSITY VERSUS PERCENT NON-FAT SOLIDS

ductivity in watts/m-C and W is water content expressed as percent by weight, wet basis.

The correlation between thermal conductivity and fat content is shown in Fig. 7 (correlation coefficient = 0.75). This relationship is similar to that between fat content and water content which reinforces the strong correlation between water content and thermal conductivity.

The data compare favorably with that from the literature although it is difficult to make direct comparisons because of differences in water or fat contents. The value for butter at 0 °C was 0.20 W/m °C which is nearly the same as that reported by Hooper and Chang (1953) for butter (0.198 W/m °C). The value for half and half at 20 °C was 0.47 W/m °C compared to 0.531 W/m °C reported by Fernandez-Martin and Montes (1952) at 25 °C; however, their product was at a higher water content and lower fat content which would account for much of the difference.

The results for butter, margarine, and whipped margarine were similar except for density, while diet margarine was closer in behavior to the cheeses, apparently due to its lower fat and water contents.

The variation in thermal conductivity of different cheeses does not

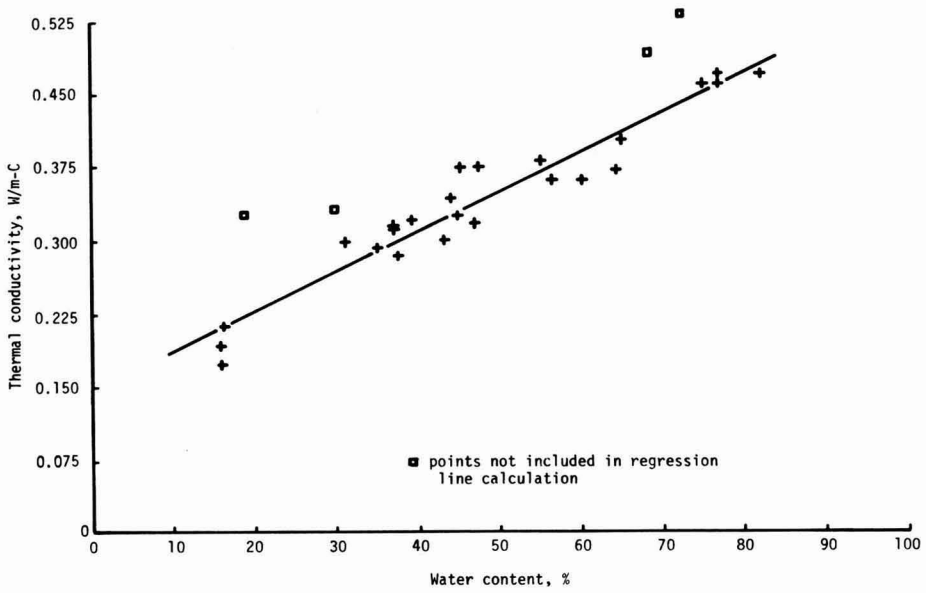

FIG. 6. EFFECT OF WATER CONTENT ON THERMAL CONDUCTIVITY OF DAIRY PRODUCTS AND MARGARINES AT 20°C.

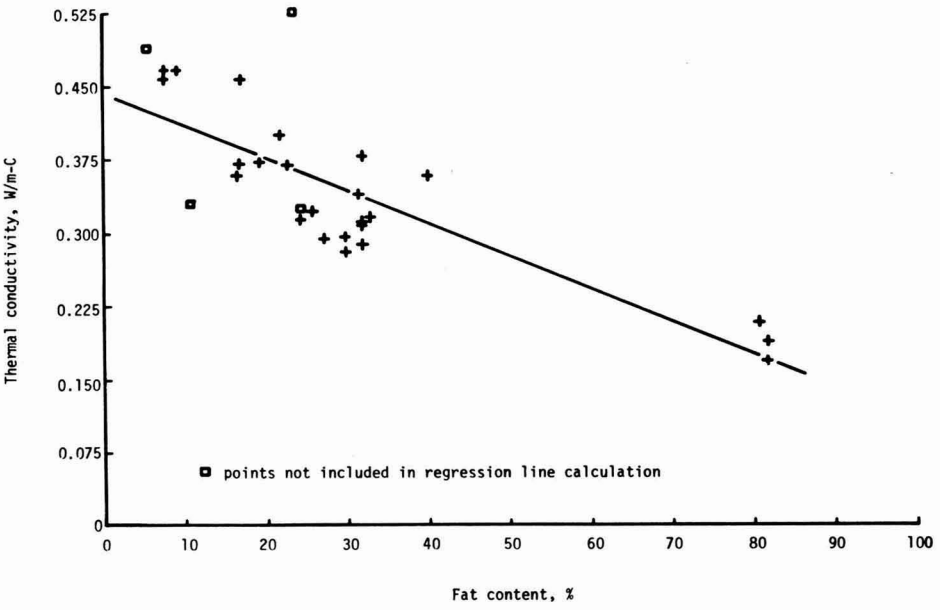

FIG. 7. THERMAL CONDUCTIVITY VERSUS FAT CONTENT FOR DAIRY PRODUCTS AND MARGARINES

appear to be accounted for solely by differences in water content, fat content, and density, although these would account for most of the differences. The accuracy of the thermal conductivity data was estimated as ± 5%.

The effect of temperature was not emphasized in this study as only three temperature levels were included; however, temperature did not appear to be a significant factor over this limited temperature range. For most products the effect of temperature was less than the estimated experimental error. The samples were completely unfrozen at 0 °C. The butter and margarine products tended to melt at 40 °C.

REFERENCES

AOAC. 1970. Official Methods of Analysis. Eleventh Ed., Association of Official Analytical Chemists. Washington, D.C.

FERNANDEZ-MARTIN, F. and MONTES, F. 1972. Influence of temperature and composition on some physical properties of milk and milk concentrations. III. Thermal Conductivity. Milchwissenschaft *27*(12).

HOOPER, F.C. and CHANG, S.C. 1952. Development of the thermal conductivity probe. Heating, Piping and Air Conditioning ASHVE, 24(10), 125-129.

KONRAD, H. and RAMBKE, K. 1971. Physikalische Eigneschaften flussiger Milchprodukte. 4. Mitt. Warmeleitfahigkeit von Milch, Rahm und Milchkonzentraten. Die Nahrung *15*(3), 269-277.

LEIDENFROST, W. 1959. Messung der Warmeleitzahl von Milch mit verschiedenem wassergehalt in temperaturbereich von 20-100 °C. Fette-Seite u. Anstrichmitt 61,1005-1010.

LENTZ, C.P. 1961. Thermal conductivity of meats, fats, gelatin, gels and ice. Food Technol. *15*(5), 243-247.

LEPILKIN, A.M. and BORISOV, V.I. 1967. Untersuchung des Einfusses der temperatur auf den termophysikalischen Eigenschaften von Milch. Molosanja Promils. *28*(9), 35-37.

NIX, G.H., LOWERY, G.W., VACHON, R.I. and TANGER, G.E. 1967. Direct determination of thermal diffusivity and conductivity with a refined line-source technique. In *Progress in Aeronautics and Astronautics: Thermophysics of Spacecraft and Planetary Bodies*, Academic Press, New York.

REIDEL, L. 1949. Warmeleitfahigkeitsmessungen an Zukerlosungen, Fruchtasaften und Milch. Chem. Ing. Technol. *21*(17/18), 340-341.

RISHOI, A.H. and SHARP, P.F. 1938. Specific heat and the physical state of the fat in cream. J. Dairy Sci. *21*, 399.

SPELLS, K.E. 1960. Thermal conductivity of some biological fluids. Phys. Medic. U. Biol. *5*(7), 139.

SWEAT, V.E., HAUGH, C.G. and STADELMAN, W.J. 1973. Thermal conductivity of chicken meat at temperatures between —75 ° and 20 °C. J. Food Sci. *38*, 158.

SWEAT, V.E. 1974. Experimental values of thermal conductivity of selected fruits and vegetables. J. Food Sci. *39*, 1080-1083.

DYNAMIC PROGRAMMING FOR PROCESS OPTIMIZATION 1. AN ALGORITHM FOR DESIGN OF MULTI-STAGE GRAIN DRYERS

ROGER C. BROOK

Agricultural Engineering Department
Purdue University
West Lafayette, Indiana 47907

AND

FRED W. BAKKER-ARKEMA

Agricultural Engineering Department
Michigan State University
East Lansing, Michigan 48823

Received for Publication July 7, 1978
Accepted for Publication November 21, 1978

ABSTRACT

A dynamic programming algorithm for determining the optimum operational parameters and size of a multi-stage concurrent flow dryer with intermediate tempering stages was developed. The objective function was based on energy and capital costs. The operational parameters were constrained by the desired final moisture content and the maximum allowable value of important grain quality factors.

The two- and three-stage concurrent flow dryers have a higher investment cost than the single stage unit, but were less expensive to operate due to the decreased grainflow rate in the single-stage unit. On the basis of operating cost, the multi-stage concurrent flow dryer was preferable to a comparable crossflow dryer for drying corn.

INTRODUCTION

Dynamic programming is an extremely powerful technique for optimization problems in the food process industry. It is especially applicable to processes involving multi-stage units. The following outlines the development of a dynamic programming algorithm for finding the optimum operational parameters and size of a multi-stage concurrent flow dryer with intermediate tempering stages (Fig. 1). The objective function was based on costs for energy consumed during the drying and for fixed and (design) variable costs. The operational parameters were constrained by the desired final moisture content, the maximum allowable exit tem-

Journal of Food Process Engineering 2 (1978) 199—211.

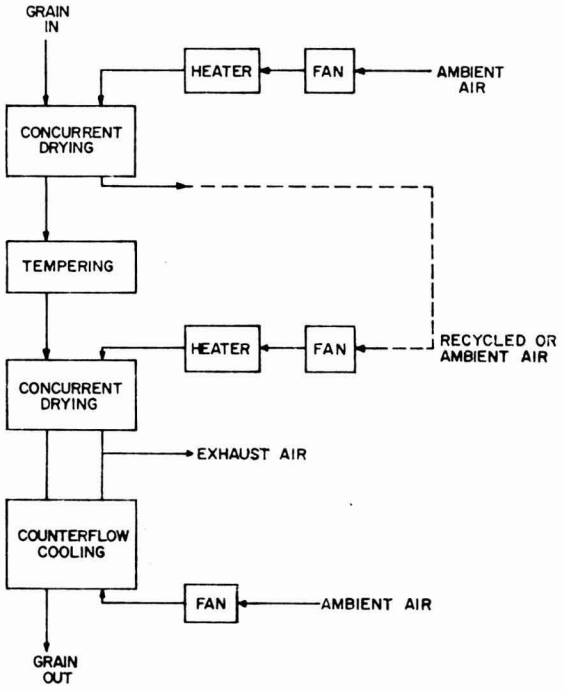

FIG. 1. SCHEMATIC REPRESENTATION OF A TWO-STAGE CONCURRENT FLOW DRYER WITH COUNTERFLOW COOLER

perature of the grain from each drying stage, and the maximum allowable value of an important grain quality factor. For shelled corn the quality factor used was the susceptibility to breakage as measured by the Stein breakage test. For pea beans or soybeans the quality factor might be the percentage of cracked seed coats. For wheat the quality factor might be an index based on baking quality factors.

LITERATURE REVIEW

Thompson (1967) and Farmer (1972) developed multivariable search techniques, based on single dimensional search algorithms, for use in studying the optimal design of convection grain dryers. Thompson studied single-stage crossflow and concurrent flow dryers. Farmer studied the optimal design of batch-in-bin dryers.

Brook and Bakker-Arkema (1976) developed a computer simulation model for minimizing operating costs for drying shelled corn in three fre-

quently used dryer types: (1) the continuous crossflow dryer, (2) batch-in-bin dryer, and (3) the column-batch dryer. The objective function was based on the heat and electrical energy costs per bushel of corn dried. After calculating the optimum drying costs, several associated corn quality factors were estimated for the optimum drying conditions.

Dynamic programming was used by Ahn *et al.* (1964) and Schroeder and Peart (1967) to study optimal air distribution patterns in crossflow grain dryers. Schroeder and Peart defined a "biostrain index" as the ratio of the moisture removed per section to the average moisture content in that section, and used it as the objective function.

Farmer (1972) developed a dynamic programming algorithm for a single-stage concurrent flow dryer with a counterflow cooler. The objective function considered energy costs and used grain quality constraints. Two cases were studied: (1) exhausting the air leaving the dryer and (2) recycling the cooler exhaust air to the heater inlet for the drying section. Bakker-Arkema *et al.* (1973) compared results obtained using Farmer's algorithm to a commercial concurrent flow grain dryer with a counterflow cooler. The results indicate that for minimum cost the concurrent flow dryer should be operated at higher air temperatures and lower airflow rates (to increase the relative humidity of the outlet air).

Bakker-Arkema *et al.* (1977) reviewed the effect of concurrent flow drying on the quality of several grains, including shelled corn, soybeans, wheat, rice, and pea beans. They reported that multi-stage concurrent flow dryers can produce high quality dried grain, if properly designed and operated.

OPTIMIZATION ALGORITHM

Dynamic programming was initially introduced by Bellman (1957). The standard form of dynamic programming used in the previously cited references was "backward" dynamic programming. Backward dynamic programming begins the computations at the final time and proceeds to the initial time in order to find the optimal solution. A useful technique outlined by Larson (1968) was "forward" dynamic programming where the computations begin at the initial time and proceed to the final time in order to find an optimal solution. Forward dynamic may be outlined as follows:

(1) Let X denote the state vector which describes the dynamic behavior of the multi-stage system.

(2) Let U denote the control vector, the components of which are varied by the dynamic programming algorithm so that the progress of the

state vector with time is controlled in an optimal fashion.

(3) The system equations relate the dynamic behavior of the state fector to the applied control vector. The system equations are often non-linear, time varying differential equations, such as:

$$\frac{dX}{dt} = F(X, U, t) \tag{1}$$

(4) The objective function (cost function) determines the effectiveness of the applied control vector and is minimized by the dynamic programming procedure. The cost function is dependent on the applied control vector, the associated state vector for the nth stage and also the minimum of the sum of the cost function for the preceding stages:

$$I(X, n) = i(X, U, n) + \min \sum_{j=1}^{n-1} i(X_{j-1}, U_{j-1}, j) \tag{2}$$

The state vector for the multi-stage concurrent flow dryer studied consisted of a single component, the moisture content of the grain. The control vector consisted of three components for each stage: (1) heated air temperature, (2) airflow, and (3) stage length. A schematic flowchart of the dynamic programming algorithm is presented in Fig. 2.

DRYING SYSTEM EQUATIONS

The phenomena of heat and mass transfer was calculated for individual kernels represented by a sphere of equivalent radius. Young and Whitaker (1971) concluded that for most agricultural products no thermal gradient exists within the kernel even though the kernel temeprature may change with time. Moisture transfer within the kernel was represented by diffusion for a sphere (Chu and Hustrulid 1969). The second order partial differential equation was transformed into a set of coupled ordinary differential equations (ODE's) by the method of lines (Carver 1976), with the spatial derivatives approximated by central finite difference.

At the surface of the kernel, interaction with passing air transfers both heat and moisture. The variation of air and grain conditions was described by ODE's developed from energy and mass balance for the concurrent flow drying process (Brooker *et al.* 1974).

The effect of tempering after concurrent flow drying was estimated

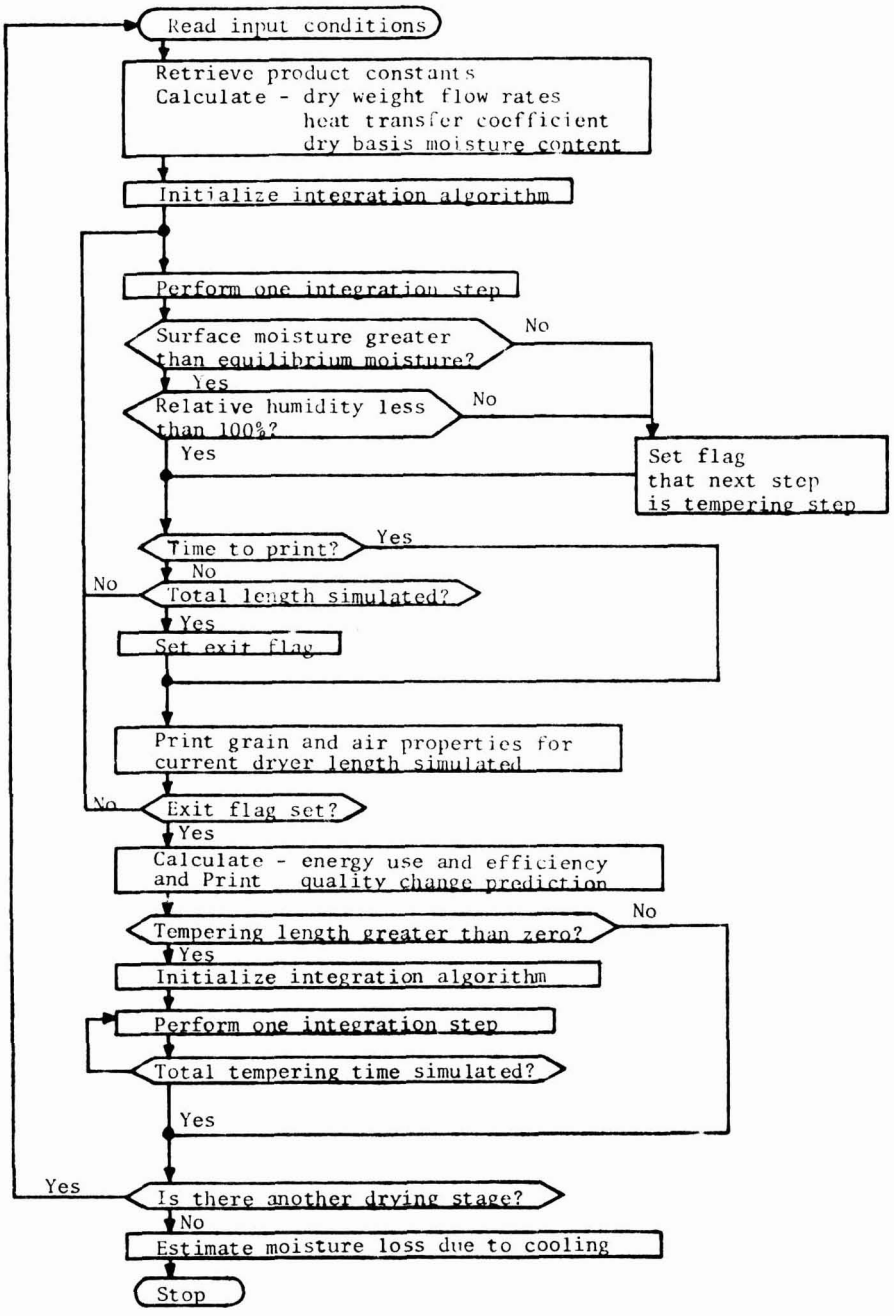

FIG. 2. FLOW CHART OF DYNAMIC PROGRAMMING ALGORITHM

using the ODE's previously described for any desired tempering time. The derivatives representing heat and moisture transfer at the surface were set to zero assuming the kernel does not change temperature or average moisture during tempering (Sabbah *et al.* 1972). During tempering the moisture within the kernel redistributes by diffusion; the moisture concentration at any point within the kernel asymptotically approaching an average value as the tempering time approaches infinity. Additional details of the drying system equations were presented by Brook (1977) and Brook and Bakker-Arkema (1978a).

ENERGY COST

One component of the objective function was the operating cost based on energy consumed during drying. The two operational parameters included in the control vector which directly affect the energy supplied were: (1) heated air temperature, and (2) airflow. The cost equations used were developed by Farmer (1972). The LP fuel and electrical energy costs used were 0.0004 cents/kJ (based on 40 cents/gal. LP) and 0.0014 cents/kJ (based on 5 cents/kWh), respectively.

CAPITAL INVESTMENT COST

The second component of the objective function was the operating cost based on capital investment. Capital cost was affected by: (1) length of the drying stage, and (2) airflow. In addition there was a fixed capital cost for auxiliary equipment. The total investment was calculated from:

$$IC = CC_{fixed} + CC_{fan}\, Q + CC_{length}\, L \tag{3}$$

Sales costs obtained from Westlake Agricultural Engineering, Inc., St. Marys, Ontario, Canada for one-, two-, and three-stage concurrent flow dryers for 1976 were used to approximate the capital cost factors in equation (3). The values of the three cost factors obtained were:

Fixed cost, $/stage	$7225.00(bottom stage)
	3270.00(top stages)
Fan Cost, $/(m/min)	5.00
Length cost, $/m	975.00(bottom stage)
	250.00(top stages)

The cost factors were determined as cost per square meter of dryer column area so as to be applicable for a wide range of dryer sizes. An economy of scale existed (approximately -$172/m2) but was not considered by the optimization routine.

Riggs (1977) described two methods for calculating annual costs for a given investment: (1) approximate calculation, and (2) exact calculation. The exact annual cost calculation includes the time value of money. The discounting of the annual cash flow is normally the preferred means for capital budgeting analysis. However, for use in the optimization procedure the simplicity of the approximate annual cost is preferred and does not affect the optimization results.

The approximate annual cost calculation was based on straightline depreciation and average interest, plus yearly maintenance and insurance costs. The annual cost divided by the yearly throughput yielded the budgeted capital cost (cost per kilogram of grain dried) which can be directly incorporated with the energy costs. Operational time was estimated at 24 h/day and 30 days per corn harvest season. The resulting budgeted capital cost was calculated from:

$$BC = \frac{((IC-SV)/N)+0.5(IC+SV)(IN+IM+II)}{720\ GF} \quad (4)$$

where

SV — Zero salvage value
N — Ten year life for the drying equipment
IN — Interest rate of 8%
IM — Maintenance factor of 5% of investment per year
II — Insurance factor of 1% of investment per year

GRAIN QUALITY CONSTRAINTS

The cost associated with deterioration in grain quality could be used as an additional cost factor. At the present time the estimation models for grain quality are not sufficiently accurate for this approach. Therefore, grain quality was not used as a cost factor but as an operational constraint.

One factor used for corn was the kernel temperature at the end of each drying stage. Corn to be used for feed can withstand a higher temperature than corn which was to be used for wet or dry milling

(Peplinski *et al.* 1975). Corn to be used for seed or milling is very sensitive to high grain temperature (Kreyger 1972). The temperature criterion used was the outlet grain temperature from any stage which indicates that the corn was at that temperature or greater throughout the drying process. The time/temperature results of Muehlbauer and Christ (1974) indicate 80 C to be a suitable constraint for feed grain, mainly to prevent heat damage discoloration.

A second quality factor for the shelled corn is the kernel breakage percentage obtained from the stein breakage test. The U.S. grade standard for shelled corn limits broken corn to 3.0% for No. 2 yellow corn (the most common trade grade). Stephens and Foster (1976) found that a handling breakage of 3.0% resulted from repeated handling of shelled corn with a Stein breakage of 17.0—23.0%. A value for the maximum allowable Stein breakage of 23.0% was used in obtaining the optimization results in the following sections. The change in Stein breakage was estimated (Brook 1977).

$$B = 143.65\ M - 8.40\ (r = 0.50,\ p < 0.01) \tag{5}$$

During the dynamic programming procedure, if any of the quality parameters (temperature or breakage percentage) exceeded the predetermined limit, the corresponding control vector was considered as an infeasible set.

RESULTS OF OPTIMIZATION FOR SHELLED CORN

The dynamic programming optimization routine was used to analyze the design of a multi-stage concurrent flow dryer for shelled corn. Three variables were considered for each drying stage: (1) heated air temperature, (2) airflow rate, and (3) length. The tempering time and thus the length of the tempering stages was, in most cases, set at a length resulting in 1.25 h tempering time. Brook (1977) determined this to be the necessary tempering time for corn at 50 °C. The inlet moisture content to the first stage was 25% w.b. The desired final moisture content was 15% w.b. The counterflow cooler was assumed to remove 1% w.b. moisture. The ranges of the variables used to obtain the results in the following sections were: (1) air temperature 150—200 °C except the top stage range of 200—230 °C, (2) airflow 30—60 m3/m2-min, and (3) dryer length 1-2 m. Additional results and discussion of design factors can be found in Brook (1977) and Brook and Bakker-Arkema (1978b).

Effect of Staging

Table 1. Optimization results for various stage concurrent flow dryers for drying corn

	Grainflow, Tonne/h-m2		
	1.0	2.5	4.0
Stage 1			
Inlet air temperature, °C	200	230	212
Airflow, m3/m2-min	42	48	60
Dryer length, m	1.5	1.1	1.1
Outlet grain temperature, °C	53	48	43
Outlet moisture, % w.b.	15.7	20.7	22.3
Stein breakage, %	22.7	11.9	10.0
Fixed cost, $	7225	3270	3270
Fan cost, $	210	240	300
Length cost, $	1463	1525	2275
Electrical energy cost, cents/kg	.004	.002	.002
Fuel energy cost, cents/kg	.226	.120	.086
Drying cost, cents/kg	.569	.198	.143
Stage 2			
Inlet air temperature, °C		200	200
Airflow, m3/m2-min		48	54
Dryer length, m		1.7	1.3
Outlet grain temperature, °C	62	57	
Outlet moisture, % w.b.		15.7	19.1
Stein breakage, %		22.7	15.5
Fixed cost, $		7225	3270
Fan cost, $		240	270
Length cost, $		1658	2325
Electrical energy cost, cents/kg		.002	.002
Fuel energy cost, cents/kg		.101	.073
Drying cost, cents/kg	.245	.130	
Stage 3			
Inlet air temperature, °C			190
Airflow, m3/m2-min			54
Dryer length, m			1.5
Outlet grain temperature, °C			68
Outlet moisture, % w.b.			15.7
Stein breakage, %			22.7
Fixed cost, $			7225
Fan cost, $	270		
Length cost, $			1463
Electrical energy cost, cents/kg			.002
Fuel energy cost, cents/kg			.069
Drying energy cost, cents/kg			.156
Total drying cost, cents/kg	.569	.443	.429
Efficiency, kJ/kg water	3867	3782	3883

The results for the one-, two-, and three-stage dryers are presented in Table 1. The grainflow rates were representative of commercial concurrent flow dryers. The variation in energy cost and energy efficiency between the three configurations was not significant. The capital cost was about 60% of the total cost for a single-stage dryer, and decreases to about 45% for the 3-stage dryer. The multi-stage dryers have a cost advantage over the single-stage dyrer. There was no apparent advantage (on the basis of average total drying cost) between 2- and 3-stage concurrent flow grain dryers.

Comparison With Crossflow Drying

Average dyring costs for crossflow dryers (Anon. 1976) were used along with the previously presented costs for multi-stage concurrent flow dryers for evaluation of investment feasibility. Comparison was based on the Internal Rate of Return (IRR) as presented by Riggs (1977).

A single-stage concurrent flow dryer rated at 8.0 tonne/h can be purchased for $43,000; an equivalent 2-stage dryer for $48,000; an equivalent 3-stage dryer for $49,000 (Westelaken 1977). All concurrent flow dryers were shown previously to have an operating cost of about 0.230 cents/kg. The average operating cost for an equivalent crossflow dryer is 0.302 cents/kg with an average purchase price of $21,000 (Anon. 1976). Based on the previous assumption of 720 yearly operating hours, the net yearly savings would be $4150. The corresponding IRR for additional investment in a concurrent flow dryer instead of a crossflow dryer would be:

(1) Single stage dryer 14.6%; added investment $22,000
(2) Two-stage dryer 8.7%; added investment $27,000
(3) Three-stage dryer 7.9%; added investment $28,000

CONCLUSIONS

The 2- or 3-stage concurrent flow dyers have a higher investment cost than a single-stage dryer. However, on a per square meter of column area basis, the single-stage concurrent flow dryer was more expensive to operate than a 2- or 3-stage concurrent flow dryer due to the decreased grainflow rate of the single-stage units. The multi-stage concurrent flow dryers have lower energy costs than comparable crossflow dryers. The multi-stage dryers do have a higher investment cost, but with the energy savings they exhibit an acceptable rate of return on investment.

The numerical results obtained were dependent on the factors used for estimating capital costs. However, operational and design factors calculated by the optimization routine were unaffected by even major changes in the capital cost factors.

The quality of the dried grain is affected by the drying process. The concurrent flow dryer produces dried corn which is less susceptible to damage than that produced by a crossflow dryer. Since the increase in Stein breakage (and thus increased susceptibility to breakage) can be related to the moisture removal rate, a multi-stage concurrent flow dryer with tempering was preferable to a single-stage concurrent flow dryer, or to a conventional crossflow dryer.

LIST OF SYMBOLS

B Stein breakage, %
BC budgeted capital cost, $/kg product dried
CC capital cost factor, $
GF dry weight flow rate of corn, kg/h-m
IC Investment cost, $
II Insurance factor, %
IM maintenance factor, %
IN interest rate, %
IRR internal rate of return, %
L total dryer length, m
M moisture removed in one stage, dec. d.b.
N assumed product life, yr
Q volumetric airflow, m3/m2-min
SV equipment salvage value, $
T air temperature, °C
U DP control vector
X DP state vector
P linear correlation significance
r linear correlation coefficient
t time

ACKNOWLEDGEMENTS

Partial financial support for this study, arranged through the Anderson Agricultural Research Fund, Columbus, Ohio, and Westlake Agricultural Engineering, Inc., St. Marys, Ontario, Canada, was greatly appreciated.

REFERENCES

Anon. 1976. Costs of Drying and Storage Grain from the Farmer's Point of View, Research Report, Comm. Div., Ill. Farm Bureau.

AHN, Y.K., CHEN, H.C., FAN, L.T. and WAN, G.G. 1964. Optimum design of a moving bed grain dryer by dynamic programming. Can. J. Chem. Eng. *42,* 117-120.

BAKKER-ARKEMA, F.W., FARMER, D.M. and LEREW, L.E. 1973. Optimum dryer design through simulation. In *Preservation of Wet Harvested Grains,* (J.L. Multon and A. Guilbot eds.), Inst. Nat. Recherche Agronomique, Paris.

BAKKER-ARKEMA, F.W., BROOK, R.C., WALKER, L.P., KALCHIK, S.J. and AHMADNIA-SOKHANSANJ, A. 1977. Concurrent flow grain drying — Grain quality aspects. Tech. Paper. Corn Quality Research Conf., Univ. Ill. Urbana, IL.

BELLMAN, R. 1957. *Dynamic Programming.* Princeton Univ. Press, Princeton, NJ.

BROOK, R.C. 1977. Design of multi-stage grain dryers. Ph.D. Thesis. Mich. State Univer., East Lansing, MI.

BROOK, R.C. and BAKKER-ARKEMA, F.W. 1976. Batch and crossflow corn dryers, TELPLAN program, Special Research Report, Agric. Engineering Department, Mich. State Univ., East Lansing, MI.

BROOK, R.C. and BAKKER-ARKEMA, F.W. 1978a. Design of commercial concurrent flow grain dryers. Trans. ASAE: *21,* 978-981.

BROOK, R.C. and BAKKER-ARKEMA, F.W. 1978b. Design of multi-stage corn dryers using computer optimization. Trans. ASAE (In press).

BROOKER, D.B., BAKKER-ARKEMA, F.W. and HALL, C.W. 1974. *Drying General Grains.* Avi Publishing Co., Westport, CT.

CARVER, M.B. 1976. The choice of algorithms in automated method of lines solution of partial differential equations. In *Numerical Methods for Differential Systems,* (L. Lapidus and W.E. Schiesser eds.) Academic press, New York.

CHU, S.T. and HUSTRULID, A. 1968. Numerical solution of the diffusion equation. Trans ASAE *11,* 705:710, 715.

FARMER, D.M. 1972. Optimization techniques for grain dryer design and analysis. Ph.D. Thesis. Mich. State Univ., East Lansing, MI.

KREYGER, J. 1972. Drying and storing grains, seeds and pulses in temperate climates. Institute for Storage and Processing of Agricultural Produce, Wageningen, Netherlands.

LARSON, R.E. 1968. *State Increment Dynamic Programming,* Am. Elsevier, New York.

MUEHLBAUER, W. and CHRIST, W. 1974. Die zulassige Einwirkungszeit verschiedner Korntemperaturen bie der Trocknung von Mais fur die tierische Ernahrung. Grundl. Landtechnik *24,* 161-164.

PEPLINKSI, A.J., BREKKE, O.L., GRIFFIN, E.L., HALL, G. and HILL, L.D. 1975. Corn quality as influenced by harvest and drying conditions. Cereal Foods World *20,* 145-149, 154.

RIGGS, J.L. 1977. *Engineering Economics,* McGraw-Hill, New York.

SABBAH, M.A., FOSTER, G.H., HAUGH, C.G. and PEART, R.M. 1972. Effect of tempering after drying on cooling shelled corn. Trans. ASAE *15,* 763-765.

SCHROEDER, M.E. and PEART, R.M. 1967. Dynamic programming method for air allocation in a grain dryer. Trans. ASAE *10,* 96-99.

STEPHENS, L.E. and FOSTER, G.H. 1976. Breakage tester predicts handling damage in corn. ARS-NC-49. USDA, Washington, DC.
THOMPSON, T.L. 1967. Predicted performances and optimal designs of convection grain dryers. Ph.D. Thesis, Purdue Univ., West Lafayette, IN.
WESTELAKEN, C.M. 1976. Personal communications. Westlake Agr. Eng., St. Marys, Ontario, Canada.

SIMULATION OF ASCORBIC ACID STABILITY DURING HEAT PROCESSING AND CONCENTRATION OF GRAPEFRUIT JUICE

I. SAGUY, I.J. KOPELMAN and S. MIZRAHI

Department of Food Engineering and Biotechnology
Technion — Israel Institute of Technology
Haifa, Israel

Received for Publication June 15, 1978
Accepted for Publication August 28, 1978

ABSTRACT

The kinetics of ascorbic acid loss in grapefruit juice was determined for thermal and concentration processes. The results indicate an apparent first order anaerobic reaction which is dependent on temperature and degree of product concentration but not on initial ascorbic acid content. The effect of temperature on rate of reaction follows the Arrhenius equation with energy of activation ranging from 5 to 11.3 Kcal/mole for solids content of 11 to 62°Bx, respectively. Using a polynomial curve fitting technique, an empirical kinetic equation correlating rate of reaction with temperature and degree of concentration was established. Based on this empirical equation, a prediction mathematical model was formulated and proved useful in analyzing the extent of ascorbic acid retention in grapefruit juice during commercial thermal and concentration processes.

INTRODUCTION

Losses of heat sensitive nutrients during processing and storage is of great concern, especially in the era of nutrient labeling. In dry foods this subject was extensively reviewed by Labuza (1972). To minimize nutrient loss efficiently, one needs a kinetic model and a simulation technique whereby the optimal process parameters can be determined.

Ascorbic acid is a typical heat sensitive nutrient and its mode of degradation has been the subject of numerous works. The destruction of ascorbic acid follows either an aerobic or an anaerobic pathway (Tannenbaum 1976); both of these reactions have common intermediates and are hardly distinguishable. The specific pathway and the degradation rate are determined by factors such as temperature, oxygen, pH, metal catalysts, enzymes, sugar concentration and amino acids (Clegg and Morton 1965; Clegg 1966; Huelin *et al.* 1971; Joslyn 1957; Kurata and Sakurai 1967a,b,c). In foods such as canned citrus juices the ascorbic

Journal of Food Process Engineering 2 (1978) 213—225.

acid degrades through first order consecutive reactions (Brenner *et al.* 1948; Davidek *et al.* 1974; Huelin 1953; Joslyn and Miller 1949). In dry foods, moisture content also plays a major role in accelerating the destruction rate of ascorbic acid (Karel and Nickerson 1964; Jensen 1967; Lee and Labuza 1975; Vojnovitch and Pfeifer 1970; Labuza 1972).

Ascorbic acid degradation results not only in lowering vitamin C content, but also in contributing to non enzymatic browning (Clegg 1966; Curl 1949; Dulkin and Friedman 1956; Joslyn and Marsh 1935; Joslyn 1957; Lalikainen *et al.* 1958). The prediction of ascorbic acid loss during storage has been the subject of intensive studies (Bauernfeind and Pinkert 1970; Lee *et al.* 1977; Nagy and Smoot 1977; Riemer and Karel 1977; Wanninger 1972). However only limited kinetic data are available on ascorbic acid losses during thermal and concentration processes.

The objectives of this study were: (1) to investigate the rate of ascorbic acid loss in grapefruit juice and concentrate as a function of temperature and degree of product concentration; (2) to develop a mathematical kinetic model describing the deterioration which occurs; (3) to use the kinetic model to predict the retention of ascorbic acid in commercial thermal and concentration processes.

EXPERIMENTAL

Grapefruit (Marsh Seedless) juice (pH 3.05, 1.65% acidity as anhydrous citric acid, and 11.8 °Bx), was taken immediately after an industrial pasteurization and cooling system (Milos-Citrus Extraction Plant, Israel). The juice was concentrated up to approximately 70 °Bx in a freeze drier (Grenco, RI-25 2.5m²) with condenser being kept at −40 °C and plate temperature lower than 35 °C for ca. 20 h. Concentration by the freeze-drying process was used to minimize the degradation of ascorbic acid.

Samples of grapefruit juice at various degrees of concentration were made by reconstituting the 70 °Bx concentrate with appropriate amounts of distilled water. These samples were used in the thermal unit (Fig. 1) for the ascorbic acid kinetic studies. The heat processing unit (Fig. 1) was designed to meet the following requirements: (1) short come-up time; (2) constant temperature during process; (3) a desired atmosphere in the headspace; (4) continuous sampling.

The experimental procedure was as follows: the unit was preheated by steam (2 atm.) in the stainless steel heating coil which was connected to a steam trap at the outlet. Head space atmosphere of the unit was established by bleeding in gas. The bleeding device may also be attached

1 Sample inlet and connection to gas bubbling device
2 Valve for withdrawing samples
3 Hot water inlet
4 Hot water outlet
5 Stirrer
6 Stirring shaft
7 Engagement to stirring motor
8 Constant temperature jacket
9 Thermocouple
10 Steam inlet
11 Steam trap outlet
12 Stainless steel heating coil
13 Flange lid
14 Ground sleeve gland
15 Support stand

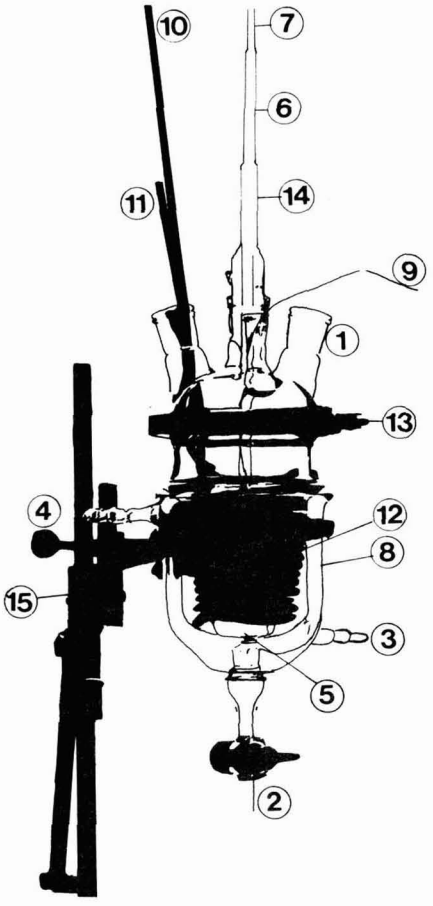

FIG. 1. EXPERIMENTAL THERMAL TREATMENT UNIT

to the sample inlet. Sample (up to 500 g) was poured into the preheated unit and when sample temperature reached the prescribed level the steam was manually turned off. The prescribed temperature was maintained during the process by the constant temperature (± 0.1 °C) water jacket. Temperature was measured by a 24 gauge copper constantan thermocouple, and was continuously recorded. Constant mixing (50 rpm) was maintained by a speed controller (Cole parmer, M-4420). The come-up time was less than 50 s for the most viscous grapefruit concentrate (62.5 °Bx). Portions (up to 50 g) were periodically withdrawn, collected in vials and cooled immediately and rapidly in an ice water shaking bath.

Ascorbic acid was determined by titration with 2.6 dichloroindophenol (Official Methods of Analysis AOAC 1970). The extraction solution used was metaphosphoric acid. Solids content was determined as °Bx by Abbe refractometer (Carl Zeiss). The obtained value was corrected for acidity.

Statistical analysis was performed by a linear and a polynomial regression (BMDO2R and BMDO5R, Dixon 1971), on the Technion IBM 370/168 digital computer.

The accuracy of prediction of ascorbic acid retention was tested on samples of commercial juice and concentrate withdrawn from an industrial evaporator (TASTE 10,000 lb capacity, Gulf Machinery, Florida). Time, temperature and concentration data at the beginning and the end of each stage of the commercial process were determined through monitoring and sampling. The work was carried out by Mr. Z. Albert of Milos-Citrus Extraction Plant, Israel. The obtained data are summarized in Table 1. To evaluate changes in temperature and concentration within a stage, a linear interpolation was used.

Table 1. Time-temperature-concentration data during a commercial grapefruit juice concentration in the TASTE evaporator

Sequence of Operations	Residence Time (S)	Concentration (°Bx)	Temperature (°C)		
Juice	———	11.0		25	
Heating	20	11.0	25		80
1st evaporator Stage	50	15.2	80		65
Pasteurization	60	15.2		96	
2nd Evaporator Stage	50	24.3[a]	96		80
3rd Evaporator Stage	35	40.1	80		65
4th Evaporator Stage	50	48.8	65		50
5th Evaporator Stage	45	61.0	50		45
6th Evaporator Stage + Flash	130	62.2	45	35	8

[a]Estimated

The "hot pack" like thermal treatment was simulated by heating and cooling 52.6 °Bx concentrate. The time-temperature history is given in Fig. 5.

RESULTS AND DISCUSSION

Order of Reaction

Ascorbic acid retention during heat treatment of grapefruit juice and

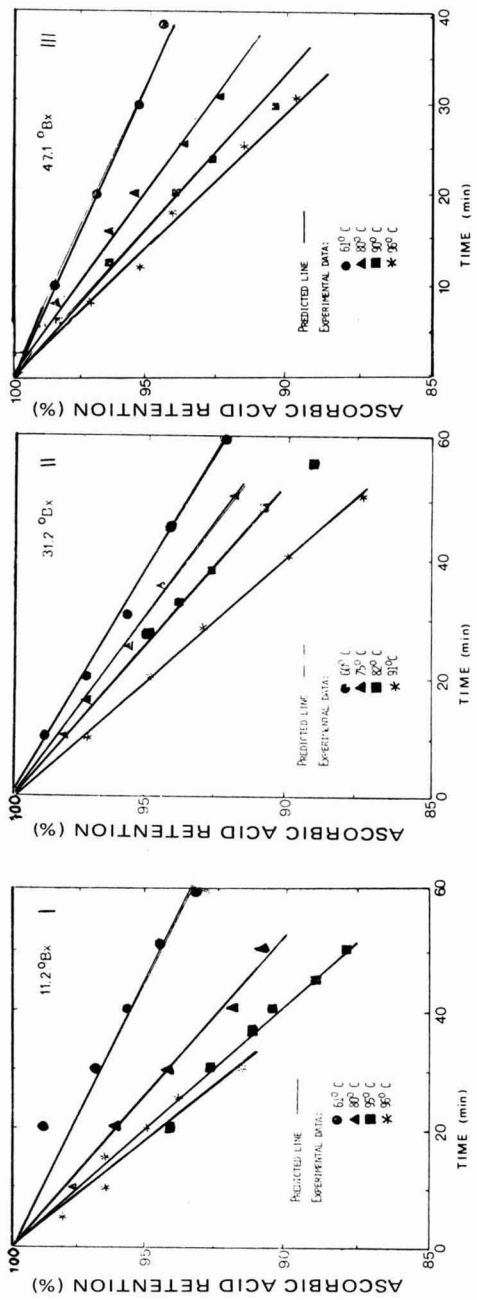

FIG. 2. EFFECT OF SOLIDS CONTENT, TEMPERATURE AND TIME ON ASCORBIC ACID RETENTION (LOGARITHMIC SCALE) (INITIAL CONCENTRATION 34.8/.100 GP IN 10.0°Bx. JUICE)

concentrate have been plotted (Fig. 2) and a regression analysis was carried out on each data set (Table 2). Results indicated that ascorbic acid degradation followed practically a first order reaction, expressed as:

$$-\frac{dc}{dt} = kc \; ; \; \ln\frac{c}{c_o} = -kt \; ; \; T_{1/2} = \frac{\ln 2}{k} \qquad (1)$$

where:

c = concentration of ascorbic acid (c_o = initial value);
t = time; k = rate constant; $T_{1/2}$ = half life time

Table 2. Effect of temperature and solids content on degradation of ascorbic acid in grapefruit juice and concentrate

Solids Content (°Bx)	Temperature (°C)	Rate Constant $k\times10^3$ (min^{-1})	Half Life $T_{1/2}$ (min)	Correlation Coefficient -r
	61.0	1.276	543.2	0.968
	80.0	1.899	365.0	0.983
11.2	95.0	2.503	276.9	0.983
	96.0	2.642	264.2	0.968
	60.0	1.349	514.0	0.962
	75.0	1.874	369.7	0.987
31.2	82.0	2.165	320.1	0.978
	91.0	2.701	256.8	0.989
	61.0	1.430	485.0	0.981
	80.0	2.460	281.8	0.988
47.1	90.0	3.121	221.9	0.982
	96.0	3.777	183.8	0.967
	61.0	1.618	428.4	0.975
	75.0	2.715	255.3	0.985
55.0	81.0	3.348	207.0	0.986
	91.0	4.712	147.1	0.994
	68.0	3.022	229.4	0.973
	76.0	4.261	162.7	0.964
62.5	81.0	5.365	129.2	0.972
	96.0	10.680	64.9	0.961

This apparent first order reaction pattern, which is in good agreement with previous findings (Labuza 1972), is valid at least within the time range of common thermal and concentration processes. To establish whether the reaction is truly a first order one, data should be obtained also for process time much beyond practical range and thus it is beyond the scope of this work.

Effect of Temperature and Solids Content

Data in Table 2 indicate that degradation rates of ascorbic acid increase with temperature and solids content. At constant solids content, the effect of temperature on ascorbic acid destruction rate followed the Arrhenius model (Equation 2):

$$k = K_0 \exp(-E_a/RT) \quad (2)$$

where:

E_a = activation energy, Kcal/mole
T = absolute temperature, °K
R = gas content, Kcal/mole °K
K_0 = frequency factor, min^{-1}

The activation energy (E_a) and the frequency factor (K_0) were determined by a linear regression for each data set and are expressed in Table 3. The values obtained for the energy of activation are within the range reported in the literature (Lee *et al.* 1977; Labuza 1972). On the other hand, values of k extrapolated to common storage temperature are about 2 to 3 order of magnitude higher than those in the literature. Lee *et al.* (1977) reported k of 1.84×10^{-3} $days^{-1}$ for ascorbic acid degradation in tomato juice at 37.8 °C and pH 3.8. Karel and Nickerson (1964) reported a value of 2.3×10^{-2} for the same reaction in orange crystals at 37 °C and water activity of 0.54. In comparison, calculated value for k of single strength grapefruit juice at 37 °C is about 1 day^{-1}. Since rate of ascorbic acid loss in grapefruit juice during storage is not so fast, the high value of k seems to indicate a drastic increase in rate of reaction at elevated temperatures. A similar trend was reported by Nagy and Smoot (1977) who found that rate of vitamin C retention in orange juice was markedly decreased above the temperature of 27 °C.

Table 3. Effect of solids content on Arrhenius equation coefficients value (K_0 expressed in min^{-1})

Solids Content (°Bx)	Arrhenius Equation Coefficient		
	E_a (Kcal/mole)	$\ln(K_0)$	Correlation Coefficient (-r)
11.2	4.98	0.845	0.998
31.2	5.24	1.297	0.989
47.1	6.69	3.531	0.999
55.0	8.60	6.528	0.999
62.5	11.28	10.802	0.972

Since the loss of ascorbic acid during the concentration process is dependent on both temperature and solids content, the relationship between Arrhenius coefficients (E_a and K_o) and solids content has to be determined. Such relationship was established by a polynomial regression analysis of the data listed in Table 3. This analysis yielded the following empirical expressions:

$$E_a = 4.2 + 0.12\,(Bx/10) - 0.55\,(Bx/10)^2 + 0.09\,(Bx/10)^3 \quad (3)$$

$$K_o = \exp[-0.61 + 2.18\,(Bx/10) - 0.95\,(Bx/10)^2 + 0.14\,(Bx/10)^3] \quad (4)$$

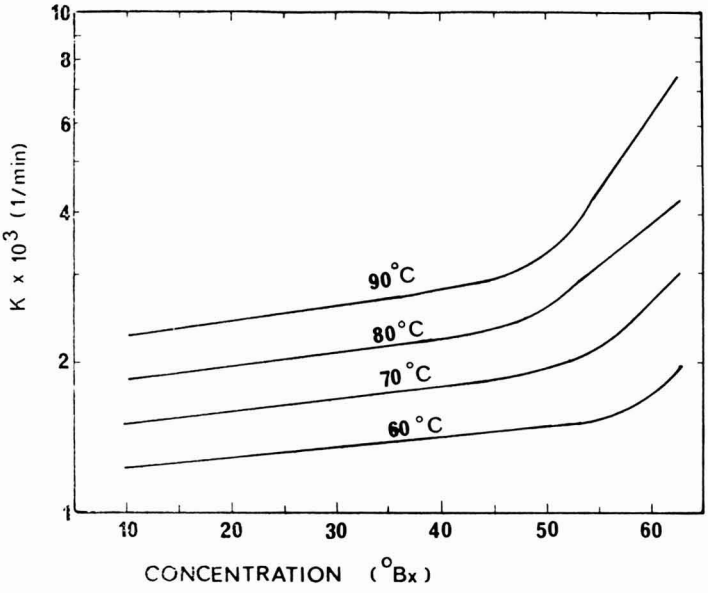

FIG. 3. EFFECT OF SOLIDS CONTENT ON RATE CONSTANT (PREDICTED RESULTS)

Using equations 1, 2, 3 and 4, the ascorbic acid destruction rate as a function of solids concentration was generated (Fig. 3). The figure indicates a sharp increase in the value of the destruction rate coefficient at high solids concentration. The reason for such effect is not clear. It may be attributed to the accelerating effect of fructose (Curl 1947; Heulin 1953) or to the increase in citric acid concentration which is known to have an important role in the nonenzymatic browning (Clegg 1966).

Effect of Ascorbic Acid Initial Concentration

To determine whether the initial concentration of ascorbic acid affects

its rate of destruction or its degradation mechanism, grapefruit juice samples were fortified with 77.7 and 170.0 mg ascorbic acid/100 g juice (corresponding to ascorbic acid content of 32.1 and 57.1 °Bx concentrate) and were heat treated at 95 °C. Results of the ascorbic acid loss (Table 4) show that its initial concentration has no significant effect either on the rate of deterioration or on the mechanism.

Table 4. Effect of initial ascorbic acid concentration in grapefruit juice (11.2 °Bx) treated at 95.0 °C on the vitamin retention

Time	Ascorbic Acid Concentration					
(min)	mg/100 g	%	mg/100 g	%	mg/100 g	%
0	34.8	100.0	34.8+77.7[a]	100.0	34.8+170.0[a]	100.0
10	33.6	96.6	109.2	97.0	198.1	96.7
20	32.7	94.0	106.2	94.4	192.2	93.8
30	32.2	92.5	103.8	92.3	188.1	91.8
40	31.4	90.2	102.2	90.8	185.3	90.5
50	30.6	87.9	99.9	88.3	180.1	87.9

[a]amount of ascorbic acid added to the juice

Effect of Oxygen

The amount of dissolved oxygen in grapefruit juice during the concentration process is obviously low, mainly due to liquid boiling during evaporation. However, even a low concentration of oxygen was found to have a detrimental effect in altering the ascorbic acid deterioration mechanism (Singh *et al.* 1976). In order to determine the effect of the dissolved oxygen on the deterioration rate of grapefruit juice and concentrates (47.1 and 62.5 °Bx), a heat treatment was carried out on de-aerated samples (2 h vacuum followed by nitrogen flushing) with a nitrogen atmosphere maintained in the heat processing unit. The additional treatment to remove oxygen had no effect on the general kinetic mechanism established previously for the ascorbic acid loss thus indicating that destruction of ascorbic acid in grapefruit juice during concentration is dominated mainly by the anaerobic mechanism.

Kinetic/Mathematical Prediction Model

The model used for predicting ascorbic acid loss during thermal concentration embodied the following information:

(1) Ascorbic acid loss follows a first order reaction (Equation 1).
(2) The temperature effect is expressed by the Arrhenius equation.
(3) The effect of solids content on the rate constant is expressed by Equations 3 and 4.

These assumptions lead to the following kinetic equation;

$$\int_{C_o}^{C_t} -\frac{dc}{c} = \int_{t=o}^{t} K_o \exp[-Ea/RT]\, dt \qquad (5)$$

Equation 5 was solved numerically using input data: initial ascorbic acid concentration (C_o); tabulated data of solids content (Bx_t) and temperature T_t as a function of the time, t. A linear interpolation was used to determine the values of temperature and solids content within the range of the tabulated input values. Using very small time intervals (3 s) the intergral was calculated by:

$$\sum_{i=1}^{n} \ln \frac{C_i}{C_i\text{-}1} = \sum_{i=1}^{n} - K_o \exp[E_a i/RT_i]\, \Delta t_i \qquad (6)$$

where:

i = 1,2 . . . . . n; n = number of intervals.

Monitoring a commercial evaporator (Table 1), the measured and predicted concentration (Equation 6) of the ascorbic acid during the evaporation process are shown in Fig. 4. Calculated on a single strength basis, ascorbic acid losses during the commercial process are small (< 1.5%). Such small losses are of no surprise due to the short thermal treatment in modern commercial citrus evaporators. Prediction of ascorbic acid retention was proven also to be successful in a longer thermal treatment such as a "hot pack"-like process (Fig. 5).

CONCLUSIONS

The kinetics of ascorbic acid loss was determined for common conditions of thermal and concentration processes of grapefruit juice. Data were found to follow an apparent first order reaction and Arrhenius equation with concentration dependent parameters. A model combining kinetic data with process variables was devised and proved useful in predicting and optimizing vitamin C retention in any process where grapefruit juice is subjected to any combination of thermal and concentration treatments.

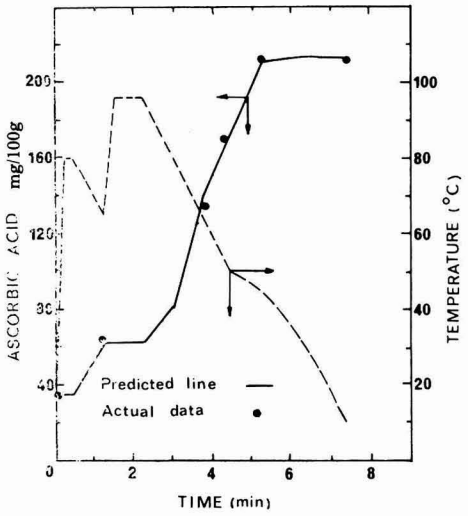

FIG. 4. ACTUAL AND PREDICTED VITAMIN C RETAINED IN AN INDUSTRIAL CONCENTRATION PROCESS

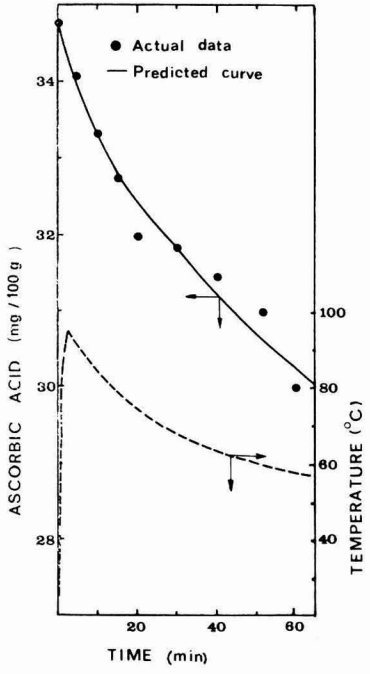

FIG. 5. ACTUAL AND PREDICTED VITAMIN C RETAINED IN AN ALTERATE TEMPERATURE PROCESS OF GRAPEFRUIT JUICE CONCENTRATE (52.6°Bx).

REFERENCES

AOAC, 1970. *Official Methods of Analysis,* 10th Ed., Washington D.C.

BAUERNFEIND, J.C. and PINKERT, D.M. 1970. Food processing with added ascorbic acid. Adv. Food Res. *18,* 219.

BRENNER, S., WODICKA, V.O. and DUNLOP, S.G. 1948. Effect of high temperature storage on the retention of nutrients in canned foods. Food Technol. *2,* 207.

CLEGG, K.M. and MORTON, A.D., 1965. Carbonyl compounds and the nonenzymatic browning of lemon juice. J. Sci. Food Agric. *16,* 191.

CLEGG, K.M., 1966. Citric acid and the browning of solutions containing ascorbic acid. J. Sci. Food Agric. *17,* 546.

CURL, A.L., 1947. Concentrated orange juice storage studies. The effect of degree of concentration and temperature of storage. Canner *105* (13), 14.

CURL, A.L. 1949. Ascorbic acid losses and darkening on storage at 49°C (120°F) Food Res. *14,* 9.

DAVIDEK, J., VALISEK, J. and JANICEK, G. 1974. The stability of vitamin C in orange drink. Lebens — Wiss. u. Technol. *7,* 285.

DIXON, W.J. 1971. *Biomedical Computer Programs,* Univ. of California Press, Berkeley, Calif.

DULKIN, S.I. and FRIEDMAN, J.E. 1956. The role of dehydroascorbic acid and dehydroreductic acid in the browning reaction. Food Res. *21,* 519.

HUELIN, F.E. 1953. Studies on the anaerobic decomposition of ascorbic acid. Food Res. *18,* 633.

HUELIN, F.E., COGGIOLA, I.M., SINDHU, G.S. and KENNETT, B.H. 1971. The anaerobic decomposition of ascorbic acid in the pH range of foods and in more acid solutions. J. Sci. Food Agric. *22,* 540.

JENSEN, A., 1967. Tocopherol content of seaweed and seameal. 3. Influence of processing and storage on the content of tocopherol, carotenoids and ascorbic acid in seaweed meal. J. Sci. Food Agric. *20,* 622.

JOSLYN, M.A. and MARSH, G.L. 1935. Browning of orange juice. Ind. Eng. Chem. *27,* 186.

JOSLYN, M.A. and MILLER, J. 1949. Effects of sugars on oxidation of acid. II. — General and specific effects. Food Res. *14,* 340.

JOSLYN, M.A. 1957. Role of amino acids in the browning of orange juice. Food Res. *22,* 1.

KAREL, M. and NICKERSON, J.T.R. 1964. Effects of relative humidity, air and vacuum on browning of dehydrated orange juice. Food Technol. *18,* 1214.

KURATA, T. and SAKURAI, Y. 1967. Degradation of L-ascorbic acid and mechanism of nonenzymatic browning reaction. a. *ibid* (I) Agric. Biol. Chem. *31,* 101; b. *ibid* (II) Agric. Biol. Chem. *31,* 170; c. *ibid* (III) Agric. Biol. Chem. *31,* 177.

LABUZA, T.P. 1972. Nutrient losses during drying and storage of dehydrated foods. CRC Crit. Rev. in Food Technol. *3,* 217.

LALIKAINEN, T., JOSLYN, M.A. and CHICHESTER, C.O. 1958. Mechanism of browning of ascorbic acid — citric acid — glycine systems. J. Agric. Food Chem. *6,* 135.

LEE, S.H. and LABUZA, T.P. 1975. Destruction of ascorbic acid as a function of water activity. J. Food Sci. *40,* 370.

LEE, Y.C., KIRK, J.R., BEDFORD, C.L. and HELDMAN, D.R. 1977. Kinetics and computer simulation of ascorbic acid stability of tomato juice as a function of temperature, pH and metal catalyst. J. Food Sci. *42,* 640.

NAGY, S. and SMOOT, J.M. 1977. Temperature and storage effects on percent retention and percent U.S. recommended dietary allowance of vitamin C in canned single-strength orange juice. J. Agric. Food Chem. *25,* 135.

RIEMER, J. and KAREL, M. 1977. Shelf life studies of vitamin C during food storage: Prediction of ascorbic acid retention in dehydrated tomato juice. J. Food Proc. Pres. *1,* 293.

SINGH, R.P., HELDMAN, D.R. and KIRK, J.R. 1976. Kinetics of quality degradation: Ascorbic acid, oxidation in infant formula during storage. J. Food Sci. *41,* 304.

TANNENBAUM, S.R. 1976. Vitamins and Minerals. In "*Principles of Food Science,*" Part I — Food Chemistry (O.R. Fennema, ed.). Marcel Dekker, New York.

VOJNOVITCH, C. and PFEIFER, V.F. 1970. Stability of ascorbic acid in blends with wheat flour, CSM and infant cereals. Cereal Sci. Today *15,* (9) 317.

WANNINGER, JR. L.A. 1972. Mathematical model predicts stability of ascorbic acid in food products. Food Tech. *26,* (6), 42.

THE LETHALITY-FOURIER NUMBER METHOD. HEATING RATE VARIATIONS AND LETHALITY CONFIDENCE INTERVALS FOR FORCED-CONVECTION HEATED FOODS IN CONTAINERS

M.K. LENZ

The Pillsbury Company
Minneapolis, Minnesota

and

D.B. LUND

Department of Food Science
University of Wisconsin-Madison
Madison, Wisconsin 53706

Received for Publication December 1, 1978
Accepted for Publication February 9, 1979

ABSTRACT

Heat transfer and lethality in foods heated by force-convection in agitated, reel-type retorts (Steritort) were investigated. Equations describing the temperature profile at any position in the food were developed and experimentally verified for fluids and fluids with particles. For both types of food, the temperature profiles are a function of the heat transfer coefficient (h) at the inside surface of the container (the fluid container interface). For foods with particulate pieces, the temperature profiles, in both the fluid and the particle, are also a function of the heat transfer coefficient (h_p) at the fluid particle interface. Empirical models are presented correlating both heat transfer coefficients (h or h_p) with system parameters.

Equations describing the temperature profile at the coldest point in the food (i.e. the point receiving least lethal treatment) were used in a modified form of the lethality-Fourier number equation (Lenz and Lund 1977a*) to calculate lethality. This method of calculating lethality agreed with lethalities calculated by the Improved General Method.*

*Confidence intervals for lethality for forced-convection heated products were determined using the Monte Carlo procedure described in Lenz and Lund (*1977b*). The* 95% *confidence intervals for the lethality ranged from* 20-60% *of the median value of the lethality depending on process conditions. The fluid/particle interface heat transfer coefficient (h_p) had a significant effect on the lethality distributions.*

Journal of Food Process Engineering 2 (1978) 227—271.

INTRODUCTION

Most investigations in the area of thermal processing concentrate on calculating lethality as a function of system parameters (heating time, heating temperature, initial product temperature, cooling temperature) and biological parameters (product heating rate, microorganism destruction rate). In general, these investigations do not consider the effect of variations in system and/or biological parameters on the lethality (Lenz and Lund 1977a). These variations in system and/or biological parameters result in a distribution of lethalities for any real situation. If the distribution or confidence interval of the lethality could be calculated, this could form the basis for designing safety factors for thermal processes (Lenz and Lund 1977b). Safety factors, such as increased processing time, are added to the median process time to account for the distribution of lethality due to system and biological parameter variations in a real situation. This study was designed to calculate lethality confidence intervals from known variations in system or biological parameters. Knowledge of these confidence intervals could lead to design of processes which include safety factors that minimize the deleterious effects of overprocessing on food quality (color, flavor, texture, nutrition) and yet maintain public health safety.

In two earlier papers (Lenz and Lund 1977a, b), a procedure was developed to estimate the confidence interval for calculated lethality of conduction-heated, thermally-processed food. To augment this earlier work on conduction-heated food, this study was designed to investigate the confidence intervals for calculated lethality of convection-heated products. The investigation was limited to forced-convection heating products processed in agitated retorts because this situation is representative of a large class in the total volume of food preserved by canning. These products are typified as pure fluids (e.g. juice) or fluids with solid particles suspended in the fluid (e.g. peas in brine). To limit the scope of this study, only spherical particles were considered.

The procedure developed by Lenz and Lund (1977a,b) to calculate lethality confidence intervals involved four steps. First, variations in heating rates and microorganism destruction rates are estimated using experimental data. Next, equations for both heating rates and microorganism destruction rates are developed and/or experimentally verified as statistically adequate models. Then, these equations for heating rates and microorganism destruction rates are combined to develop an equation for calculating lethality. Finally, the variances in heating rates and microorganism destruction rates were used to estimate lethality confidence intervals. This procedure involves combining Monte Carlo procedures with a lethality calculation method as shown in Lenz and Lund (1977b).

This procedure only estimates the effects of variations in the biological parameters on the lethality confidence interval (Lenz and Lund 1977b). If the effects of variations in system parameters on lethality confidence intervals are desired, the suggestions in Lenz and Lund (1977b) for exploring these variations also applies to this study.

Variation in Biological Parameters

It was assumed that the model for microorganism destruction rates and the variation of these rates are not affected by the mode of product heating (i.e. conduction versus convection). Therefore, the model and variation of these rates given in Lenz and Lund (1977a,b) apply in this case. The Arrhenius equation was found to be an adequate model. The standard deviation of the logarithm of microorganism destruction rates (i.e. D-value or rate constant (k)) was 0.10 (Lenz and Lund 1977b).

Variation in Heating Rates

Hicks (1961) states that the standard deviations (σ) for the heating rates of forced-convection heated foods are greater than the standard deviations for the rates of conduction-heated foods. The heating rates of conduction-heated foods have a σ of $\pm$ 4% of the value of the rate (Hicks 1961; Lenz and Lund 1977a). In contrast, for forced-convection heated foods σ is $\pm$ 5—10% of the value of the rate (Hicks 1961; Bird *et al.* 1960).

Models for the heating rates or temperature profiles for convection-heating product characterized as a fluid or a fluid containing suspended spherical particles can be derived by solving the energy balance equations for forced-convection heating given in Bird *et al.* (1960). These equations account for the accumulation of energy in the product (i.e. temperature increase in the product) as affected by the rate at which energy is added to the product. For forced-convection heating, the rate of energy addition to the product is described by the resistance to heat transfer (i.e. heat transfer coefficient at the container surface (h)) and the driving force (i.e. retort temperature (T_s) minus temperature of the product at the container surface).

For pure fluids, the energy balance becomes quite simple if all the fluid is assumed to be at one temperature (i.e. no temperature gradients in the fluid). Using this assumption, Charm (1971) gives an equation for a fluid heated by a constant temperature heating medium (T_s). This equation shows that the temperature of the fluid in the container asymptotically approaches the retort temperature (T_s) as time progresses. Charm (1971) does not mention the limitations of the "constant fluid temperature" assumption.

For fluids with particles, the energy balance involves both the fluid and particle temperatures. In order to solve this equation, a relation between the fluid and particle temperature profiles is needed. de Ruyter and Brunet (1973) derived an equation by assuming the particles heat by conduction, the fluid is all at one temperature (i.e. no gradients) and the fluid and particle surface are at the same temperature (i.e. no resistance to heat transfer at the particle surface). de Ruyter and Brunet (1973) do not mention the limitations of the assumptions used.

Model for Calculating Lethality

Once equations (that adequately model experimental data) for the temperature profiles in the products have been developed, the temperature profile and microorganism destruction models can be combined to calculate lethality. A rationale for developing a method for calculating lethality is given in Lenz and Lund (1977a). Basically this procedure involves developing equations for dimensionless lethality (lethality number) as a function of dimensionless time (Fourier number). Since there is no true Fourier number for forced-convection heating (i.e. no thermal diffusivity), the final equations for dimensionless lethality (L) and dimensionless time ($\tau_f t$) will be different than those developed previously. As with the lethality-Fourier number (L-τ) method described in Lenz and Lund (1977a), the final equation is numerically integrated to give charts of L versus $\tau_f t$ which are used to calculate lethality.

Variability in Lethality

Finally, this lethality calculation method is used with the Monte Carlo procedure outlined in Lenz and Lund (1977b) to estimate the lethality confidence interval. This procedure involves calculating the distribution of lethalities obtained for a given process time and constant system parameters when the variability in the biological parameters are considered. For each calculation, the values of the biological parameters are chosen at random from the known distributions for these parameters. For this study, the biological parameters were the fluid and particle heating rate time constants (τ_f, τ_p), the microorganism destruction rate activation energy (E_a) and the fluid/particle surface dimensionless resistance (Biot number, Bi). One hundred calculated lethalities were used to define the distribution.

THEORY

Heating Rate Modulus

Convection-heating products can be characterized as either a fluid or a fluid with suspended spherical particles. In both cases, it was assumed that the main mode of heating in agitated retorts was forced-convection. This assumption was verified experimentally. Using the basic equations for forced-convection heat transfer (Bird *et al.* 1960), temperature profiles for these products during both the heating and cooling portions of a thermal process were derived.

For fluids, the time-temperature profile is derived by solving the unsteady-state heat balance for a container in which there are no thermal gradients (Bird *et al.* 1960):

$$\rho_d C_p V \frac{dT}{dt} = h A (T_h - T) \quad (1)$$

with the boundary condition at $t = O$, $T = T_i$
where

T = temperature of the product
T_i = initial temperature of the product
T_h = temperature of the heating medium
ρ_d = density of the product
C_p = heat capacity of the product
V = volume of the product
h = heat transfer coefficient between the surface of the container and the product
A = area of the container
t = heating time

If the retort temperature (T_h) is constant (T_s), Equation (1) is easily solved using Laplace transforms (Charm 1971) to give:

$$T = T_s - (T_s - T_i) \exp(-\tau_f t) \quad (2)$$

where $\tau_f = h A/\rho_d C_p V$ = fluid time constant

If the retort exhibits a thermal lag during heat up, the temperature can be described by the analogous equation:

$$T_h = T_s - (T_s - T_{si}) \exp(-\tau_s t) \quad (3)$$

where

T_s = ultimate steam temperature
T_{si} = initial retort temperature
τ_s = retort time constant.

Under these conditions, Equation (1) is solved using Laplace transforms to give:

$$T = T_i + (T_s - T_i)(1 - \exp(-\tau_f t)) + (T_s - T_{si})\left(\frac{\tau_f}{\tau_f - \tau_s}\right)(\exp(-\tau_f t)) \quad (4)$$

Equation (1) can also be solved numerically using a 4th-order Runge Kutta procedure (Conte and de Boor 1972). If increments in $\tau_f t$ of 0.3 or less are used, the predicted temperatures coverage within 0.1 °F of the predicted temperatures using smaller intervals. The temperatures predicted by Equations 2 and 4 can also be calculated within 0.1 °F using this interval size. Considering typical food processing conditions, this increment size is equivalent to 30 sec time intervals for 608 × 700 cans and 15 sec time intervals for 303 × 406 cans.

Equations (3) and (4) were developed specifically for this study. In commercial practice, the retort would be at a constant temperature (T_s). However, the simulated agitated retort (Steritort) used in this study experienced a thermal lag. Equation 3 was found to be an adequate model for describing the retort temperature for these circumstances.

The equation for cooling a fluid is easily obtained since cooling can also be described by Equation 1. For cooling, T_w, the cooling water temperature, is substituted for T_h and T_i is the temperature of the fluid at the end of the heating period. Similarly, Equation 2 can be used to calculate the cooling temperature profile if T_w is substituted for T_s and T_i is the temperature of the fluid after heating.

For products characterized as fluid with suspended food particles and assuming there are no thermal gradients in the fluid, the energy balance for the container is (Bird *et al.* 1960):

$$\epsilon(\rho_d C_p)_f V\frac{dT_f}{dt} + (1-\epsilon) V (\rho_d C_p)_p \frac{d\overline{T}_p}{dt} = h A (T_h - T_f) \quad (5)$$

where

$_f$ refers to fluid phase
$_p$ refers to particle phase, respectively
V = volume of the container
ϵ = fraction of the container occupied by the fluid and
$\overline{T}_p$ = average temperature of the particle

The other symbols are as previously described.

In order to solve Equation 5, a functional relationship between fluid temperature (T_f) and average particle temperature ($\overline{T}_p$) is required. This equation can be derived when the following assumptions are made: (1) the particles are spherical and heat strictly by conduction, (2) the particle has a constant initial temperature (T_i), and (3) the fluid temperature (T_f) and particle surface temperature (T_{ps}) can be interrelated by Newton's law of cooling (Bird *et al.* 1960). With these assumptions, a procedure analogous to that used by de Ruyter and Brunet (1973) can be used to relate $\overline{T}_p$ to T_f. The equations developed by de Ruyter and Brunet (1973) can not be used since they ignore the resistance to heat transfer between the fluid and the particle. Under these circumstances, a temperature profile between the bulk fluid and the particle center would be similar to that diagramed in Case A, Fig. 1. In this study it was assumed that there is a finite surface heat transfer coefficient at the fluid/particle interface. This results in a temperature profile characterized by Case B, Fig. 1.

The procedure used to relate $\overline{T}_p$ and T_f consisted of correcting the solution to the unsteady-state heat balance given by Carslaw and Jaeger (1959) for the assumption of a finite surface heat transfer coefficient. Since this solution is for a particle heated by a medium at constant temperature, Duhamel's Theorem (Carslaw and Jaeger 1959) is used to give a solution for a particle heated by a medium (i.e. the fluid with a temperature that changes with time.)

The final equation is:

$$T_p - T_i = \frac{2\alpha\,Bi}{R_p^2\,\rho_p} \sum_{n=1}^{\infty} \left(\frac{\beta_n^2+(Bi-1)^2}{\beta_n^2+Bi(Bi-1)} \right) \sin\beta_n \sin\beta_n \rho_p$$

$$\exp\left(\frac{-\alpha\beta_n^2 t}{R_p^2}\right) \int_0^t \phi(\lambda) \exp\left(\frac{\alpha\beta_n^2 \lambda}{R_p^2}\right) d\lambda \qquad (6)$$

where

β = are the roots of: $\beta \cot \beta + Bi - 1 = 0$ and
α = thermal diffusivity of the particle
R_p = radius of the particle
Bi = Biot number of the particle $R_p h_p / k_p$
h_p = heat transfer coefficient between heating medium and particle surface
k_p = thermal conductivity of the particle
ρ_p = dimensionless radial position (r/R_p)
r = radial position in particle
$\phi(\lambda)$ = Equation (4) or a similar fluid temperature model

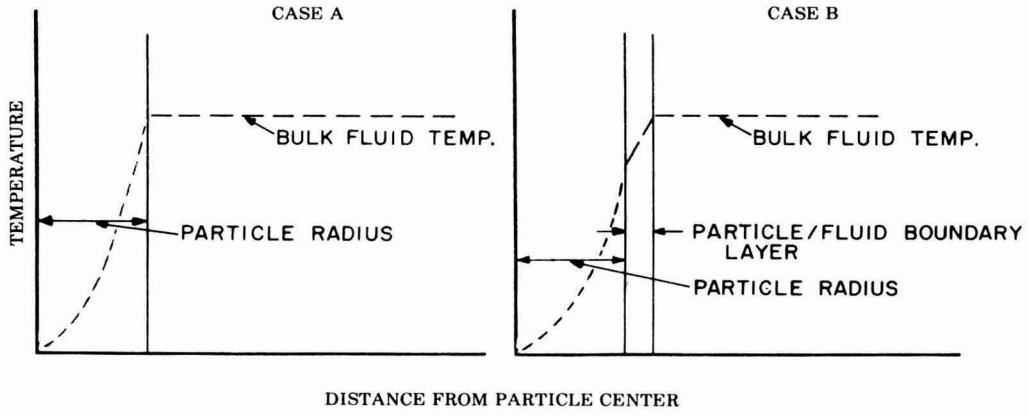

FIG. 1. TEMPERATURE PROFILE FROM PARTICLE CENTER TO BULK FLUID FOR THE SITUATIONS IN WHICH NO RESISTANCE TO HEAT TRANSFER AT THE SURFACE EXISTS (CASE A) AND THE SITUATION IN WHICH A RESISTANCE TO HEAT TRANSFER BETWEEN THE FLUID AND PARTICLE EXISTS (CASE B)

Using Equation 4, the integral in Equation 6 becomes:

$$\int_o^t (1-\exp(-\tau_f\lambda) + \delta \left(\frac{\tau_s}{\tau_f-\tau_s}\right) (\exp(-\tau_f\lambda) - \exp(-\tau_s\lambda))\exp(\tau_p\lambda)\, d\lambda$$

where $$\delta = \frac{T_s - T_{si}}{T_s - T_i}$$

and $$\tau_p = \frac{\alpha\beta^2}{R_p^2}$$

Evaluating this integral, the solution for the temperature at any position in the particle (ρ_p) versus time is:

$$\frac{T_s - T_p}{T_s - T_i} = \frac{2\,Bi}{\rho_p} \sum_{n=1}^{\infty} \left(\frac{\beta_n^2 + (Bi-1)^2}{\beta_n^2 + Bi\,(Bi-1)}\right) \frac{\sin\beta_n}{\beta_n^2} \sin\,\beta_n\,\rho_p$$

$$\left[\exp(-\tau_p t) + \left(\frac{\tau_{s+(\delta-1)\tau_f}}{\tau_s-\tau_f}\right)\left(\frac{\tau_p}{\tau_p-\tau_f}\right) \{\exp(-\tau_f t) - \exp(-\tau_p t)\}\right. \qquad (7)$$

$$\left. - \left(\frac{\delta\,\tau_f}{\tau_s-\tau_f}\right)\left(\frac{\tau_p}{\tau_p-\tau_s}\right) \{\exp(-\tau_s t) - \exp(-\tau_p t)\}\right]$$

The average temperature is obtained from Equation (7) by evaluating the integral:

$$\frac{T_s - \overline{T}_p}{T_s - T_i} = \frac{\int_V (T_s - T_p)\, dV}{\int_V dV} = \frac{\int_o^1 (T_s - T_p)\, \rho_p^2\, d\rho_p}{\int_o^1 \rho_p^2\, d\rho_p} \qquad (8)$$

$$= 6\,Bi^2 \sum_{n=1}^{\infty} \frac{\sin^2\beta_n}{\beta_n^4} \left(\frac{\beta_n^2 + (Bi-1)^2}{\beta_n^2 + Bi(Bi-1)}\right) \left\{\begin{array}{l}\text{same series of exponential}\\ \text{terms as those in brackets}\\ \text{in Equation (7).}\end{array}\right\}$$

The infinite series solutions given by Equations 7 and 8 converge very slowly. Therefore, an approximation was used to calculate the summations.

To establish this approximation, it was first noted that the terms:

$$6\,\mathrm{Bi}^2 \sum_{n=1}^{\infty} \frac{\sin^2 \beta_n}{\beta_n^4} \left(\frac{\beta_n^2 + (\mathrm{Bi}-1)^2}{\beta_n^2 + \mathrm{Bi}(\mathrm{Bi}-1)} \right)$$

and

$$\frac{2\,\mathrm{Bi}}{\rho_p} \sum_{n=1}^{\infty} \frac{\sin \beta_n}{\beta_n^4} \left(\frac{\beta_n^2 + (\mathrm{Bi}-1)^2}{\beta_n^2 + \mathrm{Bi}(\mathrm{Bi}-1)} \right)$$

are both Fourier series which are identically equal to 1 (Carslaw and Jaeger 1959). Secondly, M is defined as the value of n for which $(\tau_p(\tau_p - \tau_s) - 1)$ or $(\tau_p/(\tau_p - \tau_f) - 1)$ are ≤ 0.01. This occurs when $\tau_p \gg \tau_f$ or τ_s.

Using these definitions, the final terms for the summations in Equations (7) or (8) can be approximated. The equation for $\overline{T}_p$ becomes:

$$\frac{T_s - \overline{T}_p}{T_s - T_i} = 6\,\mathrm{Bi}^2 \sum_{n=1}^{M} \frac{\sin^2 \beta_n}{\beta_n^4} \left(\frac{\beta_n^2 + (\mathrm{Bi}-1)^2}{\beta_n^2 + \mathrm{Bi}(\mathrm{Bi}-1)} \right) \left\{ \begin{array}{l} \text{same series of exponential terms as those in brackets in Equation (7).} \end{array} \right\}$$

$$+ \left[1 - 6\,\mathrm{Bi}^2 \sum_{n=1}^{M} \frac{\sin^2 \beta_n}{\beta_n^4} \left(\frac{\beta_n^2 + (\mathrm{Bi}-1)^2}{\beta_n^2 + \mathrm{Bi}(\mathrm{Bi}-1)} \right) \right] \left[\left\{ \left(\frac{\tau_s + (\delta - 1)\tau_f}{\tau_s - \tau_f} \right) \exp(-\tau_f t) \right\} - \left(\frac{\delta\,\tau_f}{\tau_s - \tau_f} \right) \exp(-\tau_s t) \right] \quad (9)$$

This approximation is accurate to within 0.1 °F of the solution when the summation is completed. However, the approximation converges in 10-20 terms whereas the solution as written in Equations 7 and 8 require 100-200 terms to converge.

Using Equation 9, Equation 5 was solved for T_f. A 4th-order Runge Kutta procedure (Conte and de Boor 1972) was used to solve Equation 5. The stepsizes used in this method were identical to those used in solving Equation 1 (i.e. 15 sec for 303 × 406 containers and 30 sec for 608 × 700 containers).

To calculate the derivative of the average particle temperature needed in Equation 5, a centered-difference approximation was used:

$$\frac{d\,\overline{T}_p}{dt} = \frac{\overline{T}_p\ (t + d/2) - \overline{T}_p\ (t - d/2)}{d}$$

where d is the time interval in the numerical method.

The approximation was used rather than an analytical solution for d $\overline{T}_p$ dt because it was less sensitive to minor variations in τ_s, τ_f, δ and Bi.

The equation for the cooling of a spherical particle is obtained in much the same way Equation 7 was obtained. However, for cooling, the initial temperature is not constant but is equal to the temperature gradient that exists at the end of heating. Again, a solution is given in Carslaw and Jaeger (1959) for this situation if the cooling medium temperature is constant. Duhamel's theorem (Carslaw and Jaeger 1959) is used to correct this solution for the fact that the fluid temperature changes with time. The final solution for the cooling temperature profile at any position (ρ_p) of a spherical particle is:

$$T_p - T_w = \frac{2\,Bi}{\rho_p} \sum_{n=1}^{\infty} \left[\exp(-\tau_p t) + \left(\frac{\tau_p}{\tau_p - \tau_f}\right) \left\{ \exp(-\tau_f t) - \exp(-\tau_p t) \right\} \right]$$

$$\left[\left(\frac{\beta_n^2 + (Bi-1)^2}{\beta_n^2 + Bi(Bi-1)} \right) \frac{\sin \beta_n \sin \beta_n \rho_p}{\beta_n^2} \right] \left[\delta_1 - \left(\frac{\beta_n^2 + (Bi-1)^2}{\beta_n^2 + Bi(Bi-1)} \right) \right.$$

$$\left(1 + \frac{(Bi-1)\sin^2 \beta_n}{\beta_n^2} \right) \left(\exp(-\tau_p\ t_h) + \left(\frac{\tau_p}{\tau_p - \tau_f}\right) \left\{ \exp(-\tau_f\ t_h) \right. \right.$$

$$\left. \left. \left. - \exp(-\tau_p\ t_h) \right\} \right) \right] \qquad (10)$$

where $$\delta_1 = \frac{T_s - T_w}{T_s - T_i}$$

and t_h = heating time

The initial temperature profile used in this derivation was Equation 7 corrected for τ_s equal to infinity (i.e. the retort is instantly at its ultimate temperature). For this correction, everything remains the same in Equation 7 except the series of exponential terms in brackets which become:

$$\exp(-\tau_p t) + \left(\frac{\tau_p}{\tau_p - \tau_f}\right)\left\{\exp(-\tau_f t) - \exp(-\tau_p t)\right\} \qquad (11)$$

The correction shown in Equation 11 can also be used in other situations where the retort "come-up" time is zero. This, of course, is the usual case for commercial operations where the retort is always at a constant temperature (T_s).

EXPERIMENTAL

The strategy for this study was to: (1) establish the errors in heating rates or temperature profiles for these types of products, (2) develop equations based on heat transfer principles for temperature profiles and statistically verify that these are adequate models, and (3) use the models for predicting temperature profiles to calculate lethality and lethality confidence intervals. The types of products which exhibit forced convection-heating were characterized as a fluid and a fluid with suspended spherical particles.

To establish the variation or standard deviation within fluid temperature profiles for these type of products, the range between fluid temperatures at the center of three containers of identical product were measured at appropriate time intervals for a variety of process conditions. The ranges were measured at 15-sec time intervals for 303 × 406 containers and 30-sec intervals for 608 × 700 containers. The various processing conditions investigated were: (1) container size (303 × 406; 608 × 700), (2) fluid viscosity (distilled water, μ 40°C = 21 cp), (3) presence or absence of 0.95 cm (3/8 in.) diameter spherical particles (peas; $\varepsilon = 0.32$), and (4) reel speed (ω = 2, 3.5 or 4 rpm). All experiments were conducted using an agitated retort simulator (FMC Steritort). A steam temperature of 121°C (250°F) and an initial product temperature of approximately 27°C (80°F) were used for these triplicate trials. All tempera-

tures were recorded on a recording potentiometer (Leeds and Northrup Company, North Wales, PA). This potentiometer was periodically calibrated against a standard thermometer and a manually-operated potentiometer.

The measured ranges between triplicate temperatures at selected times were used to estimate the standard deviation (σ) of the heat penetration curves. This was accomplished using the following formula given by Guttman *et al.* (1971):

$$\sigma = \text{Cn} \times \text{range}$$

For n = 3, Cn is 0.6.

Heating times for all heat penetration experiments in this paper were selected such that at the end of heating, the product temperature would be within 6—11 °C (10—20 °F) of retort temperature. These times were chosen so that only the effect of biological variability on heating curves was measured (Lenz and Lund 1977a). At temperature differences less than 6 °C, recorder error can be significant.

To determine if there are temperature gradients in the fluid in the container during heating, thermocouples were placed at various positions in both 608 × 700 and 303 × 406 containers. The product was either water or 60% (w/w) aqueous sucrose solution or one of these fluids with 0.95 cm (3/8 in.) diameter peas ($\varepsilon = 0.32$). The thermocouple locations are given in Table 3. Experiments were conducted in an agitated retort (FMC Steritort) at a steam temperature of 121 °C (250 °F), initial temperature of 27 °C (80 °F) and reel rotation speeds of 3.5 and 8 rpm.

To test the adequacy of Equation 1 or its solutions, Equations 2 and 4, as models for the temperature profiles of forced-convection heating fluids during thermal processing, experimental and theoretical heat penetration curves for a wide variety of processing conditions were compared. Variables were container size (303 × 406 or 608 × 700), fluid viscosity (distilled water or 60% (w/w) aqueous solution of sucrose), steam temperature (110 °C (230 °F) or 121 °C (250 °F)) and reel speed (2, 3.5 or 8 rpm). All experiments were conducted in an FMC Steritort.

For each experiment, the value of the heat transfer coefficient (h) was determined using a least squares procedure (Seinfeld and Lapidus 1974) by selecting, through a computer program, the heat transfer coefficient which minimized the sum of the square of the deviations between the actual temperature and the temperature predicted by Equation 1. This is illustrated in Fig. 2. To eliminate the effect of a variable retort temperature (e.g. in our simulator, the retort temperature rises exponentially from an initial temperature (T_{si}) to the steam temperature (T_s)), Equation 1 was

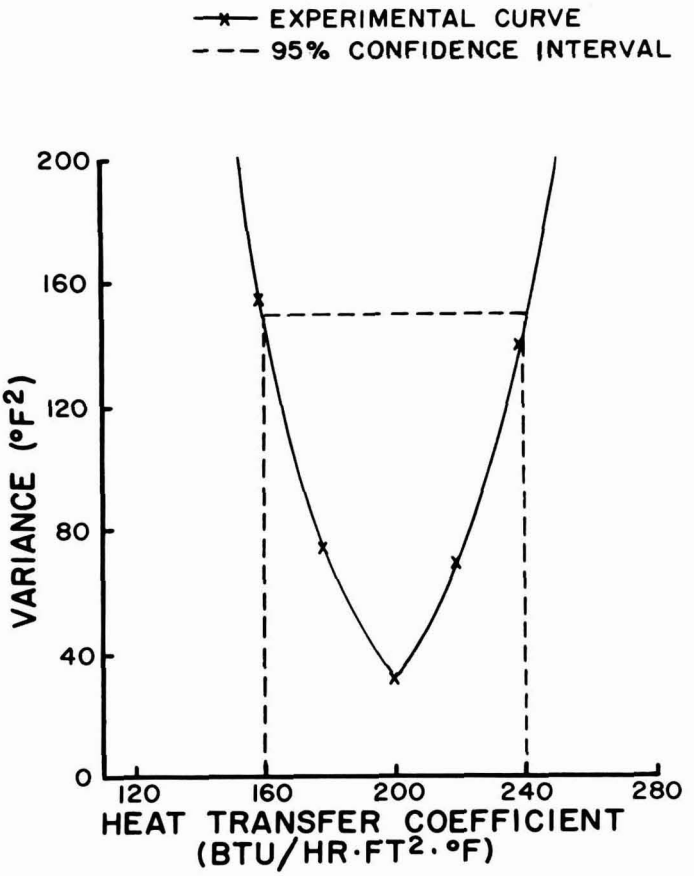

FIG. 2. VARIANCE VERSUS HEAT TRANSFER COEFFICIENT FOR DETERMINING LEAST SQUARES VALUE OF h

solved numerically using a 4th-order Runge Kutta procedure (Conte and de Boor 1972) to predict fluid temperature (T_f). Actual values of retort temperature (T_h), measured by a copper/constantan thermocouple in the retort, were used to predict T_f. Time intervals of 15 sec for 303 × 406 containers and 30 sec for 608 × 700 containers were used for the Runge Kutta method. Smaller intervals produced identical results (i.e. values of T_f) as these intervals. Experimental values of T_f were measured using a shielded copper/constantan thermocouple (Ecklund Thermocouple) mounted in the center of the container by means of a locking receptacle (Ecklund Thermocouple, Cape Coral, Fla.). The minimum sum of the square of the deviations (SSD) of the experimental minus theoretical

values of T_f was used to estimate the variance (σ^2) (Guttman *et al.* 1971). This estimate of σ^2 was compared to the variance between replicate trials to assess the adequacy of Equation 1 as a model.

It should be noted that the 95% confidence interval of h can be estimated from the SSD versus h plots for obtaining the least square value of h (Fig. 2). The values of h at four times the minimum SSD are estimates of the extreme values of the 95% confidence interval (Seinfeld and Lapidus 1974).

The next objective in our study was to test the adequacy of Equation 5 as a model for the fluid temperature in a system containing spherical particles suspended in a fluid. Equation 5 is somewhat confounded, since it interrelates three temperatures (T_f, T_h and $\overline{T}_p$). However, since T_f and $\overline{T}_p$ can be related by the use of Equation 8, experimental values of T_h can be used to predict the values of T_f as was done in verifying Equation 1. These predicted values of T_f are compared to experimental values to verify Equation 5.

In order to use the interrelation between fluid (T_f) and average particle ($\overline{T}_p$) temperatures given by Equation 8, the heat transfer coefficient (h_p) between fluid and particle has to be known. Since values for h_p were unknown, a set of experiments were designed to measure h_p under a wide variety of processing conditions.

The procedure used to measure the fluid-particle interface heat transfer coefficient consisted of measuring the fluid (T_f) and particle surface (T_{ps}) temperatures and calculating the heat transfer coefficient from these measurements using Newton's law of cooling (Bird *et al.* 1960). To measure the surface temperature of the particle, spherical particles were made from a material whose thermal conductivity was very large compared to the anticipated surface heat transfer coefficient. Under these conditions it could be assumed that thermal gradients did not exist in the particle. In other words, all points in the particle are assumed to be at one temperature, the surface temperature. Lead which has a large thermal diffusivity (α = 14.6 cm^2/min (2.26 in.^{2}/min) Perry (1963) was selected as the material to test. To determine if the temperature in a lead sphere is uniform and equal to the surface temperature during heating under our conditions, surface and center temperatures were calculated for representative process conditions using Equation 7. The process conditions used were Biot numbers (Bi) of 2, 10 and 20 and the respective values of β_n at these values of Bi, τ_f of 0.9 min^{-1}, τ_s of 0.2 min^{-1}, T_s = 121 °C (250 F), T_i = 27 °C (80 F), δ of 0.75 and α_{lead} as given earlier. The values of τ_f, τ_s and δ were typical of those experienced in verifying Equation 1. The surface and center temperatures were compared at 15-sec intervals for times long enough to bring the temperatures to 116 °C (240 °F). Temperatures were

compared for three sizes of spheres (i.e. diameters of 0.95 cm (3/8 in.), 2.1 cm (13/16) in. and 3 cm (19/16 in.)). For the 2 smaller sizes, the temperatures were less than 0.5 °C (1 °F) apart and usually 0.1—0.3 °C (0.2—0.5 °F) apart over the whole temperature range. For the largest sphere, the temperatures were 1 °C (2 °F) apart at the lower temperatures (i.e. 27—66 °C) and 0.5 °C (1 °F) or less apart at the higher temperatures. Since the temperature gradients were within the limits of measurement error, it was assumed that the lead spheres equilibrated to one temperature at all points and that a thermocouple could be placed anywhere in the particle to measure surface temperature. The procedure to measure the heat transfer coefficient (h_p) between the fluid and the spherical particle then consisted of measuring the fluid (T_f) and particle surface (T_{ps}) temperatures and relating these to h_p. The equation which relates these temperatures to the heat transfer coefficient (h_p) is:

$$(\rho_d \; C_p)_p \; V_p \frac{d \; T_{ps}}{dt} = h_p \; A_p \; (T_f - T_{ps}) \qquad (12)$$

where

V_p = volume of the spherical particle
A_p = surface area of the spherical particle
T_{ps} = temperature of the surface of the particle

and the other symbols are as previously defined. To calculate the value of h_p which relates a series of T_{ps} and T_f data, a range of values of h_p are chosen and Equation 12 is solved numerically for the values of T_{ps} given the values of T_f. The calculated values of T_{ps} are then compared to the experimentally measured surface particle temperatures and the value of h_p is found which minimizes the sum of the square of the differences (SSD) between T_{ps} (measured) and T_{ps} (predicted). (Fig. 2). An estimate of the standard deviation (σ) of h_p is obtained by comparing h_p at SSD (minimum) and h_p at SSD (four times minimum) as mentioned previously (Seinfeld and Lapidus 1974). This is also illustrated in Fig. 2. Equation 12 was solved numerically using a 4th-order Runge Kutta procedure (Conte and de Boor 1972) with a time interval of 10 sec for 303 × 406 cans and 20 sec for 608 × 700 cans. These time intervals were found to be as accurate as smaller intervals for predicting T_{ps}. The computer program and original data used to find the value of h_p which relates a given set of T_{ps} and T_f data are available in Lenz (1977).

As noted earlier, three sizes of lead spheres with thermocouples imbedded inside were used to measure T_{ps}. The diameters of these spheres were 0.95, 2.1 and 3 cm. To make these spheres a thermocouple was inserted

into molten lead and was intimately imbedded into the lead after the lead solidified. The thermocouple wire was 32 gauge copper/constantan and the thermocouple tip was sealed in a 0.95 cm (3/8 in.) piece of stainless steel tubing with epoxy. The thermocouple bead extended approximately one quarter of the diameter of the lead sphere onto the end of the tube so that by inserting the bead to the center of the lead ball, the lead would also surround some of the tubing. This was done to lend support to the setup.

The 0.95 cm diameter spheres were purchased from a gun shop (i.e. lead shot). A hole in the sphere was formed by melting the lead with a pen soldering iron and the thermocouple bead and tubing were inserted into about the center of the sphere. The larger lead spheres were made by making plaster of paris molds of the desired diameter, melting chemically pure lead and pouring the lead slowly (i.e. pour lead over 30 sec interval to allow air to escape) into the mold with the thermocouple and tubing in place. Upon cooling, the mold was separated from the sphere, any large overflows were trimmed off with a knife and the surface was polished with a buffing wheel. This lead sphere was then used in the apparatus shown in Fig. 3. This apparatus was designed to accommodate the rotating contacts (Ecklund, Coral Gables, Fla.) normally used to measure temperatures in agitated retorts (FMC Steritort).

Two procedures were used to ensure that intimate contact between the lead and thermocouple bead had been achieved (i.e. no extra resistance at this interface). First, the resistances between the end of either the copper or constantan wires (i.e. the end inserted into part 2 in Fig. 3) and the lead sphere were measured. These were identical to either copper or constantan wires of equivalent length. Secondly, the time to heat the lead spheres from 100°F to 212°F with steam was measured. This was compared to the theoretical time (i.e. the time to achieve a Fourier number (τ_p) of 1; Carslaw and Jaeger (1959). The measured times compared within 10% of the calculated times of 1 sec (0.95 cm sphere), 5 sec (2.1 cm sphere) and 9 sec (3 cm sphere).

Figure 3 shows the apparatus used to measure T_{ps} with the lead spheres. The fluid temperatures (T_f) were measured in another container with the setup previously described for measuring T_f in fluids without particles. The apparatus for measuring T_{ps} was designed so that the male prongs from the rotating connector for agitated retorts (Ecklund) would insert into the female receptacles of part 2. Part 2 (i.e. threaded end of a flexible thermocouple; Ecklund-type) allowed the wires from the thermocouple bead imbedded in the lead spheres to be soldered or unsoldered from it easily. Part 2 was threaded into a locking receptacle (part 1). An empty container (part 4) was used to hold parts 1 and 2 in place and was

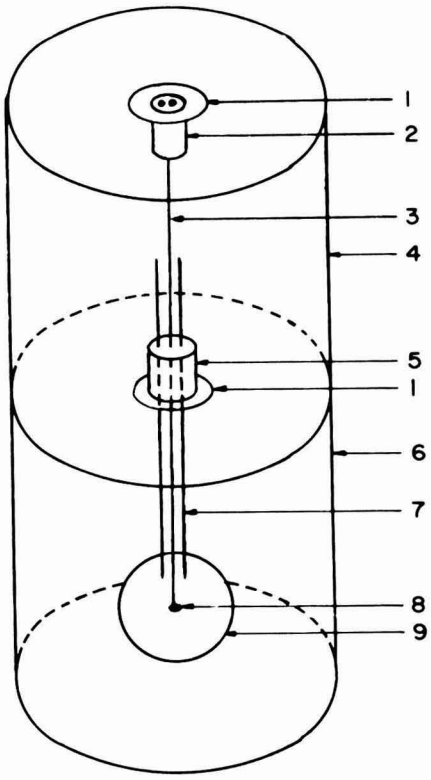

FIG. 3. EXPERIMENTAL SETUP USED TO DETERMINE HEAT TRANSFER COEFFICIENTS AT THE FLUID/PARTICLE INTERFACE

Parts as numbered are: (1) locking receptacle, (2) receptacle for the wires of a flexible thermocouple (3), (3) 32 gauge copper/constantan thermocouple wires which are sealed in (8), epoxied in (7) and soldered in (2), (4) empty 303 × 406 can with 1/2" diameter hole in bottom, (5) 3/8" compression fitting with appropriate gaskets, (6) 303 × 406 test container which is taped to (4), (7) 3/8" stainless steel tubing, (8) thermocouple bead, and (9) lead ball.

connected to the test container (part 6) with a water-resistant tape. The lead spheres were held in place in the test container by means of stainless steel tubing (part 7) and a compression fitting (part 5) threaded into a

locking receptacle (part 1). This setup was quite sturdy and survived the strenuous conditions of agitation and immersion in both steam and water with minimal mechanical or electrical failures.

The lead spheres were used to measure heat transfer coefficients (h_p) under a variety of conditions. For each of the 3 spheres, the conditions used were: (1) 2 can sizes (303 × 406 or 608 × 700), (2) 2 fluids (water or 60% (w/w) sucrose solution), (3) fluid alone or fluid with particles of the diameter of the lead ball, (4) 3 reel speeds (3.5, 6 and 8 rpm), and (5) 3 retort temperatures (110 °C, 121 °C and 132 °C). The particles used were peas for the 0.95 cm ball, carrots pared into 2.1 cm spheres and radishes pared down as needed for the 3 cm spheres.

The following thermal properties of lead given by Perry (1963) were used in calculating h_p from Equation 10: ρ_d = 11.35 g/cm^3 (0.41 lb/in.^{3}), Cp = 0.03 cal/g °C (0.03 BTU/lb · °F) and kp = 0.0827 cal/sec cm °C (20 BTU/hr ft °F).

The next step was to qualitatively check the accuracy of Equation 7. This was done by measuring the temperature profiles at the center of a plastic sphere undergoing various processes. A 2.1 cm diameter plastic sphere was molded similarly to the lead spheres with a thermocouple at the center. The plastic was an epoxy which was resistant to steam temperatures of 121 °C or less. The exact location of the thermocouple bead was found by cutting the sphere in half after the tests were run. The thermal diffusivity (α) of the plastic spheres was calculated by measuring the temperature profile of the sphere when exposed to 100 °C steam. From this profile, the plastic sphere exhibited an f-value (Stumbo 1973) of 5 min which corresponded a thermal diffusivity (α) of 0.06 cm^2/min (0.0095 in.^{2}/min). Next the temperature profiles in the plastic spheres were measured under various processing conditions in the agitated retort. The conditions were a 303 × 406 container filled with either distilled water or 60% (w/w) aqueous sucrose solution processed at 121 °C with reel speeds of 3.5 or 8 rpm. These measured profiles were compared to profiles calculated from Equation 8 using experimentally measured values of τ_f and τ_s. The values of Bi used were assumed to be equal to those of an equal-sized sphere of food under identical process conditions. These values can be calculated using the values of h_p measured earlier. Thus, for the experiments with water, the Biot number was 27 and for the sucrose solution experiments, Bi was 9.

To verify Equation 5, the steam and fluid temperatures were measured for the same can sizes, reel speeds, fluids and ultimate retort temperatures as those used to verify Equation 1. For these tests, 4 particle diameters were also used: (1) 0.95 cm (3/8 in., peas), (2) 1.6 cm (5/8 in., carrots pared into spheres), (3) 2.5 cm (1 in., radishes pared down), and

(4) 3.8 cm (1.5 in., potatoes pared down). As previously described, the value of h which minimized the sum of squares of the deviations (SSD) between the measured and predicted fluid temperatures (from Equation 5) was determined. Again the concept is illustrated in Fig. 2. The computer program and temperature profile data used in this study are available in Lenz (1977).

Equation 9 was used to predict the average particle temperature. The values of Biot number needed in Equation 9 were obtained using the values of h_p measured earlier. An average thermal conductivity (k_p) for food of 2.1×10^{-3} cal/sec cm °C (0.5 BTU/hr ft °F) (Charm 1971) was used. The thermal diffusivities used for the various particles were: (1) peas 0.11 cm²/min (0.0171 in.²/min) (Lenz and Lund 1975a), (2) carrots 0.11 cm²/min (0.0171 in.²/min) (Lenz 1977), (3) radishes 0.09 cm²/min (0.0140 in.²/min) (i.e. an average value for foods; Olson and Jackson 1942), and (4) potatoes 0.09 cm²/min (0.0140 in.²/min) (Wadsworth and Spadaro 1969).

To predict the values of T_f, Equation 5 was solved numerically using a 4th-order Runge-Kutta method (Conte and de Boor 1972). The step sizes used in the earlier experiments with Equation 1 were also adequate here.

As mentioned earlier, the value of SSD (minimum) (Fig. 2) was used to estimate the variance (σ^2) between the model (Equation 5) and experimental data. This value of σ^2 was compared to the variance between replicate trials to assess the adequacy of Equation 5 as a model.

The standard deviations for the values of h were calculated from the SSD versus h plots as explained earlier.

In confirming Equations 1 and 5 as adequate models, a considerable number of values of h versus various processing conditions were calculated. It was decided to correlate these values of h with the appropriate processing parameters. Based on correlations for heat transfer coefficients in packed beds (Bird *et al.* 1960), h or the Nusselt number (hS/k) should be dependent on Reynolds number (Re), Prandtl number (Pr) and a dimensionless number which relates the ratio of total volume of particles to total surface area of packed bed [Dp/(1—ε)S] to the characteristic dimension of the system (in this case, reel radius, S). The reel radius, S, was chosen as the characteristic dimension of the system (rather than diameter of the container, D_c because: (1) observations on heat transfer coefficients indicated that the h value was not dependent on container diameter, and (2) the characteristic velocity of the container was calculated using the reel radius (S) and reel speed (ω). That is, the values of h could be correlated with Re, Pr and Dp/S(1—ε) if S was the characteristic dimension. Using these dimensionless parameters, the values of h converted to Nusselt numbers (Sh/k = Nu) were fitted to

either the equation $Nu = A + B\ Re^a\ Pr^b$ for fluids alone or $Nu = A + B\ Re^a\ Pr^b\ (DP/S(1-\varepsilon))^c$ for fluids with suspended spherical particles. Values of A, B, a, b and c (where applicable) were found, by trial and error, which minimized the sum of the square of the deviations of predicted values of Nu and actual values.

In calculating the Reynolds number ($Re = S^2\omega\rho_d/\mu$) and the Prandtl number ($Pr = Cp\ \mu/kp$), various properties of the fluids were needed. For the correlations, all properties were evaluated at 121 °C (250 F). For distilled water, these are $\rho_d = 0.943$ g/cm^3, $Cp = 1$ cal/g · °C, $k = 2.1 \times 10^{-3}$ cal/sec cm °C (0.5 BTU/hr ft °F) and $\mu = 0.2$ cp (Perry, 1963). For the 60% aqueous sucrose solution, these are $\rho_d = 1.215$ g/cc., $Cp = 0.95$ cal/g °C, $k \fallingdotseq 2.1 \times 10^{-3}$ cal/sec cm °C (0.5 BTU/hr ft. °F) and $\mu = 1.65$ cp (Perry 1963).

The final step in this study was to incorporate the models for predicting temperature profiles into an equation for calculating lethality. This can be accomplished by modifying the lethality number equation given in Lenz and Lund (1977a). Modifications are needed because the Fourier number used for conduction heating products is not the correct form of dimensionless time for forced-convection heating products. In the present study, the dimensionless time is defined as $\tau_f t$. Therefore, the lethality number for forced-convection heating is:

$$L = \frac{-\tau_f \ln x}{k_r} = \int_0^{\tau_f t} \exp\left[\frac{-E_a}{R_g}\left(\frac{1}{T} - \frac{1}{T_r}\right)\right] d(\tau_f t) \qquad (13)$$

The integral in Equation 13 was numerically integrated using Simpson's rule (Conte and de Boor 1972) with stepsizes in $\tau_f t$ of 0.2. This stepsize gave values of L within 0.1% of the L values using smaller stepsizes. The lethality number was obtained by adding the lethality number from the heating cycle to that obtained from the cooling cycle of the process. For pure fluids, the value of L for heating was calculated using the temperature profile predicted by Equation 2 in Equation 13. For cooling the lethality was calculated using temperature profiles predicted by Equation 2 with the previously mentioned modifications. For fluids with particles, two situations existed. If the "cold point" (i.e. point receiving least lethality) was the particle surface (i.e. the particle is sterile on the interior), then for calculating lethality during heating, Equation 7 is used as the temperature profile in Equation 13 with $\rho_p = 1$. For cooling, Equation 10 with $\rho_p = 1$ is used as the temperature profile in Equation 13 for calculating lethality. If the "cold" point is at the center of the particle,

the same equations are used with $\rho_p = 0$. In calculating lethality number, it was assumed that the retort had no come-up time (i.e. retort was at constant temperature (T_s)). This means that in temperature models with terms for retort come-up time (τ_s), the value of τ_s was set at infinity.

Lethalities were calculated from the lethality number (L) versus dimensionless time ($\tau_f t$) charts by a procedure analogous to that described in Lenz and Lund (1977a). For comparison, lethalities (expressed as F_o) were calculated using the General Method (Bigelow *et al.* 1920) for actual heating and cooling profiles.

The last objective in this study was to determine the confidence intervals for calculated lethality of thermally-processed, forced-convection heated products. For products with particles, this was accomplished using the Monte Carlo procedue outlined in Lenz and Lund (1977b). For the present case, this consisted of choosing values of τ_f, E_a, Bi and τ_p at random from the previously established distributions. Then, for a given process time (t), values of lethality were calculated using the set of random values of τ_f, E_a, Bi and τ_p. The appropriate lethality number/dimensionless time charts were generated to calculate lethality. Process times (t) of 4.45, 6.67 and 8.90 min were used. The 95% confidence intervals for τ_f and E_a were 0.90 ± 0.18 min^{-1} and 65 ± 10 kcal/mole (Lenz and Lund 1977b), respectively.

Two circumstances were examined: (1) particles were sterile on the interior, and (2) particles were not sterile on the interior. In part one, the values of Bi and τ_p were those typical of spherical particles like peas. Thus, the 95% confidence intervals as determined in the initial phase of this study for Bi and τ_p were 3 ± 1.5 and 0.43 ± 0.03 min^{-1}, respectively. In part two, the values of Bi and τ_p were 17 ± 8 and 0.093 ± 0.006 min^{-1}, respectively. In both studies, 100 lethalities (F_o) were calculated at each process time. Finally, for both cases, the distributions of F_o were also determined for each process time assuming the value of Bi is infinity. This was done to evaluate the effect on calculated lethality of the assumption that the heat transfer at the fluid/particle interface can be ignored. The distribution of lethalities generated for this case (i.e. Bi = ∞) would also apply to the situation in which no particles are present (i.e. thermal processing of fluids alone).

RESULTS AND DISCUSSION

The overall objective of this study is to determine the effect of variability in parameters subject to biological variability on confidence intervals of the lethality accomplished during the thermal processing of

forced-convection heating products. Parameters subject to biological variability are heating rates of the products and destruction rates of the microorganisms. The variability in destruction rates is available in Lenz and Lund (1977a). Thus only variability in heating rates of forced-convection heating products must be evaluated in order to estimate the confidence interval of the calculated lethality.

Variability in Heating Rates

Variability in heating rates depends on the type of forced-convection-heating product and within this limitation, three types of products were considered: (1) fluids (e.g. juices or drinks), (2) fluids with particulates which are sterile in the interior (e.g. vegetables in brine or sauce), and (3) fluids with particulate pieces which are not sterile in the interior (e.g. meatballs or other formed pieces in sauces). Fluids considered in this study were Newtonian and it was assumed that heat transfer by forced-convection of the nature provided in the FMC Steritort was much more important than natural convection within the normal range of fluid viscosities in foods (1—100 cp at 77°F) (Blaisdell 1963). This is a reasonable assumption and all of the observations could be explained by assuming forced-convection heat transfer as the sole mechanism of heat transfer in the fluid.

The approach in this study was to drive theoretical temperature profiles appropriate for each type of product and subsequently experimentally verify these temperature profiles. The procedure for verification of a theoretical temperature profile was to compare the variation between theoretical and experimental temperature profiles to the variation between replicate temperature profiles. Equations for these temperature profiles were then used in a modified form of the lethality-Fourier number equation (Lenz and Lund 1977a) to prepare charts for predicting process lethality. Several lethality predictions were also verified experimentally. Finally, the variation in heating rates experienced during verification of the temperature profile was combined with the variation of microorganism destruction rates (Lenz and Lund 1977a) to predict a confidence interval for the calculated lethality (Lenz and Lund 1977b).

The variation of temperature profiles was established by measuring temperatures at the center of three cans of the same product. The range of these temperatures were measured at convenient increments of time (every 15 sec for 303 × 406 cans and every 30 sec for 608 × 700 cans). The effect of several variables on these temperature ranges was also measured. The variables were: (1) can size (608 × 700 versus 303 × 406), (2) fluid viscosity (water versus 60% sucrose solution) (μ), (3) presence or absence of 0.95 cm diameter particles (peas; $\varepsilon = 0.32$), and (4) reel speed

Table 1. Triplicates of temperature profiles at the center of 608 × 700 containers for the products and operating conditions stated

	Case 1			Case 2		
Fluid	Water			60% Sucrose Solution		
Particles	0.95 cm Spheres (peas);			None		
Reel Speed	$\varepsilon = 0.32$					
(ω)	3.5 rpm			3.5 rpm		
Retort Temp	121 C (250 F)			121 C (250 F)		
Time	Temperatures (°F)			Temperatures (°F)		
(sec)	(1)	(2)	(3)	(1)	(2)	(3)
0	60	60	60	100	100	100
30	60	65	90	104	100	111
60	106	94	112	103	100	128
90	138	130	142	116	120	148
120	144	150	152	143	140	158
150	164	173	173	162	158	174
180	189	189	185	175	174	182
210	197	195	195	183	188	192
240	200	209	205	196	196	200
270	210	217	214	203	203	207
300	220	222	216	210	210	214
330	224	224	222	213	215	219
360	226	231	228	220	220	224
390	233	233	232	222	223	227
420	236	237	236	226	228	230
450	237	237	238	229	231	233

(ω) (2, 3.5 and 8 rpm). Table 1 gives the triplicate temperature profiles for two representative experiments. One fact is clearly evident from the data in Table 1. The greater the temperature difference between the retort and the product the greater the ranges of the triplicate temperatures. This was expected because the temperature of the product increases exponentially with time and a heating rate variation will be exhibited as a larger range of measured temperatures the further the temperature is from the retort temperature. This phenomena was also observed for conduction-based products but to a lesser degree (Lenz and Lund 1977a). To eliminate the effect of heating time on the observed temperature ranges, each temperature range was divided by the difference between retort temperature (T_s) and the average of the triplicate temperatures (T prod., average). Figure 4 represents the compilation of these normalized ranges for triplicate product temperatures. The median of this distribution is

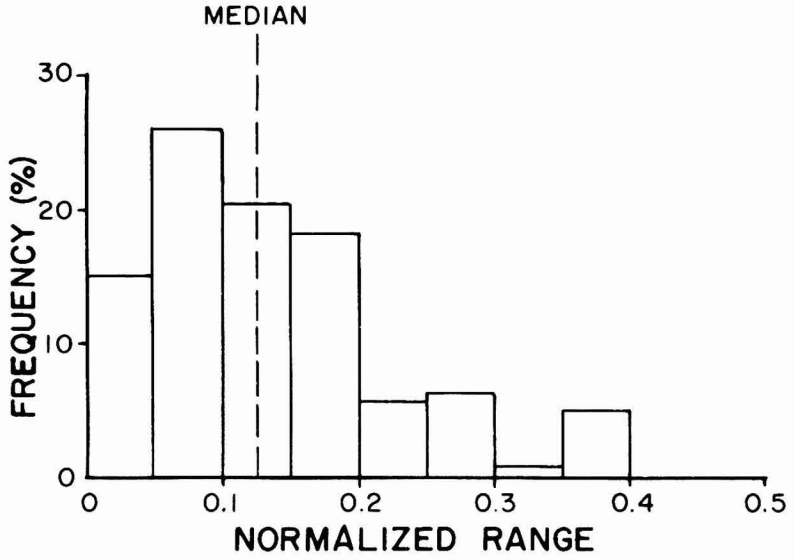

FIG. 4. FREQUENCY DISTRIBUTION OF THE NORMALIZED RANGE OF TEMPERATURES EXPERIENCED BETWEEN TRIPLICATES OF HEATING TEMPERATURE PROFILES

0.125. The standard deviation for various average ranges could be calculated using a procedure given in Guttman *et al.* (1971). The results are presented in Table 2 where it can be seen that the average range between triplicate product temperatures is about 12% of the retort/product temperature difference.

Table 2. Expected ranges and standard deviations for various retort/product temperature differences ($\Delta T = T_s - T$)

T (°F)	Range (°F)	σ (°F)
150	20	12
100	12	7
75	9	5
50	6	4
30	4	2
20	2-3	1-2
10	1	0.5

The dependence of standard deviation on retort/product temperature difference was observed between replicate measurements, between temperature comparisons at different container positions (i.e. experiments verifying that temperature gradients do not exist in these products) and between actual and predicted temperatures. To complete the calculations, however, it was necessary to establish one standard deviation which could be used for all retort/product temperature differences. This seemed justified since the products had similar heating rates and were heated between similar initial and final temperatures (i.e. same overall product temperature rise). The average of all data used to prepare Fig. 4 resulted in a standard deviation of 3.3 °C (6 °F).

In order to derive an adequate model to predict product temperature, it was necessary to determine if there were temperature gradients within the product in the container. Temperature at nine positions represented by the combinations of the axial positions (ζ = 0, 0.12, 0.70) and the radial positions (ρ_c = 0, 0.3, 0.45) were measured. Temperatures at these positions were compared at the same time increments and for the same series of processing conditions (i.e. can size, fluid viscosity, particle presence and size, reel speed) as those temperatures determined in triplicate in the earlier study. For each combination of processing conditions, only the temperatures at 3 of the 9 positions were compared. The three positions used were chosen at random. Table 3 illustrates the typical position-to-position temperature variation experienced. An average standard deviation (σ) for each experiment was calculated from the ranges (Guttman *et al.* 1971) and compared to the σ of 6 °F determined previously. Based on this comparison, it was evident that position-to-position variation in temperature was no greater than the variation in triplicate temperature measurements and that it could be assumed that temperature gradients do not exist for this type of product under these processing conditions.

Since temperature gradients were not found in the fluid, the simple energy balance given by Equation 1 was solved to give equations for predicting product temperature of simple fluid products. Equations 2 and 4 are solutions to this energy balance for the situations in which the retort temperature is constant and asymptotically approaches a constant temperature from a lower temperature, respectively. Equation 2 describes the profile normally observed. This is equivalent to a temperature profile presented by Charm (1958) for similar situations.

However, in our simulation work, the product could not be introduced into the retort if the retort was at final processing temperature (i.e. our retort was not equipped with a pressure lock through which containers could be introduced). Therefore, the containers were placed in the retort

Table 3. Temperature profiles at a series of positions in 608 × 700 containers for products and process conditions as stated

	Case 1 Axial Positions			Case 2 Radial Positions		
Fluid	Water			60% Sucrose Solution		
Particles	None			0.95 cm Spheres (peas);		
Reel Speed				$\varepsilon = 0.32$		
(ω)	8 rpm			3.5 rpm		
Retort Temp	121 C (250 F)			121 C (250 F)		
Axial Pos	$\xi = 0.16, 0.107, 0.700$			$\xi = 0.125$		
Radial Pos	$\rho_c = 0.0$			$\rho_c = 0.0, 0.463, 0.327$		
Time	Temperatures (°F)			Temperatures (°F)		
(sec)	$\xi = 0.16$	$= 0.107$	$= 0.70$	$\rho_c = 0.0$	$= 0.463$	$= 0.327$
0	100	100	100	95	95	95
30	109	112	122	103	95	103
60	129	149	134	118	110	148
90	157	173	159	128	120	136
120	176	176	178	152	138	154
150	186	193	193	150	186	174
180	203	202	206	188	170	187
210	216	216	212	189	182	180
240	215	218	220	192	203	190
270	232	224	224	201	208	207
300	231	236	227	216	217	208
330	236	228	232	222	218	210
360	239	238	234	223	220	218
390	238	237	234	226	229	222
420				231	229	232
450				235	232	235

and the steam temperature was then brought up to processing temperature. Equation 3 was found to adequately describe this retort temperature rise. Equation 4 was needed to model the fluid temperature in our simulation apparatus.

To verify that Equation 2 or 4 is an adequate model for predicting the temperature profile of fluids, experimental and predicted temperature profiles were compared. Since our simulation retort experienced a come-up time in steam temperature, experimental temperature profiles were compared to profiles predicted by Equation 4. The profiles were compared for a wide range of processing conditions which included changes in retort temperature, type of fluid, container size, thermocouple position and reel speed. The actual temperature profiles are available in

Table 4. Variances (σ^2) between the predicted and actual fluid temperatures for selected processing conditions

Variance (σ^2)		Thermocouple Position in Container			Particles (Spheres) Diameter	Void Fraction	Reel Speed
°F²	Can Size	ρ_c	ξ	Fluid[1]	(in.)		(rpm)
46	600 × 700	0.0	0.11	Water	None	———	3.5
14	608 × 700	0.0	0.43	Water	None	———	8
52	608 × 700	0.0	0.68	Water	0.38	0.32	8
24	608 × 700	0.0	0.68	60% S.S.	0.38	0.32	8
50	608 × 700	0.0	0.11	60% S.S.	0.38	0.32	3.5
5	608 × 700	0.0	0.43	60% S.S.	None	———	8
7	608 × 700	0.0	0.43	60% S.S.	None	———	3.5
86	608 × 700	0.46	0.13	60% S.S.	0.38	0.32	3.5
29	608 × 700	0.46	0.13	Water	0.38	0.32	3.5
18	608 × 700	0.33	0.13	Water	0.38	0.32	8
30	608 × 700	0.33	0.13	60% S.S.	None	———	3.5
84	608 × 700	0.0	0.11	60% S.S.	0.63	0.36	8
21	608 × 700	0.0	0.11	Water	1.0	0.41	2
23	608 × 700	0.0	0.43	60% S.S.	1.0	0.41	8
18	608 × 700	0.0	0.43	60% S.S.	1.0	0.41	2
36	608 × 700	0.0	0.11	Water	1.5	0.45	2
59	608 × 700	0.0	0.11	60% S.S.	1.5	0.45	3.5
25	608 × 700	0.0	0.43	60% S.S.	1.5	0.45	2
32	303 × 406	0.0	0.40	Water	None	———	3.5
12	303 × 406	0.0	0.40	60% S.S.	None	———	3.5
5	303 × 406	0.0	0.08	Water	0.38	0.32	8
32	303 × 406	0.0	0.08	60% S.S.	0.38	0.32	3.5
31	303 × 406	0.0	0.25	Water	0.63	0.36	8
28	303 × 406	0.0	0.25	60% S.S.	0.63	0.36	3.5
36	303 × 406	0.0	0.08	Water	1.0	0.41	8
20	303 × 406	0.0	0.08	60% S.S.	1.0	0.41	8

[1]60% S.S. = 60% aqueous sucrose solution
T_s = 250 F; T_i = 100 F; T_w = 60 F

Lenz (1977). When the variances between the predicted and experimental profiles were compared to the variance experienced between replicate measurements ($\sigma^2 = 36\,°F^2$) and tested using an F-test (Guttman *et al.* 1971), Equations 2 and 4 were found to be adequate models for 100% of the test runs. Several representative variances are given in Table 4. Table 4 also gives variances for systems with particulates. This will be discussed later in the paper.

Next, the temperature profiles in fluids with particulate pieces were investigated. To predict the temperature profiles for the other two situations considered in this paper, solutions for the complete energy balance given by Equation 5 and for the temperature profile throughout the particulate pieces were needed. Equation 5 accounts for the energy throughout the container. This entails the energy accumulating in the fluid and particulate pieces and the energy entering through the container surface. Since the fluid and particulates do not heat at the same rate, these components are accounted for separately in Equation 5. This is in contrast to Equation 1 where energy was accumulating in only one component (the fluid). The solution to Equation 6 was used to calculate the particulate heating rate or temperature profile once the fluid heating rate or temperature profile is known. This solution is given in Equation 7 for temperatures at individual positions in the particulate and Equation 8 for the average temperature profile of the piece. It should be noted that these solutions are for spheroidal geometries which were the only type of particulates investigated in this study.

In order to use Equations 7 or 8, the value of the heat transfer coefficient (h_p) between the particle surface and the fluid was needed. This is illustrated as the particle/fluid boundary layer in Case B of Fig. 1. In order to establish that this boundary layer existed (i.e. that the temperature profile did not look like Case A of Fig. 1) and to quantify the value of h_p for a variety of processing conditions, the experimental setup illustrated by Fig. 3 was designed and built. Lead was used to construct the spheres rather than food pieces or another material with low thermal diffusivity so that the problem of conducting heat throughout the piece was eliminated. In other words, once heat penetrated the particle/fluid boundary layer, the thermal energy immediately equilibrated throughout the piece of lead. Thus, the total piece of lead was at one temperature. This assumption that heat is instantly dispersed in these lead spheres was confirmed by separate experiments. By using lead spheres, the heat transfer coefficient could be measured independent of heat conduction effects. This also eliminated the problems with variability of thermal properties and positioning the thermocouple accurately in the piece.

With the setup illustrated by Fig. 3, the fluid and particle temperatures

could be measured. These temperatures were used to calculate the fluid/particle boundary layer heat transfer coefficient (h_p) by using Equation 10. Table 5 lists values of h_p for various processing conditions.

Table 5. Values of heat transfer coefficients h_p for the interface of the particles and the surrounding fluid at stated processing conditions.[1]

h_p[2] (BTU/ft² hr °F) Without Particles	With Particles	Particle Diameter (D_p) (in.)	Fluid[3]	Reel Speed (ω) (rpm)	Can Size
92	60	0.375	Water	3.5	303 × 406
86	132	0.375	Water	5.5	303 × 406
94	116	0.375	Water	8	303 × 406
167	94	0.375	60% S.S.	3.5	303 × 406
144	91	0.375	60% S.S.	5.5	303 × 406
207	144	0.375	60% S.S.	9	303 × 406
269	222	0.813	Water	3.5	303 × 406
236	223	0.813	Water	5.5	303 × 406
309	256	0.813	Water	8	303 × 406
	76	0.813	60% S.S.	3.5	303 × 406
	73	0.813	60% S.S.	5.5	303 × 406
95	86	0.813	60% S.S.		303 × 406
367	273	1.187	Water	3.5	303 × 406
361		1.187	Water	5.5	303 × 406
319		1.187	Water	8	303 × 406
123	211	1.187	60% S.S.	3.5	303 × 406
116	193	1.187	60% S.S.	5.5	303 × 406
134		1.187	60% S.S.	8	303 × 406
	33	0.375	Water	3.5	608 × 700
	38	0.375	Water	8	608 × 700
54		0.813	Water	3.5	608 × 700
83		0.813	Water	8	608 × 700

[1]Retort temperature = 250°F

[2]Experiments with fluid containing only the lead ball are listed as without particles. Experiments with fluid containing the lead ball and other particles of the same size as the lead ball are listed as with particles

[3]60% S.S. = 60% aqueous sucrose solution

Figure 5 correlates the values of h_p from Table 5 with type of fluid and normalized particle diameter (Dparticle/Dcontainer). Table 6 indicates variances between the model given in Equation 10 and the actual particle

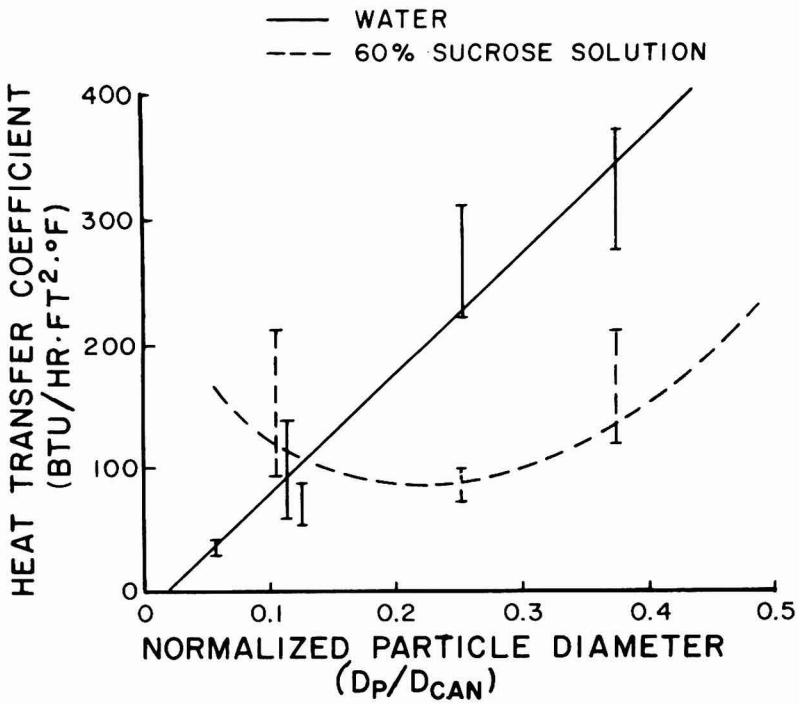

FIG. 5. VALUES OF HEAT TRANSFER COEFFICIENTS (h_p) FOR THE PARTICLE/FLUID INTERFACE FOR VARIOUS PARTICLE/CONTAINER RATIOS AND FOR TWO FLUIDS

surface temperatures. The actual temperature data is available in Lenz (1977). The average of the variances (σ^2) given in Table 6 yields a standard deviation (σ) between the model and actual data of 4 °F. Since this value of σ is close to the range between several replicates trials which were run, Equation 10 was assessed as an adequate model. Also, this value of σ is between those for pure conduction (σ = 3 °F; Lenz and Lund 1972) and for forced convection (σ = 6 °F). This standard deviation was related to the standard deviation of h_p using the procedure illustrated in Fig. 2. The standard deviation of h_p is 27% of the value of h_p. Figure 5 shows that for water, h_p increases linearly with Dp/Dc. However, for the more viscous sucrose solution, Dp/Dc has little effect on h_p. Since the intent of this study was to establish only representative values of h_p, the effect of fluid viscosity on h_p was not investigated further to explain these observations. In addition to the processing conditions stated in Table 5, other trials were also run at retort temperatures of 230 and 270 °F. For those conditions the values of h_p were not significantly different within the error of h_p.

Table 6. Variances (σ^2) between predicted and actual particle surface temperature for selected processing conditions

Variance (σ^2) °F[2]	Particle Diameter (in.)	Fluid[1]	Particles[2] Diameter (in.)	Void Fraction (ϵ)	Reel Speed (ω) (rpm)
12	0.33	Water	None	———	3.5
16	0.33	Water	None	———	8
21	0.33	Water	0.33	0.32	3.5
34	0.33	Water	0.33	0.32	8
9	0.33	60% S.S.	None	0.32	3.5
7	0.33	60% S.S.	None	———	8
4	0.33	60% S.S.	0.33	0.32	3.5
14	0.33	60% S.S.	0.33	0.32	8
4	0.63	Water	None	———	3.5
9	0.63	60% S.S.	0.63	0.36	8
9	0.63	60% S.S.	None	———	8
17	0.63	60% S.S.	0.63	0.36	3.5
4	1.0	Water	None	———	3.5
5	1.0	Water	None	———	8
18	1.0	Water	1.0	0.41	8
4	1.0	60% S.S.	None	———	3.5
9	1.0	60% S.S.	1.0	0.41	3.5
7	1.0	60% S.S.	1.0	0.41	8

[1]60% S.S. = 60% (by weight) aqueous sucrose solution
[2]Indicates presence or absence of extra particles (spheres) suspended in fluid

For some of the conditions described for this series of experiments other particles of food of the same diameters as the lead sphere were in the container. Those results were included in Table 5 also. Spheres of food were used as the particles to more closely simulate velocities and "wiping motions" of the particles and fluid under actual conditions of thermal processing of foods. Examination of Table 5 shows that the values of h_p did not differ significantly between fluids with and without additional particles, within the error of h_p.

This study established that the heat transfer coefficient at the interface of the fluid and particle is not infinite (i.e. negligible boundary layer as illustrated by Case A of Fig. 1) but finite as shown in Case B of Fig. 1. For the range of variables used in this study, the Biot number ranged from 2—25. This indicates that Equations 6—8 are the correct forms of the heat conduction equation to use under these circumstances. It was now necessary to establish the adequacy of the particle temperature profile given by Equations 7 and 8 and the overall temperature profile for particles suspended in a fluid given by Equation 5.

First, the temeprature at the center of the plastic ball was measured for various process conditions. The temperature profile was also predicted by inserting the experimental fluid temperature profile and the appropriate value of h_p from Table 5 in Equation 7. Two representative trials comparing actual and predicted temperatures are shown in Fig. 6.

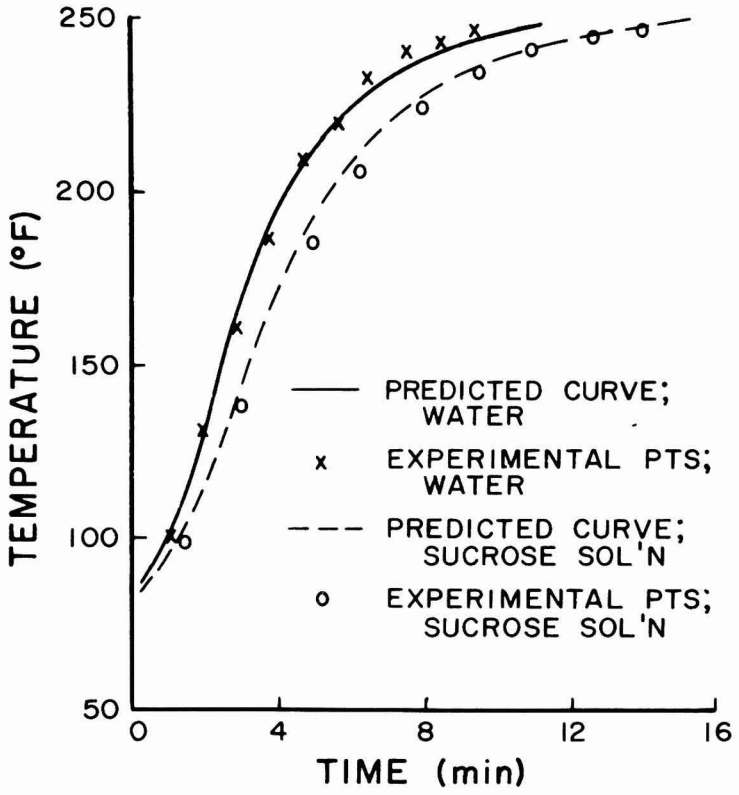

FIG. 6. EXPERIMENTAL AND PREDICTED TEMPERATURE PROFILES FOR THE CENTER OF A 5/8" PLASTIC SPHERE IN EITHER WATER OR A 60% SUCROSE SOLUTION

The fluid and sphere were processed in a 303 × 406 container at a retort temperature of 249°F and a reel speed of 3.5 rpm

Next, the average particle temperature predicted by Equation 8 was used with the appropriate value of h_p from Table 5. Actual fluid temperatures were compared to fluid temperatures predicted by Equation 5 for a series of processing conditions. The results are shown in Table 4. The actual temperature profiles are available in Lenz (1977). When the

variances given in Table 4 were compared to the replicate measurement variance ($\sigma^2 = 36\,°F^2$) and tested using an F-test (Guttman *et al.* 1971), Equation 5 was found to adequately represent 90% of the trials.

It should be noted that, as with Equation 4, Equations 7 and 8 were derived assuming the retort temperature asymptotically approaches the ultimate retort temperature. As mentioned previously, this was the case with our simulation retort. The modification to Equations 7 and 8 for the usual case (i.e. retort temperature is constant and at the ultimate temperature) is given by Equation 13.

Correlations for Heat Transfer Coefficients

In assessing the adequacy of Equations 4 and 5 as models, the values of the heat transfer coefficient between the container surface and the fluid (h) were determined. These values of h as a function of the various processing parameters used in this study are given in Table 7. Correlations were developed using the data in Table 7 which related characteristic dimensionless groups for the separate cases of fluids and of particles suspended in fluids (Bird *et al.* 1960). These correlations are shown in Fig. 7 and 8, respectively. The equations describing these correlations are:

$$\text{Fig. 7: } Nu = 115 + 15\ Re^{0.3}\ Pr^{0.08} \tag{14}$$

$$\text{Fig. 8: } Nu = -33 + 53\ Re^{0.28}\ Pr^{0.14}\ D_p/S(1-\varepsilon))^{0.46} \tag{15}$$

The standard deviation between Equations 14 and 15 and the actual data is less than the standard deviation between replicate values of Nu or h.

Before proceeding, several observations should be mentioned about the correlations given in Fig 7 and 8. First, the correlation shown in Fig. 8 and given in Equation 15 should not be used for values of ε greater than 0.5. Spurious results were obtained in this range. This is also the case for packed beds (Bird *et al.* 1960). Normally, however, one would not be in this range. The values of ε in our study usually ranged from 0.32—0.45 as shown in Table 7. Next, it is interesting to note that the diameter of the container is not the characteristic length in these correlations. The values of h were independent of the container size used in this study. Because the characteristic velocity in the study contained a dimension (i.e. the radius of the reel (S)), this dimension (S) was used as the characteristic length. We were not able to repeat the study with a different reel length to confirm this finding. As with most heat transfer coefficients, the values of h or dimensionless h (Nu) are correlated with the Reynolds number (Re) and Prandtl number (Pr) (Bird *et al.* 1960). However, the

Table 7. Heat transfer coefficients (h) for the interface of the container and either a fluid medium or a fluid medium with particulate spheres at the stated process conditions

h (BTU/hr ft² °F)	Fluid[1]	Reel Speed (ω) (rpm)	Particle Diameter (in.)	Relative Fluid Volume in Container (ε)
146, 129, 143	Water	3.6	None	———
164, 168, 171	Water	8	None	———
102, 104, 99	60% S.S.	3.5	None	———
125, 125, 114	60% S.S.	8	None	———
37, 44, 49	Water	3.5	0.375	0.32
52, 58	Water	8	0.375	0.32
62	Water	3.5	0.625	0.36
78	Water	8	0.625	0.36
68	Water	2	1.00	0.41
85, 75	Water	3.5	1.00	0.41
102, 94	Water	8	1.00	0.41
76	Water	2	1.50	0.45
88	Water	3.5	1.50	0.45
126	Water	8	1.50	0.45
34	60% S.S.	2	0.375	0.32
30, 31, 32	60% S.S.	3.5	0.375	0.32
43, 32, 41, 42	60% S.S.	8	0.375	0.32
32, 39	60% S.S.	3.5	0.625	0.36
57	60% S.S.	2	1.00	0.41
59, 60	60% S.S.	3.5	1.00	0.41
72, 77	60% S.S.	8	1.00	0.41
60	60% S.S.	2	1.50	0.45
87	60% S.S.	8	1.50	0.45

[1]60% S.S. = 60% (by weight) aqueous sucrose solution

exponents for Re, Pr in Equations 14 and 15 are much smaller than similar correlations for heat transfer coefficients in packed beds (Bird *et al.* 1960). This is probably caused by the starting and stopping nature of this process (i.e. cans rotate quickly at the bottom of the cycle when the reel rolls the can along the shell and do not rotate at the top of the cycle when the can is held in the reel). Finally, when particles are suspended in the fluid, the values of h are decreased. It was suspected that the particles exerted a drag on the fluid. This decreased the relative fluid velocity which increased the boundary layer and decreased h. To test this, the values of h were correlated with a term which reflected the ratio of bed volume to particle surface area [Dp/S (1—ε)]. The positive correlation shown in Fig. 8 supports this theory.

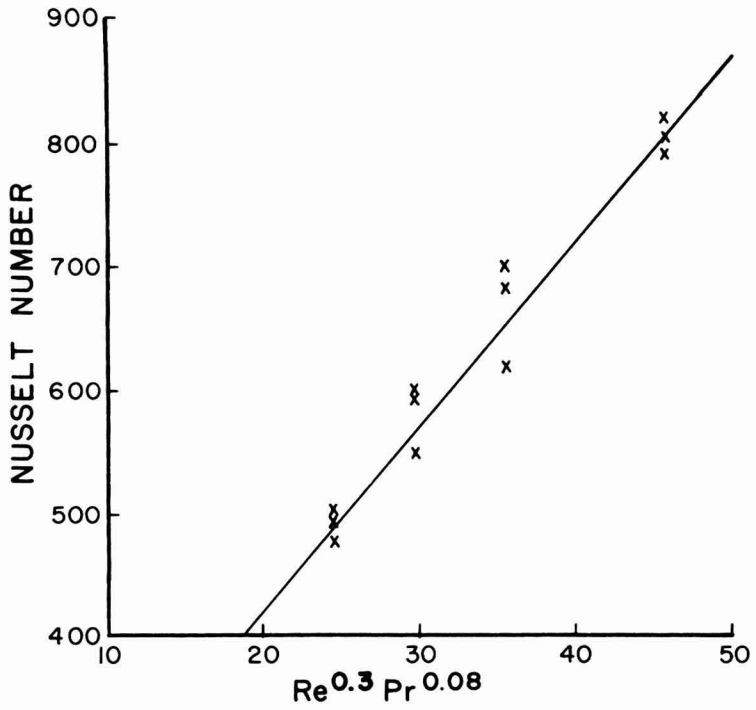

FIG. 7. VALUES OF DIMENSIONLESS HEAT TRANSFER COEFFICIENTS (h in Nu) AT THE CONTAINER/FLUID INTERFACE FOR FLUIDS WITHOUT PARTICLES AS INFLUENCED BY REYNOLDS NUMBER (Re) AND PRANDTL NUMBER (Pr)

Lethality-Fourier Number Model for Convection-Heating Foods

The final step in this study is to use the temperature prediction models to calculate the lethality and lethality confidence interval of a thermal process. The temperature profiles established to this point have only been for heating, and the profiles for cooling are needed to calculate total lethality. Since the fluid is at one temperature, the cooling profile for cooling fluid only is obtained by substituting T_w for T_s and the final temperature accomplished during the heating cycle for T_i. For fluid containing suspended particles, several corrections to Equation 7 pointed out in Carslaw and Jaeger (1959) are needed. The final profile is given in Equation 12. This equation is a straight-forward derivation using the starting profile for a sphere with an initial temperature gradient and a heat transfer resistance (Carslaw and Jaeger 1959) and then using the procedure used to obtain Equation 7 from Equation 6 (Duhamel's Theorem).

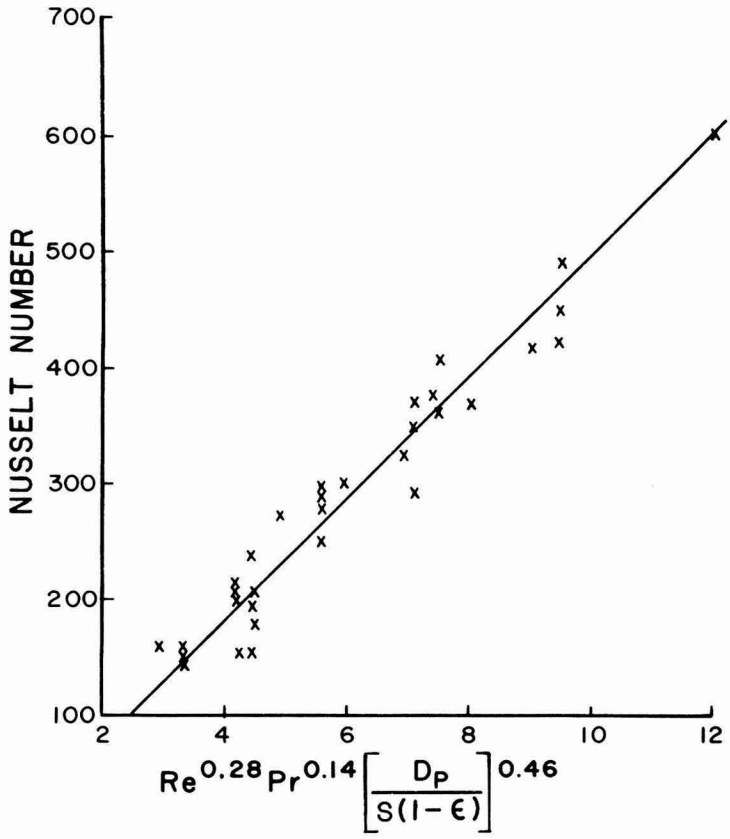

FIG. 8. VALUES OF DIMENSIONLESS HEAT TRANSFER COEFFICIENT (h in NU) AT THE CONTAINER/FLUID INTERFACE FOR FLUIDS WITH SPHERICAL PARTICLES AS INFLUENCED BY REYNOLDS NUMBER (Re), PRANDTL NUMBER (Pr) AND PARTICLE SURFACE AREA/VOLUME RATIO ($D_p/S(1-\varepsilon)$)

The necessary temperature profiles can now be inserted into the lethality number equation (Equation 13) and desired lethalities can be calculated. As mentioned previously, Equation 13 is a modification of the lethality number equation given in Lenz and Lund (1977a). This modification occurs because forced-convection heating does not involve thermal diffusivities (this is a property used in conduction heating) and therefore does not have a Fourier number. Thus, it was necessary to define a new dimensionless time. This was done using a heating time constant (τ_f) which is equal to $h\ A/\rho_d C_p V$ (Equation 2). Dimensionless time is therefore $\tau_f t$ because τ_f has units of reciprocal time (i.e. sec^{-1}, min^{-1}, etc.). This then

modifies the definition of the lethality number to:

$$L = \frac{\tau_f \ln x}{k_r} = \tau_f U$$

Using Equation 13 and the appropriate temperature profile for heating (Equation 2 or 7) or cooling (Equation 2 modified or Equation 10), the lethality number charts for the three types of products were calculated. These products are characterized as: (1) fluids, (2) particles sterile on interior suspended in fluid, and (3) particles not sterile on interior suspended in fluid. For each of these situations, the lethality number for heating was added to the lethality number for cooling to establish the total lethality number at the "cold point" or point receiving least lethal heat treatment in the product. The "cold point" for the products was (1) anywhere in the container for fluids (i.e. no temperature gradients), (2) at the surface of the particle for particles sterile on the interior, and (3) at the center of the particle for particles not sterile in the interior. Figure 9

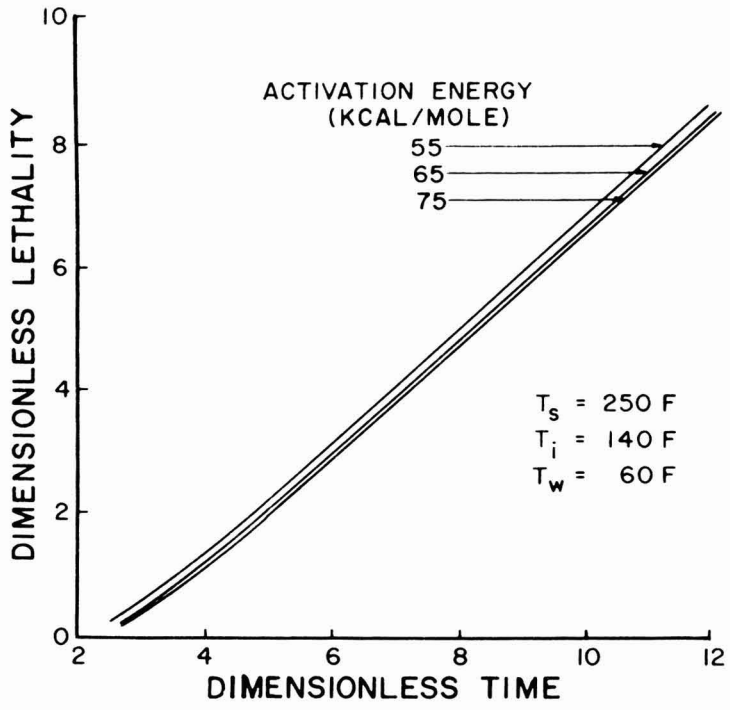

FIG. 9. TYPICAL LETHALITY NUMBER (DIMENSIONLESS LETHALITY) ($\tau_f U$) VERSUS DIMENSIONLESS TIME ($\tau_f t$) PLOTS FOR THREE ACTIVATION ENERGIES (E_a)

is a typical lethality number-dimensionless time chart for particles which are sterile on the interior suspended in fluid (product 2). It should be pointed out that the lethality numbers and dimensionless times for forced-convection heating are about 10 times larger than those reported for conduction-heating (Lenz and Lund 1977a). This is related to the form of the conduction heating equations which contain eigen values (β_n^2) in the exponential terms.

Table 8. Process times determined by the general method and lethality number-dimensionless time (L-τ_ft) method which accomplish an F_0 = 12 min. Experimental heating curves with the specified conditions were used to obtain appropriate parameters

Fluid[1]	Retort Temperature (°F)	Reel Speed (ω) (rpm)	Heating Time Constant (τ_f) (min^{-1})	General	L-τ_ft
60% S.S.	249	3.5	0.62	20.7	20.6
60% S.S.	250	8	0.71	17.2	17.5
60% S.S.	239	8	0.74	62.9	63.6
60% S.S.	259	3.5	0.78	9.2	8.2
Water	249	3.5	0.90	17.5	18.2
Water	249	8	1.15	16.5	17.3

[1]60% S.S. = 60% (by wt.) aqueous sucrose solution (Container size was 303 × 406)

To test this lethality calculation method, several experimental heating and cooling curves with fluids in containers were generated. The exact conditions for these trials are presented in Table 8. Table 8 also presents the process times required to achieve an F_0 of 12, under the experimental conditions, calculated by the General method (Stumbo 1973) and the lethality number-dimensionless time (L-τ_ft) method. Since the calculation of process times using L-τ_ft is comparable to the lethality-Fourier number method (Lenz and Lund 1977a) with the appropriate corrections previously mentioned, a sample calculation will not be given. The values of τ_f used in Table 8 for the L-τ_ft method were determined by fitting Equation 2 to the experimental temperature profiles. The least squares procedure described earlier and illustrated in Fig. 2 was used to determine the value of τ_f.

Confidence Intervals on Calculated Lethality

Since the results shown in Table 8 indicated that the L-τ_ft method could accurately predict lethality, the final phase of this study could be completed. That is, the lethality confidence intervals for the three products under consideration could be established. This was accomplished using the Monte Carlo procedure detailed in Lenz and Lund (1977b). Values of τ_f, E_a, Bi and τ_p werre chosen at random from the distributions previously established in this study or given by Lenz and Lund (1977b). For each situation 100 sets of values were generated to establish the confidence interval for calculated lethality. The study was designed to center the dimensionless time distributions at 4, 6 and 8 min. Since the median and 95% confidence interval for τ_f were 0.9 $\pm$ 0.18 min^{-1} for all previous experiments, this would result in process times of 4.45, 6.67 and 8.90 min. For fluids, the standard deviations for calculated lethality were $\pm$ 25% at 4.45 min, $\pm$ 13% at 6.67 min and $\pm$ 8% at 8.90 min. The distributions were similar to those shown in Fig. 10 for particles in fluid.

For particles which are sterile on the interior, the lethality is evaluated for conditions at the surface of the particle. For comparison, the lethalities were also evaluated assuming the fluid and particle surface were at the same temperature (Case A of Fig. 1). In practice, lethalities are usually calculated using this assumption (i.e. assuming the fluid and particle surface are at the same temperature). Figure 10 shows the lethality distributions for the surface of 0.95 cm (3/8 in) spheres of food. The median and 95% confidence intervals for calculated lethality are: 1.1 $\pm$ 0.7 at 4.45 min, 3.0 $\pm$ 0.8 at 6.67 min and 5.2 $\pm$ 0.9 at 8.90 min. If the surface temeprature of the particle is assumed to equal the fluid temperature (i.e. infinite fluid/particle heat transfer coefficient (h_p)), the 95% confidence intervals of F_o are 1.2 $\pm$ 0.6 min at 4.45 min, 3.2 $\pm$ 0.8 min at 6.67 min and 5.4 $\pm$ 0.8 min at 8.90 min. It is reassuring that these median values are close to those found when infinite surface heat transfer is considered. The standard practice of ignoring the fluid/particle surface heat transfer resistance seems to be justified under these conditions.

For particles which are not sterile on the interior, the lethality is evaluated at the center of the particle. Again, the purposes of comparison, the lethalities were also calculated when the heat transfer resistance is ignored (i.e. $h_p \approx \infty$). For 2 cm (4/5 in) spheres of food, the lethality distributions are given in Fig. 11. The median and 95% confidence intervals for F_o are 1.4 $\pm$ 0.8 min at 6.67 min and 3.4 $\pm$ 1.0 min at 8.90 min. When the surface heat transfer resistance is assumed to be zero the intervals are 1.7 $\pm$ 0.7 min at 6.67 min and 4.0 $\pm$ 1.2 min at 8.90 min. These median values are approximately one standard deviation higher than those obtained when surface heat transfer resistance is considered.

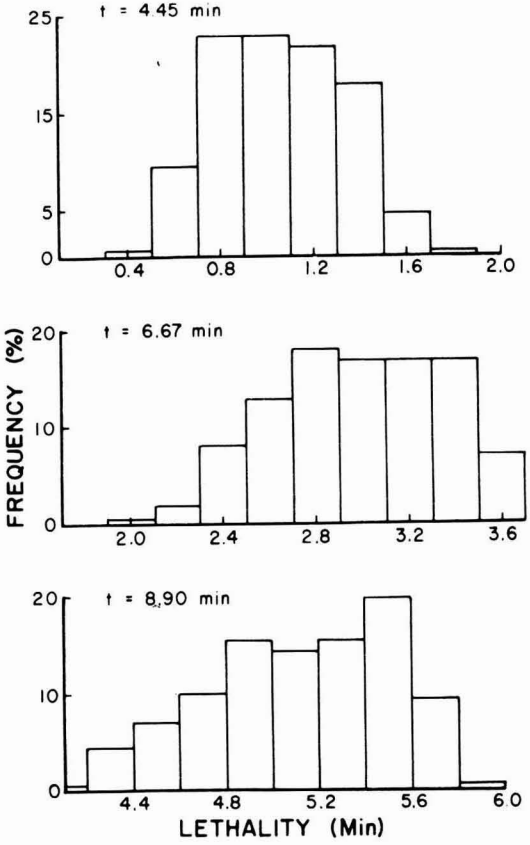

FIG. 10. DISTRIBUTION OF LETHALITIES (F_o) AT THE SURFACE OF A SPHERICAL PARTICLE FOR VARIOUS HEATING TIMES

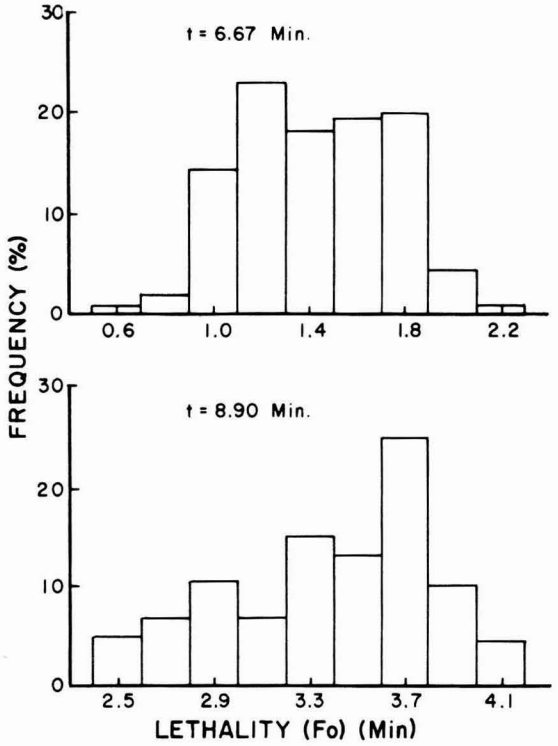

FIG. 11. DISTRIBUTION OF LETHALITIES (F_o) AT THE CENTER OF A SPHERICAL PARTICLE FOR VARIOUS HEATING TIMES

It appears that the heat transfer resistance should not be ignored under these circumstances.

SUMMARY

To summarize, equations were derived and experimentally evaluated for predicting temperature profiles in fluids and particles suspended in fluids for systems heated by forced-convection. Temperatures calculated using the models had an average standard deviation of 6°F. This variability was due to the fact that the standard deviation was equivalent to that found in replicate temperature measurements. The heat transfer coefficient at the particle/fluid interface was also evaluated. It was found that at this interface, the dimensionless heat transfer coefficient (Biot number) ranged from 2-25. The standard deviation for this fluid/particle surface heat transfer coefficient (h_p) was approximately 27%.

Finally, the temperature profiles were incorporated in a method for calculating lethality (L-τ_ft method). The L-τ_ft Method compared favorably to the General Method (Stumbo 1973) for calculating lethality. The method was also used to determine the confidence intervals of calculated lethality for the "cold point" of (1) fluids, (2) fluids with particles sterile on the interior, and (3) fluids with particles not sterile on the interior. These distributions were generated using a Monte Carlo procedure for choosing values of parameters subject to biological variability (E_a, τ_f, τ_p, Bi). For fluids, σ for lethality ranged from 8-25% of the median value as τ_ft ranged from 8-4, respectively. For particles sterile on the interior suspended in fluid, σ was similar to σ for fluids alone over the same τ_ft range. It appeared that the heat transfer resistance could be neglected, at least for small particles (0.95 cm spheres), in this case. For particles not sterile on the interior suspended fluid, σ was 29% of the median F_o value for τ_ft around 6 and 15% of the median F_o value for τ_ft around 8. For this case, the heat transfer resistance at the fluid/particle interface should not be neglected. Finally, this study would suggest that a finite surface heat transfer coefficient at the fluid/particle interface should also be considered in aseptic processing of particulates in fluid. Such a study would complement the study by de Ruyter and Brunet (1973), who assumed negligible fluid/particle heat transfer resistance.

SYMBOLS

T = temeprature of product
T_i = initial temperature of product

T_h = heating medium temperature (retort temperature)
T_s = actual (ultimate) steam temperature
T_{si} = initial retort temperature
$\overline{T}$ = average temperature of product
T_f = Temperature of the fluid
T_{ps} = surface temperature of the particle
T_w = cooling water temperature
$\phi(\lambda)$ = fluid temperature versus time (λ) model
δ = $(T_s - T_{si})/(T_s - Ti)$
δ_1 = $(T_s - T)/(T_s - Ti)$
t = time
t_h = heating time
λ = dummy variable for time
ρ_d = density
C_p = heat capacity of the particle
α = thermal diffusivity of the particle
k_p = thermal conductivity of the particle
μ = viscosity of the fluid (=) centipose (cp)
h = heat transfer coefficient at container surface
h_p = heat transfer coefficient at particle surface
V = volume of the container
A = surface area of the container
R_p = radius of the particle
S = radius of the reel in the agitated retort
V_p = volume of the particle
A_p = surface area of the particle
ι = half-length of the container
R_c = radius of the container
Dp = diameter of the particle
Dc = diameter of the container
ε = fraction of the container volume occupied by fluid
ω = rotational speed of the reel (=) rpm
τ_f = $h\ A/\rho_d Cp\ V$
τ_s = retort time constant = time it takes for the retort temperature to rise 67% of the overall temperature rise $(T_s - T_{si})$
τ_p = time constant for the particle = $\alpha\beta_n^2/R_p^2$
τ = Fourier number = $\alpha t/R_c^2$
r = radial position in the spherical particles
ρ_p = dimensionless radial position in the particle = r/R_p
Z = axial position in the container (measured from center)
ζ = dimensionless axial position in the container

ρ_c = dimensionless radial position in the container (measured from the center) = r/R_c
Bi = Biot number for heating the particle = $R_p h_p/k_p$
C = concentration of biological component
C_o = initial concentration of biological component
X = C/C_o
k_r = rate constant for destruction of a biological component at temperature (T_s)
D_r = decimal reduction time at T_s
E_a = activation energy (=) Kcal/mole
U = $D_f \log x = -\ln x/k_f$ = thermal death time at T_s
F_o = thermal death time at 250°F
L = $(-\tau_f \ln x)/k_r$
Nu = Nusselt number = Sh/k_p
Pr = Prandtl number = $Cp\ \mu/k_p$
Re = Reynolds number = $S^2\omega\rho_d/\mu$
σ = standard deviation of a measurement
σ^2 = variance of a measurement
d = time interval used for numerical integration
β = roots of the transcendental equation ($\beta \cot \beta + Bi - 1 = 0$)
$_f$ = subscript for fluid phase of product
$_p$ = subscript for particle phase of product

ACKNOWLEDGEMENT

This research was supported by the College of Agricultural and Life Sciences, University of Wisconsin-Madison, UW Computing Center, UW Graduate School, and by the United States Department of Health, Education and Welfare, FDA Research Grant Number 5-R01-FD00606. We would like to thank Professor E.N. Lightfoot for assistance in developing the methods for estimating heat transfer coefficients.

REFERENCES

BIGELOW, W.D. and ESTY, J.R. 1920. The thermal death point in relation to time of typical thermophilic organisms. J. Infect. Dis. *27*(6), 602.

BIRD, R.B., STEWART, W.E. and LIGHTFOOT, E.N. 1960. *Transport Phenomena*, John Wiley & Sons, New York.

BLAISDELL, J.L. 1963. Natural convection heating of liquids in unagitated food containers. Ph.D. Thesis, Dept. of Food Technol., Mich. State Univ., East Lansing, MI.

CARSLAW, H.S. and JAEGER, J.C. 1959. *Conduction of Heat in Solids,* 2nd Ed., Clarendon Press, Oxord, England

CHARM, S.E. 1971. *The Fundamentals of Food Engineering,* 2nd Ed., The Avi Publishing Co., Westport, Conn.

CONTE, S.D. and de BOOR, C. 1972. *Elementary Numerical Analysis,* 2nd Ed., McGraw-Hill, New York.

de RUYTER, P.W. and BRUNET, R. 1973. Estimation of process conditions for continuous sterilization of foods containing particulates. Food Technol. *27,* 44.

GUTTMAN, I., WILKS, S.S. and HUNTER, J.S. 1971. *Introductory Engineering Statistics,* John Wiley & Sons, New York.

HICKS, E.W. 1961. Uncertainties in canning process calculations. J. Food Sci. *26,* 218.

LENZ, M.K. 1977. The lethality-Fourier number method. Its use in estimating confidence intervals of the lethality or process time of a thermal process and in optimizing thermal processes for quality retention. Ph.D. Thesis, Dept. of Food Sci., Univ. of Wis., Madison, Wis.

LENZ, M.K. and LUND, D.B. 1977a. The lethality Fourier number method. I. Experimental verification of a model for calculating temperature profiles and lethality in conduction-heating, canned foods. (In press).

LENZ, M.K. and LUND, D.B. 1977b. The lethality-Fourier number method. III. Confidence intervals for calculated lethality and mass-average retention of conduction-heating, canned foods. (In press).

OLSON, F.C.W. and JACKSON, J.M. 1942. Heating curves: Theory and practical application. Ind. Engr. Chem. *34,* 337.

PERRY, J.H. (ed.). 1963. *Perry's Chemical Engineer's Handbook,* 4th Ed., McGraw-Hill, New York.

SEINFELD, J.H. and LAPIDUS, L. 1974. *Mathematical Methods in Chemical Engineering:* Vol. 3, *Process Modelling, Estimation and Identification,* Prentice-Hall, Englewood Cliffs, New Jersey.

STUMBO, C.R. 1973. *Thermobacteriology in Food Processing,* 2nd Ed., Academic Press, New York.

WADSWORTH, J.I. and SPADARO, J.J. 1969. Transient temperature distribution in whole sweet potato roots during immersion heating. Food Technol. *23,* 85.

LITERATURE ABSTRACTS

ABSTRACTS FROM THE JOURNAL OF FOOD SCIENCE

Each of the following abstracts has been reprinted with permission from the *Journal of Food Science.*

STORAGE STABILITY OF INTERMEDIATE MOISTURE FOOD PROCESS CHEESE FOOD PRODUCTS. L.N. Kreisman and T.P. Labuza, J. Food Sci. *43*, 341-344.

A series of intermediate moisture food processed cheese foods were made utilizing water, nonfat milk solids and propylene glycol to change the water activity of 0.81, 0.86, 0.90, 0.91 and 0.94. The stability of these cheeses was tested over a 6-month period at room temperature. The cheeses were challenged with three molds (*Aspergillus niger, Aspergillus glaucus* and *Penicillium roqueforti*) and two pathogenic bacteria (*Staphylococcus aureus* and *Salmonella anatum*). Changes in color, texture, meltability and organoleptic acceptability were followed. The high a_w cheeses (0.90-0.94) supported the growth of the three molds, while only the 0.94 a_w cheese food supported the growth of *Staphylococcus aureus.* The lower a_w cheeses (0.81 and 0.86) were stable microbiologically. However, the almost a_w cheese was initially not acceptable in terms of the other parameters, while the 0.86 a_w cheese became acceptable after 6-8 weeks. The IMF cheese food at a a_w 0.90 was the most acceptable, with a shelf-life of about 5 months.

OPTIMIZATION OF PROTEIN ISOLATE PRODUCTION FROM SOY FLOUR USING INDUSTRIAL MEMBRANE SYSTEMS. J.T. Lawhon, D.W. Hensley, D. Mulsow and K.F. Mattil, J. Food Sci. *43*, 361-364.

A new approach to the production of protein isolates from oilseed flours with industrial ultrafiltration and reverse osmosis membranes previously demonstrated has been further optimized for use with soy flour. The effects of membrane performance of prefiltering the flour extract feed to different degrees and processing the feed at different pH levels were examined. A wide range of industrial membrane systems embodying several configurations were tested. Prefiltration of feed to less than 100μ proved to be unnecessary for most systems. Feed at pH 7.0 processed at high permeation rates yielded products with NSI values in excess of 90.

COMPUTER CALCULATION OF THERMAL PROCESSES. M.A. Tung and T.D. Garland J. Food Sci. *43*, 365-369.

A series of computer-oriented procedures was developed to facilitate the rapid handling of heat penetration data while providing estimates of the process time required to achieve a specified lethality at a single point within the product for a particular product, container size, fill and processing conditions. Accepted thermobacteriological equations were employed with variation in the heating rate used to establish confidence limits on processes. This statistical approach was considered more pragmatic than the traditional use

Journal of Food Process Engineering 2 (1978) 273—281.

of the slowest or mean single value of the heating rate in sterilization calculations while the amount of heat penetration data necessary for process determination was minimized. Varying computer program versions permit the application of these process determination procedures to high or low acid products that are convection or conduction heating providing they exhibit single or broken straight-line heating curves.

APPARATUS FOR STUDYING FOULING OF HEATED SURFACES BY BIOLOGICAL FLUIDS. A.D. Ling and D.B. Lund, J. Food Sci. *43*, 390-393.

A laboratory-scale double tube heat exchanger was developed to study fouling phenomena of biological fluids. The test fluid is continuously circulated through the system exposing the solution to an electrically-heated stainless steel section. The stainless steel section is 0.635 cm (0.25 in.) diameter and is located on the center-axis of 2.54 cm (1 in.) diameter glass-pipe. The heat transfer characteristics of the system were determined and egg albumin solution was used to test the applicability of the system for studying fouling. The system was found to be stable and reproducible. The system can be used to study the effects of operational variables (such as surface temperature, velocity and fluid temperature) and fluid characteristics on fouling rates. The test surface can be easily interchanged to study surface characteristics also.

KERNEL HARDNESS OF WILD RICE AS AFFECTED BY DRYING AIR TEMPERATURE AND MOISTURE GRADIENT. M.A. Wirakartakusumah and D.B. Lund, J. Food Sci. *43*, 394-396.

Samples of wild rice (38-40% moisture, wet basis) were dried to 7-8% moisture using three different drying air temperatures and relative humidities, namely, 110°C-6% relative humidity, and 60°C-20% relative humidity. Samples were subsequently hulled immediately (hulled hot) or hulled after storing 24 hr at room temperature (hulled cold). Evaluations included determination of hulling efficiency, kernel hardness and degree of gelatinization. Hulling was most efficient when a high drying air temperature was used and when the kernels were hulled immediately after drying. Total yield was not affected by temperature gradient or moisture gradient which the wild rice kernels experienced during drying. Head yield was maximum when wild rice was dried under conditions of a high drying air temperature and low moisture gradient, and when it was hulled hot, immediately after drying. The kernel hardness test confirmed that kernels were harder when dried under high temperature, low moisture gradient conditions. Degree of gelatinization studies confirmed that about 90-95% of the starch in kernels dried under these conditions were gelatinized. The gelatinization of starch was influenced by both temperature and rate of drying. Susceptibility of kernels to cracking increased with increased magnitude of moisture gradient within kernels. The best processing conditions for wild rice using criteria previously described consist of drying under high air temperature and a low moisture gradient, and hulling the kernels hot, immediately after drying.

SLOPES OF MOISTURE SORPTION ISOTHERMS OF FOODS AS A FUNCTION OF MOISTURE CONTENT. P. Viollaz, J. Chirife and H.A- Iglesias, J. Food Sci. *43*, 606-608.

Values of the isotherm factor, $(\alpha a_w/\alpha X)_T$, for various dried foods (apple, beef, cod, carrot, fennel, peas, peanut, potatos and trout) were calculated and reported as a function of moisture content. The effect of sorption hysteresis on the isotherm factor was also calculated for some foods. It is hoped that these data may be useful for adequacy interpreting experimental results on rates of moisture sorption and desorption in dried foods.

MICROSTRUCTURE AND MECHANICAL PROPERTIES OF SINGLE CELL PROTEIN CURD. T.D. Tsintsadze, C.H. Lee and C.K. Rha, J. Food Sci. *43*, 625-630.

The microstructure and the physical and mechanical properties of yeast protein curds were investigated by using the scanning electron microscope and Instron Universal Testing Machine, Model 1122. Heat treatment of the protein dispersion prior to the precipitation did not remarkably influence the structure and water-holding capacity of the curds. Yeast protein curd precipitated with calcium had a micron-network structure which was not apparent in the isoelectric point precipitated curd. The calcium precipitated curd had a low value of hardness, high water-holding capacity, low value of adhesiveness and high cohesiveness compared to the isoelectric precipitated curd. The calcium precipitated curd also showed a strong structural potential which was revealed upon freezing. The freeze-thawing of the curd in general increased hardness and springiness but decreased the adhesiveness and cohesiveness. The physical, structural and mechanical properties of yeast protein curds were compared with those of soybean protein curds studied previously.

KINETIC PARAMETERS FOR THERMAL INACTIVATION OF PANTOTHENIC ACID. D.J. Hamm and D.B. Lund, J. Food Sci., *43*, 631-633.

Decimal reduction values (D values) and activation energies for destruction of pantothenic acid (PA) in KH phthalate buffer, pH 4,5 and 6, in meat puree and in pea puree at temperatures between 118-143°C were determined using the thermal death time tube method and the Arrhenius equation. Samples were assayed according to AOAC (1975) microbiological method for pantothenic acid. Activation energies ranged from 20,000-38,000 cal/mole. As pH increased from 4 to 7, activation energies also increased. The D_{121} values ranged from 4-32 hr for buffered systems and from 38-40 hr for food systems. These large D values for foods would indicate that PA is not very heat labile and is more stable in these food systems compared to buffered systems.

A GENERAL LETHAL-RATE PAPER FOR THE GRAPHICAL CALCULATION OF PROCESSING TIMES. G.F. Leonhardt, J. Food Sci. *43*, 660.

A general lethal-rate paper is proposed in order to represent directly the heat penetration data, whatever may be the Z value and whatever may be the reference temperature. A simple error analysis is carried out to determine the scale size that assures accurate results.

INFLUENCE OF CELLULAR MEMBRANE PERMEABILITY OF DRYING BEHAVIOR. E. Rothstein and A.R.H. Cornish, J. Food Sci. *43*, 926-934.

The basic transport equations and alternative cellular membrane permeability definitions are reviewed. An analysis of data on osmotic and diffusional permeability and a discussion of boundary layer resistances allows a representative water permeability value to be chosen. The rate of drying for a cellular membrane water permeability controlled drying experiment is then predicted for two extreme cases of convective contribution to the diffusional rate. Experimental results indicate that in the case of apples the drying phenomenon is not controlled by the cellular permeability.

SURFACE TEXTURIZATION OF EXTRUDED AND PREFORMED POTATO PRODUCTS BY A THREE-STEP DRY-STEAM-DRY PROCESS. M. Nonaka, R.N. Sayre and K.C. Ng, J. Food Sci. *43*, 904-907.

A dry-steam-dry process was used to make a crisp French fry from mash potatoes without additives. The times and conditions for drying, steaming and drying were varied and eval-

uated to get an organoleptically acceptable product. Long cooking times, high pressures and shearing actions that caused cellular damage and release of free starch were detrimental to the process and product. Compared with the commercially available product, the extruded French fry is more crisp, fries in a shorter time, absorbs less oil, has more natural potato flavor and has an excellent "plate-life." Other comparisons showed the process utilized less raw material and produced more strips and servings than was possible with the commercial process and product.

SOME RHEOLOGICAL PROPERTIES OF A CHEESE-LIKE PRODUCT PREPARED BY DIRECT ACIDIFICATION. J.R. Rosenau, J.F. Calzada and M. Peleg, J. Food Sci. *43*, 948-950.

A processed nonfermented cheese-like product was prepared by direct acidification of milk and heat coagulation of the curd. Modification of the textural properties was done by the incorporation of carrageenan. Textural evaluation was done by uniaxial compression. The parameters analysed were true stress-true (Hencky's) strain relationships obtained at two different histories, residual stresses after relaxation, and true stresses and strains at failure. Results showed that with respect to all these parameters the experimental nonfermented product resembled commercial processed American cheese though at generally smaller strength levels. Introduction of carrageenan contributed solid properties to the experimental processed cheese. At 1% level of carrageenan the product had mechanical properties similar to those of commercial cheese.

FLUX RESTORATION OF REVERSE OSMOSIS MEMBRANES BY INTERMITTENT LATERAL SURFACE FLUSHING FOR ORANGE JUICE PROCESSING. A. Watanabe, S. Kimura, and S. Kimura, J. Food Sci. *43*, 985-988.

A newly developed method for washing membranes and the adhesive strength of mandarin orange juice fouling on reverse osmosis membranes were studied. When the permeation rate decreased it was restored to more than 90% of its original value by a lateral surface flushing of highly accelerated mandarin orange juice driven by the expansion force of compressed gas for runs of 4-5 hr duration with 10° Brix feed. The normal operating cycle was 45 min of reverse osmosis concentration followed by a 10-sec wash. Membranes treated at higher temperature have a more condensed surface from which deposits are easily removed. However high axial flow rates which are useful for preventing the fouling on the membrane, actually promote permanent fouling.

MOISTURE SORPTION ISOTHERMS OF COFFEE PRODUCTS. K. Hayakawa, J. Matas, and M.P. Hwang, J. Food Sci. *43*, 1026-1027.

The moisture sorption isotherm of six different coffee products were determined at 20 and 30°C by a standard procedure which used saturated salt solutions. According to the analysis of variance applied to collected adsorption data, we observed that different drying methods (M), temperature of adsorption (T), and environmental relative humidity (RH) significantly influenced moisture adsorption by the product. It was also observed that interactions between M and decaffeination as well as between M and RH were also statistically significant. Monolayer values and sorption heat values were estimated from the isotherms using the BET and Clausius-Clapeyron's equations.

OPTIMAL MODES OF OPERATION FOR MICROWAVE FREEZE DRYING OF FOOD. T.K. Ang, J.D. Ford and D.C.T. Pei, J. Food Sci. *43*, 648-649.

In freeze-drying the quality of the resulting product determines the attractiveness of the drying process. Therefore, the temperature profiles within the material are as important as the total drying time required. For microwave assisted freeze drying it has been indicated both experimentally and in theoretical analysis that the maximum applicable constant field strength for beef cubes is 130 v/cm. Beyond this point melting of the ice core and/or overheating in the dried layer will occur. However, the drying time can be further reduced by 20% if a simple preprogrammed stepwise adjustment of the applied field strength is introduced.

EVALUATION OF KINETIC MODEL FOR REACTIONS IN MOISTURE-SENSITIVE PRODUCTS USING DYNAMIC STORAGE CONDITIONS. S. Mizrahi and M. Karel, J. Food Sci. *43*, 750-753.

A method using continuously changing moisture content and temperature was developed for evaluating the kinetics of deterioration in moisture sensitive products. The method can be applied to cases where the order of the reaction is known and the rate is dependent on water content and temperature. The kinetic parameters are calculated from the extent of deterioration, which is monitored in a product under continuously changing conditions. The accuracy of the method depends on the sensitivity of the analytical techniques used as well as on the proper selection of experimental conditions. The expected accuracy is adequate, but inferior to the traditional constant-moisture/constant-temperature kinetic tests.

MECHANICAL INTERPRETATION OF COMPRESSIVE STRESS-STRAIN RELATIONSHIPS OF SOLID FOODS. F.J. Calzada and M. Peleg, J. Food Sci. *43*, 1087-1092.

True compressive stress-strain relationships of various solid foods have been demonstrated in a three-dimensional display that has included the test's true strain histories. The shapes of the stress-strain curves and complementary relaxation and compressibility data indicated the existence of two antagonistic mechanisms which regulated the stress levels. These were internal fractures which tended to decrease the mechanical strength of the deformed specimens and structural compaction that had the tendency to increase it. It has also been demonstrated that the true stresses could be influenced by the specimen dimensions as well as by the strain rate.

SOME MATHEMATICAL ASPECTS OF MASTICATION AND ITS SIMULATION BY MACHINES. M. Peleg, J. Food Sci. *43*, 1093-1095.

If the deformation process of a specimen satisfies the condition: $H(t) = g(H_o) \cdot f(t)$ (Eq. 1), where H(t) is the deformed specimen length at time (t), $g(H_o)$ is a function of the initial length (H_o) only and f(t) a function of time only, then the true strain $\dot{e}(t)$ and the strain rate e(t) are: $\dot{e}(t) = \text{In } f(t)$ (Eq. 2), and $\dot{e}(t) = [d \text{ In } f(t)]/dt$(Eq.3). These imply that the stress-strain (or force-time) relationship of a homogeneous material is independent of the specimen length and is only determined by the rheological properties of the material and the selected function f(t). If the deformation histories produced in mastication satisfy the condition set by Eq. (1) it would provide a partial mathematical explanation to why sensory textural-rheological properties are not affected by the specimen dimensions in contrast to instrumental parameters obtained by existing testing machines. The construction of machines that provide such straining histories is physically possible (they would not, however, be operated at a constant deformation rate), and therefore it is theoretically possible to obtain instrumental parameters that are dimension independent. The concept

is demonstrated that some simplified rheological models and its possible application to food testing evaluated.

SHORT-CUT METHOD FOR THE CALCULATION OF STERILIZATION CONDITIONS YIELDING OPTIMUM QUALITY RETENTION FOR CONDUCTION-TYPE HEATING OF PACKAGED FOODS. H.A.C. Thijsen, P.J.A.M. Kerkhof and A.A.A. Liefkens, J. Food Sci. *43*, 1096-1011.

Based on analytical equations for the temperature distribution history in a container, the relation between the reductions of the concentrations of heat labile food components, including microorganisms, nutrients and sensory factors, and the kinetic parameters of the reactions causing these reductions, has been calculated numerically. For a constant temperature of the heating medium with time it is concluded that the loss of quality is almost minimal at one Fourier value of the heating time. This optimal Fourier value is a function of only the Biot number and the relationship between initial product temperature, cooling water temperature and retort temperature. At an infinite value of Biot and a cooling water temperature equal to the initial product temperature the optimum Fourier value amounts to 0.5. On the basis of this conclusion a short-cut calculation method is developed. The method is valid for Biot numbers larger than 10, initial homogeneous product temperatures equal to or larger than the temperature of the cooling medium and for the main container geometries including spheres, cylinders and rectangular bodies. The method does not require tedious interpolations of tables. The calculation of the optimum process conditions to obtain the desired sterility and the calculation of the retention of the quality factor of interest require only a few minutes on a pocket calculator. For routine calculations the procedure can conveniently be programmed.

TENSILE STRENGTH OF PROCESSED MEATS DETERMINED BY AN OBJECTIVE INSTRON TECHNIQUE. T.A. Gillett, C.L. Brown, R.L. Leutzinger, T.D. Cassidy and S. Simon, J. Food Sci. *43*, 1121-1124.

Union Carbide has designed an accessory for securing meat slices while tensile strength determinations are being made using an Instron Universal Testing Machine. When compared to pneumatic jaws, the sliceholding accessory (SHA) gave smaller standard deviations, handled larger sample sizes, weakened the sample less and could be used to evaluate a wider range of products. The SHA was successfully used to demonstrate the positive effects of salt, phosphate, and dry skim milk on the binding characteristics of processed meats. In addition, it illustrated the effect of sample storage temperature and slice thickness on tensile strength (g/cm^2) of selected meat items. Recommendations are discussed for determining, reporting, and comparing tensile strength values on processed meats.

SOME EFFECTS OF SELECTED PLASTICIZING AGENTS ON THE REVERSIBLE COMPRESSION OF FREEZE-DRIED COOKED BEEF CUBES. J.P. Morgan and D.F. Farkas, J. Food Sci. *43*, 1133-1136.

Ethanol (95%) and glycerin were found to plasticize freeze-dried cubes of beef for reversible compression. Both are easily applied and plasticization appears to be rapid and effective. Appearance and texture of the reconstituted, compressed product compared favorably with that of noncompressed product and product plasticized by partial rehydration to 10% moisture; however, the glycerin and ethanol treatments gave a slightly off-flavor. Vegetable oil and trichlorofluoromethane did not provide adequate plasticization. Polar liquids appear to be required for plasticization of dried beef for compression.

DEFINITION OF A PREDICTION MODEL FOR DETERMINATION OF THE EFFECT OF PROCESSING AND COMPOSITIONAL PARAMETERS ON THE TEXTURAL CHARACTERISTICS OF FABRICATED SHRIMP. H.M. Soo, E.H. Sander and D.W. Kess, J. Food Sci. *43*, 1165-1171.

The designs of Scheffe J. Royal Stat. Soc., Series B (1963) 25: 35, and of McLean and Anderson Technometrics (1966) 8(3):447 were used to study the effect of processing (mixing times and procedures) and compositional (shrimp, isolated soy protein, NaCl, and sodium tripolyphosphate) parameters on the textural changes of fabricated shrimp. Prediction equations were developed to investigate the effect of those parameters on textural changes of the cooked shrimp patties. There is not a significant interaction effect between the processing and compositional parameters. Mixing temperature has a greater effect on texture of cooked shrimp patties than does mixing time. The directional derivatives of the response surface and the contour plots were used to examine the compositional effects. Sodium tripolyphosphate (STP) causes the greatest change in response among components studied. The optimum level of NaCl for springiness is 2% whereas the optimum level of STP is dependent upon the isolated soy protein (ISP) level. Springiness of cooked shrimp patties increased with increasing ISP and decreasing shrimp levels in the mixture. The calculated optimum processing and compositional parameters for fabricated shrimp texture were obtained by using a non-linear programming routine, and agreed with the measured values. The designs and data analysis procedures can be used to develop accurate prediction models for the effect of processing and compositional parameters on textural characteristics of fabricated shrimp.

Table 2 which was published in Issue 1, Vol. 2 of the *Journal of Food Process Engineering* on page 11 contained 4 errors including 1 error in the Table data and 3 errors in the footnotes.

The corrected Table 2 is published below.

Table 2. Coefficients in the equation[a] of viscosity μ (poise) as function of shear rate γ_w (s^{-1}) and temperature T (°C/100)

Added Moisture	A_o	A_1	A_{11}	A_{12}	A_2	A_{22}	Multiple Correlation Coefficient
22%	1.1953	0.6256	−0.5815	1.1560	3.9976	−2.9588	0.991[b]
25%	−1.1733	−1.6475	−0.0930	1.0297	13.8805	−6.9624	0.998[c]
32%	4.0761	−1.0016	0.0616	−0.0378	2.7291	−1.1817	0.994[d]

[a] $\log \mu = A_o + A_1 \log \dot{\gamma}_w + A_{11} \log^2 \dot{\gamma}_w + A_{12} T \log \dot{\gamma}_w + A_2 T + A_{22} T^2$ where A_o, A_1, A_{11}, A_{12}, A_2 and A_{22} are empirical constants

[b] Valid for the range $55 \leqslant \dot{\gamma}_w \leqslant 1200$ and $1.0 \leqslant T \leqslant 1.6$

[c] Valid for the range $70 \leqslant \dot{\gamma}_w \leqslant 10500$ and $1.0 \leqslant T \leqslant 1.6$

[d] Valid for the range $60 \leqslant \dot{\gamma}_w \leqslant 5210$ and $1.0 \leqslant T \leqslant 1.6$

F
N
P

JOURNALS AND BOOKS IN FOOD SCIENCE AND TECHNOLOGY

JOURNAL OF FOOD BIOCHEMISTRY — Herbert O. Hultin
Norman F. Haard and John R. Whitaker

JOURNAL OF FOOD PROCESS ENGINEERING —
Dennis R. Heldman

JOURNAL OF FOOD PROCESSING AND PRESERVATION —
Theodore P. Labuza

JOURNAL OF FOOD QUALITY — Amihud Kramer and
Mario P. DeFigueiredo

JOURNAL OF FOOD SAFETY — M. Solberg and Joseph D. Rosen

JOURNAL OF TEXTURE STUDIES — P. Sherman and
Alina S. Szczesniak

FOOD POISONING AND FOOD HYGIENE, FOURTH EDITION —
Betty C. Hobbs and Richard J. Gilbert

FOOD SCIENCE AND TECHNOLOGY, THIRD EDITION —
Magnus Pyke

POSTHARVEST BIOLOGY AND BIOTECHNOLOGY —
Herbert O. Hultin and Max Milner

PRINCIPLES OF FOOD SCIENCE — Georg Borgstrom
VOLUME 1 — FOOD TECHNOLOGY
VOLUME 2 — FOOD MICROBIOLOGY AND BIOCHEMISTRY

THE SCIENCE OF MEAT AND MEAT PRODUCTS,
SECOND EDITION —
James F. Price and B. S. Schweigert

GUIDE FOR AUTHORS

Typewritten manuscripts in triplicate should be submitted to the editorial office. The typing should be double-spaced throughout with one-inch margins on all sides.

Page one should contain: the title, which should be concise and informative; the complete name(s) of the author(s); affiliation of the author(s); a running title of 40 characters or less; and the name and mail address to whom correspondence should be sent.

Page two should contain an abstract of not more than 150 words. This abstract should be intelligible by itself.

The main text should begin on page three and will ordinarily have the following arrangement:

Introduction: This should be brief and state the reason for the work in relation to the field. It should indicate what new contribution is made by the work described.

Materials and Methods: Enough information should be provided to allow other investigators to repeat the work. Avoid repeating the details of procedures which have already been published elsewhere.

Results: The results should be presented as concisely as possible. Do not use tables *and* figures for presentation of the same data.

Discussion: The discussion section should be used for the interpretation of results. The results should not be repeated.

In some cases it might be desirable to combine results and discussion sections.

References: References should be given in the text by the surname of the authors and the year. *Et al.* should be used in the text when there are more than two authors. All authors should be given in the References section. In the Reference section the references should be listed alphabetically. See below for style to be used.

DEWALD, B., DULANEY, J. T. and TOUSTER, O. 1974. Solubilization and polyacrylamide gel electrophoresis of membrane enzymes with detergents. In *Methods in Enzymology*, Vol. xxxii, (S. Fleischer and L. Packer, eds.) pp. 82–91, Academic Press, New York.

HASSON, E. P. and LATIES, G. G. 1976. Separation and characterization of potato lipid acylhydrolases. Plant Physiol. *57*, 142–147.

ZABORSKY, O. 1973. *Immobilized Enzymes*, pp. 28–46, CRC Press, Cleveland, Ohio.

Journal abbreviations should follow those used in *Chemical Abstracts*. Responsibility for the accuracy of citations rests entirely with the author(s). References to papers in press should indicate the name of the journal and should only be used for papers that have been accepted for publication. Submitted papers should be referred to by such terms as "unpublished observations" or "private communication." However, these last should be used only when absolutely necessary.

Tables should be numbered consecutively with Arabic numerals. The title of the table should appear as below:

Table 1. Activity of potato acyl-hydrolases on neutral lipids, galactolipids, and phospholipids

Description of experimental work or explanation of symbols should go below the table proper.

Figures should be listed in order in the text using Arabic numbers. Figure legends should be typed on a separate page. Figures and tables should be intelligible without reference to the text. Authors should indicate where the tables and figures should be placed in the text. Photographs must be supplied as glossy black and white prints. Line diagrams should be drawn with black waterproof ink on white paper or board. The lettering should be of such a size that it is easily legible after reduction. Each diagram and photograph should be clearly labeled on the reverse side with the name(s) of author(s), and title of paper. When not obvious, each photograph and diagram should be labeled on the back to show the top of the photograph or diagram.

Acknowledgments: Acknowledgments should be listed on a separate page.

Short notes will be published where the information is deemed sufficiently important to warrant rapid publication. The format for short papers may be similar to that for regular papers but more concisely written. Short notes may be of a less general nature and written principally for specialists in the particular area with which the manuscript is dealing. Manuscripts which do not meet the requirement of importance and necessity for rapid publication will, after notification of the author(s), be treated as regular papers. Regular papers may be very short.

Standard nomenclature as used in the engineering literature should be followed. Avoid laboratory jargon. If abbreviations or trade names are used, define the material or compound the first time that it is mentioned.

EDITORIAL OFFICE: Prof. D. R. Heldman, Editor, Journal of Food Process Engineering, Michigan State University, Department of Agricultural Engineering, East Lansing, Michigan 48824 USA

JOURNAL OF FOOD PROCESS ENGINEERING VOL. 2 NO. 3

CONTENTS